Time-Dependent Backgrounds of String Theory

A thesis presented

by

Alexander DeWitt Maloney

to

The Department of Physics

in partial fulfillment of the requirements

for the degree of

Doctor of Philosophy

in the subject of

Physics

Harvard University

Cambridge, Massachusetts

May, 2003

Abstract

This thesis is devoted to the study of time-dependent backgrounds in string theory. The first chapter contains a brief, non-technical introduction to the subject.

In the second chapter quantum field theory in d-dimensional de Sitter space is studied, with an emphasis on the dS/CFT correspondence. We study a one-parameter family of dS-invariant vacua; this bulk vacuum dependence is dual to a deformation of the boundary CFT by a marginal operator. In odd spacetime dimensions the state with no particles on $\mathcal{I}^-$ has no particles on $\mathcal{I}^+$, implying the absence of particle production. In Kerr-dS, a thermal density matrix is found by tracing over causally inaccessible modes. Assuming Cardy's formula, the microscopic entropy of such a thermal state in the boundary CFT precisely equals the Bekenstein-Hawking value.

Next, we construct de Sitter vacua of supercritical string theories in $D > 10$ dimensions. Compactifying $D - 4$ of these dimensions on a carefully constructed asymmetric orientifold projects out the continuous moduli of the compact directions. By adding specific fluxes we generate dilaton potentials with nontrivial minima at arbitrarily small cosmological constant and string coupling. We then discuss the decay of such metastable de Sitter vacua. For sufficiently large potential barriers the standard gravitational instantons violate both causality and low-energy decoupling, raising the possibility that these de Sitter vacua are stable.

In the final chapter we study spacelike branes as exact, boundary deformed worldsheet CFTs. Open string pair production is thermal, as can be seen from either a Bogolyubov transformation or an Unruh detector argument. Moreover, there exist exactly thermal mixed states which define a Euclidean effective field

theory on the S-brane world-volume. By computing the boundary state of this theory we determine the long range closed string production. At a critical value of the coupling the S-brane reduces to an array of sD-branes on the imaginary time axis. In real time this corresponds to a purely closed string configuration with no D-branes, yet the long range force felt by an observer is proportional that produced by the original unstable D-brane.

Contents

Chapter 1: Introduction

1. Time Dependence in String Theory 1
   1.1. Conformal Vacua and Entropy in de Sitter Space 2
   1.2. de Sitter Space in Non-Critical String Theory 4
   1.3. S-Brane Thermodynamics 5

Chapter 2: Conformal Vacua and Entropy in de Sitter Space

2. Introduction and Summary 6
3. Green Functions 11
   3.1. The Euclidean Vacuum and Wightman Function 12
   3.2. The MA Transform 14
   3.3. Analytic Continuation from AdS 16
   3.4. Particle Detection 17
4. The Sphere 19
   4.1. Solutions of the Wave Equation 20
   4.2. In and Out Vacua 21
   4.3. The Euclidean Vacuum 24
   4.4. The $|E\rangle \rightarrow |\text{in}\rangle$ Transformation 26
5. CFT Interpretation 27
   5.1. $\mathcal{I}^{\pm}$ Correlators 27
   5.2. dS Vacua as Marginal CFT Deformations 30
6. $\mathcal{CPT}$ and the Inner Product 33
   6.1. Continuous and Discrete Symmetries of de Sitter Space 34
   6.2. $\mathcal{CPT}$ 35
   6.3. The Witten Inner Product and Modifications 37
   6.4. Adjoints of the $SL(2,C)$ Generators 38
7. The Cylinder 39
   7.1. The Wave Equation 40
   7.2. The Northern and Southern Diamonds 40
   7.3. The Past and Future Triangles 42
   7.4. Matching Across the Horizon. 44
   7.5. Euclidean Modes on the Cylinder 46
   7.6. MA Transform to Euclidean Modes 47
   7.7. The Thermal State 48
8. Kerr-de Sitter 49
   8.1. Static Coordinates 49
   8.2. Kerr-dS_3 as a Quotient of dS_3 50
   8.3. Kerr-dS_3 Temperature and Angular Potential 51
   8.4. The Boundary Stress Tensor and Virasoro Charges 53
9. Entropy 56

Appendix A. Alternate Forms of Green Functions on dS_d . . . 58
Appendix B. Properties of Hypergeometric Functions . . . 60

Chapter 3: de Sitter Space in Non-Critical String Theory

10. Introduction . . . 61
11. de Sitter Compactifications of Super-Critical String Theory . . . 64
11.1. Asymmetric Orientifolds in Non-Critical String Theory . . . 65
11.2. de Sitter Solutions . . . 71
11.3. Solutions With Small Λ . . . 72
12. Metastability of the de Sitter Vacuum . . . 73
12.1. The Instantons . . . 74
12.2. Causality . . . 76
12.3. Breakdown of the Semiclassical Approximation . . . 78
12.4. Instantons in the Orientifold Model . . . 81

Chapter 4: S-Brane Thermodynamics

13. Introduction . . . 85
14. Quantum vacuum states . . . 91
14.1. The $|in\rangle_+$ vacuum for brane decay . . . 93
14.2. The $|in\rangle_-$ vacuum for brane creation . . . 96
14.3. Full s-brane modes . . . 97
14.4. $|in\rangle_s$ and $|out\rangle_s$ s-brane vacua . . . 99
14.5. The $|0\rangle_s$ Euclidean s-brane vacuum . . . 100
14.6. More vacua . . . 103
15. S-brane thermodynamics . . . 103
15.1. S-branes at finite temperature . . . 104
15.2. Unruh detection . . . 106
15.3. Thermal correlators . . . 109
16. Long-distance s-brane effective field theory . . . 110
17. Thermal boundary states . . . 112
17.1. Zero modes and winding sectors . . . 113
17.2. The superstring . . . 115
18. The $\lambda = \pm\frac{1}{2}$ sD-brane limit . . . 116
18.1. The classical closed string field . . . 117
18.2. RR field strength and s-charge . . . 120
18.3. Long-range graviton/dilaton fields . . . 121
18.4. The annulus diagram . . . 123
18.5. The finite-temperature annulus . . . 126
18.6. S-branes and D-instantons . . . 129
19. Timelike Holography . . . 130

References . . . 132

Acknowledgements

I would like to thank Andy Strominger for his guidance and support over the years. It has been a pleasure and an honor to be his student.

I am also grateful to my collaborators, Raphael Bousso, Ruth Britto, Eva Silverstein, Mark Spradlin, Mark Stern and Xi Yin, who have taught me so much.

I would like to thank the many other people who have taught me physics over the years, Nima Arkani-Hamed, Sidney Coleman, Howard Georgi, Renata Kallosh, Barry Lasker, Juan Maldacena, Shiraz Minwalla, Vahe Petrosian, Lenny Susskind and Cumrun Vafa.

I am also grateful to my fellow grad students and comrades in arms, Freddy Cachazo, Chari, Henry Chen, Matt Headrick, Jeremy Michelson, Andy Neitzke, Daniel Podolsky, Matt Schwarz, Shishir Sinha, Dave Thompson, Anastasia Volovich, Jay Wacker and Martijn Wijnholt.

I would like to thank all the other members of the particle theory group at Harvard, who have made this such an exciting place to spend five years: Mina Aganagic, Vijay Balasubramanian, Rajesh Gopakumar, Aaron Grant, Sergei Gukov, Michael Gutperle, Joanna Karczmarek, Marcos Marino, Lubos Motl, Carlos Nunez, David Tong and Nick Toumbas.

Of course, I am especially indebted to John Barrett, Nancy Partridge and the rest of the physics department administrative staff.

I would also like to thank the Harvard physics department, the NSF graduate fellowship program, the Department of Energy and everyone who pays taxes for financial support.

Finally, I would like to thank my family and friends, without whom none of this would have been possible. Foremost, I am grateful to my parents, Gail and Peter, and to my sister, Beth – their unwavering love and encouragement has been more important to me than words can describe. I would like to thank Bekah, whose love,

support and inspiration has meant so much to me over the past year. I would also like to thank the rest of my friends and family – over the years they have encouraged me, consoled me, laughed at my jokes and tolerated my antics far above and beyond the call of duty. Finally, I would like to remember my grandfather, Hans, who more than anyone set me on this path many years ago. This thesis is dedicated to his memory.

Chapter 1

Introduction

1. Time Dependence in String Theory

The study of time dependent systems – and indeed the notion of time itself – has played a crucial role in the development of modern physics. The theory of relativity, for example, describes time and space not as separate entities but in terms of a single, smooth space-time geometry. Quantum mechanics, however, implies that these classical notions of space-time break down at very short distances. The standard theories of gravity and quantum mechanics simply can not describe physics at such small scales, and something new is required – a quantum theory of gravity. String theory provides an elegant and radical solution to the problem of quantum gravity. In doing so it promises to unify the two great triumphs of the twentieth century – the theory of relativity and the standard model of particle physics – into a single coherent formulation of fundamental physics. Many aspects of string theory remain mysterious, however, and must be understood if string theory is to live up to it's early promise. Nevertheless, string theory has already solved many of the long-standing and difficult problems in theoretical physics. In the theory of gravity, for example, the list of accomplishments includes a microscopic understanding of the structure of black holes and the resolution of singularities. On the particle physics side, string theory provides insights into the fundamental structure of quantum theories and progress towards understanding the origin of the standard model of particle physics. Perhaps the most striking discovery is that these and many other seemingly unrelated problems are in fact intimately related by web of dualities.

While impressive, this list of achievements is primarily limited to static, time-independent systems. The study of time-dependent systems in string theory has proven surprisingly difficult, and until recently little progress had been made. This question is not completely academic, as quantum gravity plays a crucial role in the cosmological evolution of our universe. In fact, astronomical observations provide one of the most exciting prospects for experimental tests of string theory.

This thesis contains my contributions to the study of time-dependent systems in string theory. The following three chapters describe three different approaches to the subject, which I shall now summarize in turn. Most of the material in this thesis has appeared previously, in references [1–3].

1.1. Conformal Vacua and Entropy in de Sitter Space

We live in an expanding universe. Over the course of history, our universe has grown in size by a factor of about 10^{60}. Recent astronomical observations indicate that this expansion will continue forever, and that in the far future our universe will gradually come to resemble a geometry known as de Sitter space. Moreover, the most promising theories of the early universe posit that our universe resembled de Sitter space in the far past. An understanding of de Sitter space in quantum gravity is therefore of paramount importance.

de Sitter space is the simplest example of a time-dependent cosmology, and is one of the oldest and best studied solutions of general relativity. It is characterized by exponential expansion; every point in de Sitter space expands away from every other point with exponentially increasing velocity. Eventually this rate of expansion will exceed the speed of light, at which point no two observers will ever be able to communicate with one another. [1] The two observers will be separated by an event

[1] In de Sitter space, everyone ends up alone – it has been called "the ultimate existential nightmare."

horizon, much like the one that surrounds the interior of a black hole. This analogy between black holes and de Sitter space has guided much of the previous work on the subject. String theory successfully describes the microscopic physics of black holes, so it is natural to seek a similar understanding of de Sitter space in string theory.

Moreover, a close cousin of de Sitter space, called Anti-de Sitter space, has proven remarkably interesting in string theory. String theory in a D dimensional Anti-de Sitter space is precisely equivalent to a theory of particle physics in $D-1$ dimensions. Such an equivalence between two different theories is known as a duality; in recent years string theory has provided several amazing examples of dual theories. The Anti-de Sitter duality is especially interesting because the corresponding dual theory lives in one less dimension, a phenomenon known as holography. It is natural to speculate that string theory in a D dimensional de Sitter space has a dual holographic description as a $D-1$ dimensional theory of particle physics.

The second chapter of this thesis explores this conjecture in detail, along with several related phenomena. The duality conjecture allows us to match certain features of de Sitter space to analogous features of the dual $D-1$ dimensional theory. One such feature is the existence of conformal vacua – this is the statement that the notion of empty space, or vacuum, is not a well defined concept in de Sitter space. In fact, in any time-dependent geometry what one observer sees as empty space may appear to another observer as a bath of radiation. This ambiguity greatly constrains the structure of the dual $D-1$ dimensional theory. Moreover, the existence of a dual holographic theory explains several other mysterious features of de Sitter space. Certain properties of the event horizons, for example, have elegant descriptions in terms of the dual particle theory.

1.2. de Sitter Space in Non-Critical String Theory

The third chapter, continuing the study of time-dependent backgrounds, gives a construction of de Sitter space in a specific model of string theory. The string theory under consideration, known as non-critical string theory, has a variety of unusual features. The most well studied class of string theories – called critical string theories – contain six extra dimensions in addition to the four that we live in, for a total of ten dimensions. These six new dimensions are necessary to describe a theory in flat space, i.e. a theory without space-time curvature. Other theories, known as non-critical string theories, have more than six extra dimensions – they can be used to describe curved geometries such as de Sitter space. However, the same features that make these theories useful, namely the existence of more than six extra dimensions, make them difficult to study.

The construction of de Sitter space in string theory involves another unusual phenomenon, the appearance of non-geometric dimensions. The classical theory of gravity describes space and time in terms of smooth, continuous geometry. However, this description breaks down at very short distances. On these small scales the traditional notions of space and time are replaced by new, string theoretic quantities. These non-geometric concepts play a crucial role in the construction of de Sitter space. For example, a four dimensional de Sitter solution is found by considering a D dimensional non-critical theory, with $D-4$ of the dimensions taking this peculiar, non-geometric form.

Any construction of de Sitter space in string theory is plagued by the problem of vacuum instability. In particular, one expects that after a certain amount of time these de Sitter solutions will spontaneously decay into flat space. A quantum fluctuation will lead to the creation of a spherical bubble of flat space inside the de Sitter geometry. The walls of this bubble expand at velocities approaching the

speed of light, converting everything in their path into empty flat space. [2] The final part of this chapter describes a mechanism by which certain de Sitter constructions evade this problem. These considerations are certainly important if, as astronomical observations indicate, our universe will come to resemble de Sitter space in the far future.

1.3. S-Brane Thermodynamics

The final chapter of this thesis concerns spacelike branes, a different type of time dependent background. String theory contains, in addition to the eponymous strings, a host of additional objects called branes. Whereas strings are one dimensional objects, these branes are extended in more than one dimension – membranes, for example, are objects that extend in two dimensions. Some of these objects are unstable and if perturbed slightly will quickly decay into a bath of radiation. This decay process, often referred to as a spacelike brane or S-brane, is one of the few time-dependent backgrounds that can be readily studied in string theory.

An obvious first task is to determine the dynamics and composition of this decay. In general, an unstable brane may decay into either open strings or closed strings. Open strings – strings whose endpoints can move freely in space – are typically associated with theories of particle physics. Closed strings, whose endpoints join to form a closed loop, describe the gravitational and geometric fluctuations of space-time. Both types of decay play a crucial role in the study of S-branes.

[2] These decays have been playfully referred to as "the ultimate ecological catastrophe."

Chapter 2

Conformal Vacua and Entropy in de Sitter Space [3]

2. Introduction and Summary

Recently, following earlier work [4–15], a proposal has been made relating quantum gravity in de Sitter space to conformal field theory on the spacelike boundary of de Sitter space [16]. The proposal was motivated by an analysis of the asymptotic symmetry group of de Sitter space together with an appropriately crafted analogy to the AdS/CFT correspondence [17,18,19]. Other relevant discussions of quantum gravity in de Sitter space and dS/CFT appear in [20–42].

Unlike the AdS/CFT case, there has been no derivation of the proposed dS/CFT correspondence from string theory. Hopefully, a stringy construction of de Sitter space will be forthcoming. Meanwhile, much has been learned about AdS/CFT by analyzing solutions of the field equations and studying the propagation and interactions of fields, without directly using string theory. In this paper we pursue a parallel approach to dS/CFT, analyzing in some detail massive scalar field theory in de Sitter space. A number of surprising and interesting features emerge. Since this paper contains some rather detailed calculations, for the benefit of the reader we include a summary in this introduction.

We begin in section 2 with a discussion of dS-invariant Green functions for a massive scalar, reviewing and generalizing to d dimensions the discussion of [43,44]. We first describe the Green function obtained by analytic continuation from the Euclidean sphere. This is the so-called Euclidean Green function, and it is the two-point function of the scalar field in the Euclidean vacuum. We then construct a family of dS-invariant vacua labeled by a complex parameter α and compute the

[3] This chapter is based on the paper [1], with R. Bousso and A. Strominger.

Green functions in these α-vacua, which have several peculiarities. Singularities occur at antipodal points which are however, unobservable since antipodal points are always separated by a horizon. Moreover, these singularities do not affect the scalar commutator, which is independent of α. We also see that the coincident point singularity has two terms, with opposite-signed $i\epsilon$ prescriptions. Hence all of these α-vacua except for the Euclidean vacuum differ from the usual Minkowski vacuum at arbitrarily short distances. We also compute the response of an Unruh detector and find that it is thermal only in the Euclidean vacuum. The dual CFT interpretation of the α-vacua is deferred to section 4.

In relating the AdS/CFT and dS/CFT correspondences, it is natural to consider the particular Green function obtained by 'double' analytic continuation from AdS to dS via the hyperbolic plane. We show that the Green function so obtained, while dS-invariant, does *not* correspond to the Green function in any known dS-invariant vacuum.[4] This result underscores the non-triviality of extrapolating from AdS/CFT to dS/CFT.

In section 3 we consider scalar field theory in spherical coordinates

$$\frac{ds^2}{\ell^2} = -d\tau^2 + \cosh^2\tau\, d\Omega_{d-1}^2, \tag{2.1}$$

again generalizing [43,44] to d dimensions. A salient feature of these coordinates is that they cover all of de Sitter space and hence are suitable for studying global properties. The solutions of the massive scalar wave equation are found for arbitrary angular momentum. We then give an explicit construction in terms of these modes

[4] We benefitted greatly from discussions with M. Spradlin and A. Volovich on this point. There is in fact a four-complex-parameter family of dS-invariant Wightman functions, characterized by the (complex) strengths of the coincident and antipodal poles, as well as the two possible $i\epsilon$ prescriptions at each pole. Only a one-complex-parameter family of these is known to be realizable as two-point vacuum expectation values. Analytic continuation from AdS gives a result which is not realized within this family.

of the Bogolyubov transformations relating all the α-vacua. Special 'in' and 'out' vacua are found, which are distinct from the Euclidean vacuum. The in vacuum has no incoming particles on $\mathcal{I}^-$, while the out vacuum has no outgoing particles on $\mathcal{I}^+$. The Bogulubov transformation between them is computed. Surprisingly, it is found to be trivial in odd-dimensions. This means that for the in vacuum of odd-dimensional de Sitter space there is no particle production. This result did not appear in previous analyses, which largely considered the four-dimensional case.

In section 4 we specialize to dS_3 and consider the dual CFT_2 interpretation of these results, along the lines proposed in [16]. We first compute the boundary behavior of the massive scalar Green function as a function of the vacuum parameter α. This behavior is fixed by conformal invariance up to overall constants which are α-dependent. The boundary correlators have an especially simple form in the in vacuum. For both points on $\mathcal{I}^-$ (or both on $\mathcal{I}^+$) they vanish![5] This is related to the fact that on $\mathcal{I}^-$ the spatial kinetic terms vanish and the theory becomes ultralocal. For one point on $\mathcal{I}^-$ and one on $\mathcal{I}^+$ they do not vanish. The simplicity of this behavior suggests that the in vacuum, despite the unphysical singularities, may play an important role in understanding the dS/CFT correspondence.

One way of generating a family of correlators in a CFT is by deforming the theory by a marginal operator. In [16] it was argued that a scalar field of mass m is dual to a pair of CFT operators $\mathcal{O}_\pm$ with conformal weights $1 \pm \sqrt{1 - m^2\ell^2}$. The composite operator $\mathcal{O}_+\mathcal{O}_-$ always has dimension 2 dor any m, exactly what is required for a marginal deformation. We show explicitly for real α that this composite operator deforms the correlators in the same way as shifting α.

In section 5 we consider the definition of the adjoint in the Hilbert space of the scalar field. In standard treatments of 2D Euclidean conformal field theory, the adjoint of an operator involves a (non-local) reflection about the unit circle. This

[5] Except for a contact term which is computed.

prescription becomes the usual local adjoint when mapped to the cylinder. The "naive" adjoint for a bulk scalar field induces an adjoint in the Euclidean CFT which is local, and hence does not agree with the usual Euclidean CFT adjoint. However, in [20] Witten introduced a modified bulk inner product and corresponding adjoint. We show that, after a modification of the parity operation, Witten's bulk adjoint induces precisely the standard non-local Euclidean CFT adjoint. We further show that with the modified adjoint the $SL(2,C)$ generators obey $\mathcal{L}_n^\dagger = \mathcal{L}_{-n}$ (in a standard notation), as opposed to the relation $\mathcal{L}_n^\dagger = \bar{\mathcal{L}}_n$ implied by the naive adjoint.

As in the AdS case one expects that different coordinate systems in dS are relevant for different physical situations. In section 6 we consider static coordinates for dS_3, in which the metric is

$$\frac{ds^2}{\ell^2} = -(1-r^2)dt^2 + \frac{dr^2}{(1-r^2)} + r^2 d\varphi^2, \tag{2.2}$$

where ℓ is the de Sitter radius. These coordinates do not cover all of dS_3 with a single patch. Nevertheless, they do cover the so-called southern diamond—the region causally accessible to an observer at the 'south pole' $r = 0$. Moreover, the symmetry generating time evolution of the southern observer is manifest in static coordinates. Hence they appear well-adapted to describing the physics accessible to a single observer, as advocated in [45]. $\mathcal{I}^-$ is at $r \to \infty$ and is conformal to a cylinder.

In the (t, r, φ) coordinates, the full dS_3 spacetime can be covered with four patches separated by horizons. We solve the scalar wave equation in each patch and construct global solutions by matching across the horizon. It is shown that the in vacuum on the cylinder and the in vacuum on the sphere are equivalent. A southern density matrix is constructed from the Euclidean vacuum by tracing over modes which are supported only in the northern causal diamond and are thereby

unobservable to the southern observer. This is explicitly shown to be a thermal density matrix at temperature $T_{\rm dS} = \frac{1}{2\pi\ell}$, with energy measured with respect to the static time coordinate in (2.2). (This result is implicit in the original work [46].)

In section 7 we extend the static coordinate discussion to the Kerr-dS$_3$ geometry which represents a pair of spinning point masses at the north and south poles of dS$_3$. This has a Gibbons-Hawking temperature T_{GH} and angular potential Ω_{GH} which depend on the mass and spin. It is shown that, after tracing over northern modes, one obtains a thermal density matrix at precisely temperature T_{GH} and angular potential Ω_{GH}.

According to the dS$_3$/CFT$_2$ correspondence the quantum state on a bulk spacelike slice ending on $\mathcal{I}^-$ is dual to a CFT state on the boundary of the spacelike slice at $\mathcal{I}^-$[16]. The dS-invariant bulk vacuum should be dual to the $SL(2,C)$ invariant CFT vacuum. For pure de Sitter space, we therefore expect to see a Casimir energy $-c/12$, where $c = \frac{3\ell}{2G}$ is the central charge of the CFT computed in [16]. We find a two-parameter agreement with this expectation by computing the Brown-York boundary stress tensor in Kerr-dS$_3$. This generalizes results of [45].

Finally, in section 8 we turn to the issue of de Sitter entropy. In the case of BTZ black holes in AdS$_3$, the entropy formula can be microscopically derived, including the numerical coefficient, from the properties of the asymptotic symmetry group together with the assumption that the system is described by a consistent, unitary quantum theory of gravity [47]. String theory seems necessary in order to produce an actual example of such a theory, but the general arguments follow from the stated assumptions independently of the stringy examples. Therefore it is natural to hope that a similar discusion is possible for dS$_3$. We report here some partial results but not a complete solution of the problem. Related discussions appear in [6,11,48–53].

The main observation is that if we simply assume Cardy's formula for the den-

sity of states, then a CFT with $c = \frac{3\ell}{2G}$ at temperature T_{GH} and angular potential Ω_{GH} has a microscopic entropy precisely equal to one quarter the area of the Kerr-dS$_3$ horizon. The two-parameter fit is striking but at present should be regarded as highly suggestive numerology rather than a derivation. For one thing, the dual CFT is unlikely to be unitary [16], and so there is no reason for Cardy's formula to apply. Secondly, it is not clear how a mixed thermal state arises in the dual CFT. The natural CFT state associated to $\mathcal{I}^-$ is the $SL(2,C)$ invariant vacuum, in agreement with the pure nature of the global bulk de Sitter vacuum. A mixed density matrix arises in the bulk only after tracing over the unobservable northern modes. However, tracing over northern modes is a bulk concept. We have not succeeded in finding a natural boundary interpretation of this operation.

We believe this raises a sharp and important question whose answer may lie within the present framework and in particular may not require a stringy construction of de Sitter. What is the meaning, in terms of the dual boundary CFT, of tracing out degrees of freedom which are inaccessible to a single observer?

Two appendices detail useful properties of hypergeometric functions and de Sitter Green functions. For the rest of the paper we will set $\ell = 1$ unless otherwise stated.

3. Green Functions

The two point Wightman function of a free massive scalar can be used to characterize the various de Sitter invariant vacua. In this section we describe these Green functions and their properties. Previous studies of scalar field theory in de Sitter space, largely concentrating on the four-dimensional case, can be found in [43,44,54–63].

3.1. The Euclidean Vacuum and Wightman Function

In this subsection we review the standard Euclidean vacuum and its associated Wightman function.

d-dimensional de Sitter space (dS_d) is described by the hyperboloid in $d+1$-dimensional Minkowski space

$$P(X,X) = 1, \tag{3.1}$$

where

$$P(X,X') = \eta_{ab} X^a X'^b, \qquad a,b = 0,...,d. \tag{3.2}$$

We will use lower case x to denote a d-dimensional coordinate on dS_d and upper case X to denote the corresponding $d+1$-dimensional coordinate in the embedding space. The function $P(x,x')$ is greater than one for timelike separations, equal to one for lightlike separations, and less than one for spacelike separations. In fact, $P(x,x') = \cos\theta$, where θ is the geodesic distance between x and x' for spatial separations, or i times the geodesic proper time difference for timelike separations.

A vacuum state $|\Omega\rangle$ for a free massive scalar in de Sitter space with the mode expansion

$$\phi(x) = \sum_n \left[a_n \phi_n(x) + a_n^\dagger \phi_n^*(x) \right] \tag{3.3}$$

can be defined by the conditions

$$a_n |\Omega\rangle = 0, \tag{3.4}$$

where a_n and $a_n^\dagger$ as usual obey

$$[a_n, a_m^\dagger] = \delta_{nm}. \tag{3.5}$$

The modes $\phi_n(x)$ satisfy the de Sitter space wave equation

$$(\nabla^2 - m^2)\phi_n = 0, \tag{3.6}$$

and are normalized with respect to the invariant Klein-Gordon inner product

$$(\phi_n, \phi_m) = -i \int_\Sigma d\Sigma^\mu \left(\phi_n \overleftrightarrow{\partial_\mu} \phi_m^*\right) = \delta_{nm}. \tag{3.7}$$

The integral is taken over a complete spacelike slice Σ in dS_d with induced metric h_{ij}, and $d\Sigma^\mu = d^d x \sqrt{h}\, n^\mu$, where n^μ is the future directed unit normal vector. The norm (3.7) is independent of the choice of this slice. $|\Omega\rangle$ depends on the choice of modes appearing in (3.3).

The Wightman function, defined by

$$G_\Omega(x, x') = \langle \Omega | \phi(x) \phi(x') | \Omega \rangle = \sum_n \phi_n(x) \phi_n^*(x'), \tag{3.8}$$

characterizes the vacuum state $|\Omega\rangle$. There is a unique state, the "Euclidean vacuum" $|E\rangle$, whose Wightman function is obtained by analytic continuation from the Euclidean sphere. This state is invariant under the full de Sitter group. In d spacetime dimensions the Wightman function in the state $|E\rangle$ is

$$\begin{aligned} G_E(x, x') &= \langle E | \phi(x) \phi(x') | E \rangle = c_{m,d} F(h_+, h_-; \frac{d}{2}; \frac{1 + P(x, x')}{2}), \\ h_\pm &\equiv \frac{d-1}{2} \pm i\mu \\ \mu &\equiv \sqrt{m^2 - \left(\frac{d-1}{2}\right)^2} \\ c_{m,d} &\equiv \frac{\Gamma(h_+)\Gamma(h_-)}{(4\pi)^{d/2}\Gamma(\frac{d}{2})}. \end{aligned} \tag{3.9}$$

G_E is real in the spacelike region $P < 1$ and singular on the light cone $P = 1$. The $i\epsilon$ prescription near the singularity is

$$G_E(x, x') \sim \left((t - t' - i\epsilon)^2 - |\vec{x} - \vec{x}'|^2\right)^{1 - \frac{d}{2}}. \tag{3.10}$$

Note that this prescription cannot be written in terms of the invariant quantity P alone, which is time-reversal invariant. G_E obeys

$$(\nabla^2 - m^2) G_E(x, x') = 0. \tag{3.11}$$

In addition to the Wightman function, the Feynman propagator

$$G_F(x,x') = \Theta(t-t')G(x,x') + \Theta(t'-t)G(x',x) \tag{3.12}$$

and commutator

$$G_C(x,x') = G(x,x') - G(x',x) \tag{3.13}$$

are also of interest. With the normalization (3.9) G_F obeys

$$(\nabla^2 - m^2)G_F(x,x') = \frac{-i}{\sqrt{-g}}\delta^d(x,x'). \tag{3.14}$$

3.2. The MA Transform

In this subsection we describe the MA (Mottola-Allen) transform [43,44], which relates the various de Sitter invariant vacua and Wightman functions to one another.

Let $\phi_n^E(x)$ denote the positive frequency modes associated to the Euclidean vacuum. Explicit expressions for ϕ_n^E will be given later (sections 3.3 and 6.5), but we don't need them now. Let x_A denote the antipodal point to x on the de Sitter hyperboloid (i.e., $X_A = -X$). Then, as will be seen below, the Euclidean modes can be chosen to obey

$$\phi_n^E(x_A) = \phi_n^{E*}(x). \tag{3.15}$$

Now consider a new set of modes related by the MA transform

$$\tilde{\phi}_n \equiv N_\alpha(\phi_n^E + e^\alpha \phi_n^{E*}), \qquad N_\alpha \equiv \frac{1}{\sqrt{1-e^{\alpha+\alpha^*}}}. \tag{3.16}$$

where α can be any complex number with $\mathrm{Re}\,\alpha < 0$. The modes (3.16) can be used to define new operators $\tilde{a}_n$ and $\tilde{a}_n^\dagger$ via a decomposition of the form (3.3). These are related to the Euclidean operators a_n^E and $a_n^{E\dagger}$ by

$$\tilde{a}_n = N_\alpha(a_n^E - e^{\alpha^*} a_n^{E\dagger}). \tag{3.17}$$

This may be rewritten as

$$\tilde{a}_n = \mathcal{U}\, a_n^E\, \mathcal{U}^\dagger, \tag{3.18}$$

where

$$\mathcal{U} = \exp\left\{\sum_n c\,(a_n^{E\dagger})^2 - \bar{c}\,(a_n^E)^2\right\}, \qquad c(\alpha) = \frac{1}{4}\left(\ln\tanh\frac{-\mathrm{Re}\,\alpha}{2}\right) e^{-i\,\mathrm{Im}\,\alpha}. \tag{3.19}$$

The vacuum state

$$|\alpha\rangle = \mathcal{U}\,|E\rangle \tag{3.20}$$

is annihilated by the $\tilde{a}_n$. The operator $\mathcal{U}$ is unitary, so (3.20) is properly normalized. In the quantum optics literature, $|\alpha\rangle$ is known as a squeezed state. Equation (3.20) may be formally rewritten as

$$|\alpha\rangle = C\exp\left(\frac{1}{2}e^{\alpha^*}(a_n^{E\dagger})^2\right)|E\rangle, \tag{3.21}$$

where C is a constant. Although this expression is not normalizable (so C is technically zero), it is often more convenient than (3.20).

The Wightman function in the state $|\alpha\rangle$ is

$$G_\alpha(x,x') = \sum_n \tilde{\phi}_n(x)\tilde{\phi}_n^*(x'). \tag{3.22}$$

Using (3.15) and (3.16) this can be rewritten as a sum over Euclidean modes,

$$\begin{aligned} G_\alpha(x,x') = N_\alpha^2 \sum_n \big[&\phi_n^E(x)\phi_n^{E*}(x') + e^{\alpha+\alpha^*}\phi_n^E(x')\phi_n^{E*}(x) \\ &+ e^{\alpha^*}\phi_n^E(x)\phi_n^{E*}(x'_A) + e^{\alpha}\phi_n^E(x_A)\phi_n^{E*}(x')\big], \end{aligned} \tag{3.23}$$

and then evaluated as

$$G_\alpha(x,x') = N_\alpha^2\big[G_E(x,x') + e^{\alpha+\alpha^*}G_E(x',x) + e^{\alpha^*}G_E(x,x'_A) + e^{\alpha}G_E(x_A,x')\big]. \tag{3.24}$$

Hence it is easy to obtain the $|\alpha\rangle$ Wightman function from the Euclidean one. Since these Wightman functions depend only on the $SO(d,1)$ invariant quantity P

(away from the singularities) this construction demonstrates the invariance of the $|\alpha\rangle$ vacua under the connected part of the de Sitter group. Note however that if α is not real the collection of modes (3.16) is not mapped into itself by CPT. Therefore the $|\alpha\rangle$ vacua are CPT invariant only for real α.

Of course, since the commutator of two fields is a c-number, the commutator function G_C must be the same in all vacua. It is easy to check that the commutator constructed from the two point function (3.24) has this property.

The Wightman function (3.24) has several peculiarities. Firstly, there are antipodal singularities at $x' = x_A$. However such antipodal points are separated by a horizon so this singularity is not observable. Secondly, the singularity at coincident points has a negative frequency component coming from the second term in (3.24) (although the commutator is unaffected). This means that for $e^\alpha \neq 0$ the vacuum state does not approach the usual Minkowskian one even at distances much shorter than the de Sitter radius. This "unphysical" behavior was to be expected since the MA transform (3.16) involves arbitrarily high-frequency modes. Despite these peculiarities we will see that these vacua play an interesting role in the dS/CFT correspondence.

3.3. Analytic Continuation from AdS

An alternate way to get a dS Green function is by double analytic continuation from AdS via the hyperbolic plane.[6] In fact, we shall argue that this yields a Green function which differs from any of those discussed in the previous subsection and therefore, as far as we know, is not physically realizable as the Wightman function in any vacuum state. Hence the dS/CFT correspondence is not in any precise sense that we know of the analytic continuation of the AdS/CFT correspondence, and care must be taken in extrapolating from the latter to the former.

[6] See [5,10,64] for discussions.

AdS_d has a unique $SO(d-1,2)$ invariant vacuum whose scalar Green functions can be obtained as a sum over normalizable eigenmodes. The wave equation allows two possible falloffs (fast and slow) at infinity, but only the fast falloff appears in the Green function. Double analytic continuation from AdS to dS will therefore yield a dS Green function with only one of the two possible falloff rates (which become complex conjugates for large enough m). This cannot be the Euclidean dS Green function, as the latter involves both falloffs. There is a vacuum $|\alpha\rangle$ whose Green function has the required falloff[7]. However from (3.24) we see that the Green function for every state except $|E\rangle$ has a coincident point singularity with a coefficient larger than that of $|E\rangle$ and containing two terms with opposite-signed $i\epsilon$ prescriptions. However double analytic continuation from AdS will yield a coincident point singularity with a canonical coefficient and a single $i\epsilon$ prescription. Hence it yields a Green function which is not realized as $\langle\alpha|\phi(x)\phi(x')|\alpha\rangle$ for any α.

3.4. Particle Detection

In this subsection we discuss particle detection by a geodesic observer in the $|\alpha\rangle$ vacua. We will find a thermal spectrum only for the Euclidean vacuum.

Consider an Unruh detector moving along a timelike geodesic, which couples to the field as

$$\int dt\, m(t)\, \phi(x(t)) \tag{3.25}$$

where $m(t)$ is an operator acting on the internal states of the detector and the integral is over the proper time along the detector worldline. Without loss of generality we may take the detector to be sitting on the south pole. Let's assume that the detector has a spectrum of states $|E_i\rangle$ with energies E_i, and define the matrix element $m_{ij} = \langle E_i|m(0)|E_j\rangle$. In the vacuum state $|\alpha\rangle$ the transition rate between the states $|E_i\rangle$ and $|E_j\rangle$ may be evaluated in perturbation theory (see, e.g. the review

[7] It turns out to correspond to the in vacuum discussed below.

[65])

$$\dot{P}_\alpha(E_i \to E_j) = |m_{ij}|^2 \int_{-\infty}^{\infty} dt\, e^{-i\Delta E t}\, G_\alpha\left(x(t), x(0)\right) \tag{3.26}$$

where $\Delta E = E_j - E_i$.

First, let us study particle production in the Euclidean vacuum. For two time-like separated points x and x' we have $P(x,x') = \cosh t$ and $P(x_A, x') = -\cosh t$, where t is the proper time between x and x'. We take t to be positive (negative) if x is in the future (past) light cone of x'. As a function of t, the appropriate $i\epsilon$ prescription for the Wightman function is

$$G_E(x,x') = G_E(t - i\epsilon) \tag{3.27}$$

indicating that for positive (negative) t we should go under (over) the branch cut from $P = 1$ to $P = \infty$ in (3.9). As a function in the complex t plane G_E obeys

$$G_E(t) = G_E(-t - 2\pi i). \tag{3.28}$$

$$G_E^*(t) = G_E(\bar{t} - 2\pi i). \tag{3.29}$$

To evaluate $G_E(x', x)$ we must take $t \to -t$

$$G_E(x', x) = G_E(-t - i\epsilon) = G_E(t + i\epsilon - 2\pi i). \tag{3.30}$$

Similarly, we may evaluate

$$G_E(x, x'_A) = G_E(x_A, x') = G_E(t - i\pi). \tag{3.31}$$

The points x and x'_A are spacelike separated, so it is not necessary to insert an $i\epsilon$.

Let us consider the example of $d = 3$. As a function of t, the Green function (3.9) has singularities at $t = n\pi i$ for all $n \neq -1$. This may be seen from the alternate form of the Green function presented in Appendix A. Thus in the evaluating (3.26) we may deform the contour of integration in the complex t plane

$$\begin{aligned} \int_{-\infty}^{\infty} dt e^{-i\Delta E t} G_E(t - i\epsilon) &= e^{-\pi\Delta E} \int_{-\infty}^{\infty} dt e^{-i\Delta E t} G_E(t - i\pi) \\ &= e^{-2\pi\Delta E} \int_{-\infty}^{\infty} dt e^{-i\Delta E t} G_E(t - 2\pi i + i\epsilon). \end{aligned} \tag{3.32}$$

The $e^{-\epsilon E}$ terms have been dropped. Using (3.28) and the second line of (3.32) we find that the detector response rate (3.26) obeys

$$\frac{\dot{P}_E(E_i \to E_j)}{\dot{P}_E(E_j \to E_i)} = e^{-2\pi\Delta E} \tag{3.33}$$

in the Euclidean vacuum. This is the condition of detailed balance for a thermal system at the de Sitter temperature

$$T_{dS} = \frac{1}{2\pi}. \tag{3.34}$$

For a general vacuum state $|\alpha\rangle$ we may use the identities (3.32) to relate the integrals of all four terms in (3.24). We find

$$\int_{-\infty}^{\infty} dt e^{-i\Delta E t} G_\alpha(t - i\epsilon) = N_\alpha^2 |1 + e^{\alpha + \pi\Delta E}|^2 \int_{-\infty}^{\infty} dt e^{-i\Delta E t} G_E(t - i\epsilon). \tag{3.35}$$

So the ratio (3.33) becomes[8]

$$\frac{\dot{P}_\alpha(E_i \to E_j)}{\dot{P}_\alpha(E_j \to E_i)} = e^{-2\pi\Delta E} \left| \frac{1 + e^{\alpha + \pi\Delta E}}{1 + e^{\alpha - \pi\Delta E}} \right|^2. \tag{3.36}$$

We conclude that the detector response is not thermal. In general the detector will not equilibrate. Even though the ratio (3.36) is non-zero, we will see in the next section that there are vacua for which, in a certain sense, there is no particle creation.

4. The Sphere

In this section we study scalar field theory on dS_d in global coordinates (τ, Ω). The metric is

$$ds^2 = -d\tau^2 + \cosh^2 \tau \, d\Omega_{d-1}^2, \tag{4.1}$$

where $d\Omega_{d-1}^2$ is the usual metric on S^{d-1}, parameterized by the coordinates Ω. A important feature of these coordinates is that they cover all of dS_d and hence are suited to a global description of the quantum state.

[8] This expression was obtained for the case of a scalar with conformal mass in [62].

4.1. Solutions of the Wave Equation

In this subsection we find solutions to the massive wave equation

$$(\nabla^2 - m^2)\phi = 0. \tag{4.2}$$

This differential equation is separable, with solutions

$$\phi = y_L(\tau) Y_{Lj}(\Omega). \tag{4.3}$$

The Y_{Lj} are spherical harmonics on S^{d-1} obeying

$$\nabla^2_{S^{d-1}} Y_{Lj} = -L(L+d-2) Y_{Lj}. \tag{4.4}$$

Here L is a non-negative integer and j is a collective index $(j_1, \ldots, j_{d-2})$. We will use a non-standard choice of Y_{Lj}'s, with

$$Y_{Lj}(\Omega_A) = Y^*_{Lj}(\Omega) = (-)^L Y_{Lj}(\Omega). \tag{4.5}$$

Here Ω_A denotes the point on S^{d-1} antipodal to Ω. In terms of the usual spherical harmonics S_{Lj},

$$Y_{Lj} = \sqrt{\frac{i}{2}}\, S_{Lj} + (-)^L \sqrt{\frac{-i}{2}}\, S^*_{Lj}. \tag{4.6}$$

The functions Y_{Lj} are orthonormal,

$$\int d\Omega\, Y_{Lj}(\Omega) Y^*_{L'j'}(\Omega) = \delta_{LL'}\delta_{jj'}, \tag{4.7}$$

and complete,

$$\sum_{Lj} Y_{Lj}(\Omega) Y^*_{Lj}(\Omega') = \delta^{d-1}(\Omega, \Omega'). \tag{4.8}$$

We then have

$$\ddot{y}_L + (d-1)\tanh\tau \dot{y}_L + \left[m^2 + \frac{L(L+d-2)}{\cosh^2\tau}\right] y_L = 0. \tag{4.9}$$

In terms of the coordinate $\sigma = -e^{2\tau}$ this becomes

$$\sigma(1-\sigma)y_L'' + \left[(1-\frac{d-1}{2}) - (1+\frac{d-1}{2})\sigma\right] y_L' + \left[\frac{m^2}{4}\frac{1-\sigma}{\sigma} - \frac{L(L+d-2)}{1-\sigma}\right] y_L = 0. \tag{4.10}$$

Let us make the substitution

$$y_L^{\rm in} = \cosh^L \tau \, e^{(L+\frac{d-1}{2}-i\mu)\tau} x. \tag{4.11}$$

With

$$\mu = \sqrt{m^2 - \frac{(d-1)^2}{4}}, \tag{4.12}$$

equation (4.10) becomes a hypergeometric equation for x,

$$\sigma(1-\sigma)x'' + [c - (1+a+b)\sigma]\, x' - abx = 0, \tag{4.13}$$

with coefficients

$$a = L + \frac{d-1}{2}, \quad b = L + \frac{d-1}{2} - i\mu, \quad c = 1 - i\mu. \tag{4.14}$$

Let us consider the case of real positive μ, i.e., $2m > (d-1)$. We find that

$$y_L^{\rm in} = \frac{2^{L+d/2-1}}{\sqrt{\mu}} \cosh^L \tau e^{(L+\frac{d-1}{2}-i\mu)\tau} F(L+\frac{d-1}{2}, L+\frac{d-1}{2} - i\mu; 1-i\mu; -e^{2\tau}) \tag{4.15}$$

and its complex conjugate are two linearly independent solutions. The normalization is fixed by demanding that these modes are orthonormal with respect to the inner product (3.7), which is easily evaluated on $\mathcal{I}^-$.

4.2. In and Out Vacua

We now use the solutions (4.15) to construct in (out) vacua with no incoming (outgoing) particles, and find the Bogolyubov transformation relating them. Note that (4.9) is invariant under time reversal. Hence we obtain another pair of linearly independent solutions by defining

$$y_L^{\rm out}(\tau) = y_L^{\rm in *}(-\tau). \tag{4.16}$$

Explicitly,

$$y_L^{\rm out} = \frac{2^{L+d/2-1}}{\sqrt{\mu}} \cosh^L \tau e^{(-L-\frac{d-1}{2}-i\mu)\tau} F(L+\frac{d-1}{2}, L+\frac{d-1}{2}+i\mu; 1+i\mu; -e^{-2\tau}). \tag{4.17}$$

At the past boundary ($\tau \to -\infty$) we find that $F \to 1$ and hence

$$y_L^{\rm in} \to \frac{2^{d/2-1}}{\sqrt{\mu}} e^{(\frac{d-1}{2}-i\mu)\tau} \tag{4.18}$$

while at the future boundary ($\tau \to \infty$)

$$y_L^{\rm out} \to \frac{2^{d/2-1}}{\sqrt{\mu}} e^{-(\frac{d-1}{2}+i\mu)\tau}. \tag{4.19}$$

Thus we see that the modes

$$\begin{aligned} \phi_{Lj}^{\rm in}(x) &= y_L^{\rm in}(\tau) Y_{Lj}(\Omega) \\ \phi_{Lj}^{\rm out}(x) &= y_L^{\rm out}(\tau) Y_{Lj}(\Omega). \end{aligned} \tag{4.20}$$

are positive frequency modes with respect to the global time τ near the asymptotic past and future boundaries, respectively. They represent incoming and outgoing particle states. They define two vacua, $|{\rm in}\rangle$ and $|{\rm out}\rangle$, which are annihilated by the lowering operators associated to $\phi^{\rm in}$ and $\phi^{\rm out}$, respectively. Physically, $|{\rm in}\rangle$ is the state with no incoming particles on $\mathcal{I}^-$ and $|{\rm out}\rangle$ is the state with no outgoing particles on $\mathcal{I}^+$.

The Bogolyubov coefficients relating the two sets of modes can be found by using the hypergeometric transformation equations (summarized in Appendix B) and (4.5). One finds

$$\phi_{Lj}^{\rm in} = A e^{-2i\theta_L} \phi_{Lj}^{\rm out} + iB \phi_{Lj}^{{\rm out}*}. \tag{4.21}$$

where

$$A = \begin{cases} 1, & \text{d odd} \\ \coth \pi\mu, & \text{d even} \end{cases}, \qquad B = \begin{cases} 0, & \text{d odd} \\ (-)^{\frac{d}{2}} \operatorname{csch} \pi\mu, & \text{d even} \end{cases}; \tag{4.22}$$

we have isolated the phase

$$e^{-2i\theta_L} = (-)^{L-\frac{d-1}{2}} \frac{\Gamma(-i\mu)\Gamma(L+\frac{d-1}{2}+i\mu)}{\Gamma(i\mu)\Gamma(L+\frac{d-1}{2}-i\mu)} \tag{4.23}$$

for later convenience. The coefficients obey $|A|^2 - |B|^2 = 1$ as required for properly normalized modes.

Note that B, the coefficient mixing positive and negative frequency modes, vanishes in odd dimensions. This implies that the two sets of modes define the same vacuum:

$$|\text{in}\rangle = |\text{out}\rangle \qquad \text{in odd dimensions.} \tag{4.24}$$

Hence, there is no particle production. If no particles are coming in from $\mathcal{I}^-$, no particles will go out on $\mathcal{I}^+$.[9] This is in contrast to the even-dimensional case for which there is always some particle production.

From (4.18) it follows that $\phi^{\text{in}}_{Lj} \sim e^{h-\tau}$ near $\mathcal{I}^-$. In the language of [16], this implies the modes ϕ^{in} are dual to operators of weight h_+ on the boundary. Likewise, $\phi^{\text{in}*}$ are dual to operators of weight h_-. The de Sitter transformations act on the boundary theory as global conformal transformations, which do not mix operators of different weight. We conclude that ϕ^{in} and $\phi^{\text{in}*}$ do not mix under the de Sitter group, so the states $|\text{in}\rangle$ and $|\text{out}\rangle$ are de Sitter invariant.

It is convenient to define the rescaled global modes

$$\begin{aligned} \tilde{\phi}^{\text{in}}_{Lj}(x) &= e^{i\theta_L} y^{\text{in}}_L(\tau) Y_{Lj}(\Omega) \\ \tilde{\phi}^{\text{out}}_{Lj}(x) &= e^{-i\theta_L} y^{\text{out}}_L(\tau) Y_{Lj}(\Omega). \end{aligned} \tag{4.25}$$

This is a trivial phase shift, so $|\text{in}\rangle$ and $|\text{out}\rangle$ are the states annihilated by the lowering operators associated to $\tilde{\phi}^{\text{in}}$ and $\tilde{\phi}^{\text{out}}$, respectively. In this basis the Bogolyubov transformation

$$\tilde{\phi}^{\text{in}}_{Lj}(x) = A\tilde{\phi}^{\text{out}}_{Lj}(x) + iB\tilde{\phi}^{\text{out}*}_{Lj}(x) \tag{4.26}$$

[9] Note however that according to (3.36) an Unruh detector still observes particles.

has the form of an MA transform, and so can be used to define additional de Sitter invariant vacua. The modes (4.25) have the useful property that for any point x

$$\tilde{\phi}^{\rm in}_{Lj}(x_A) = \tilde{\phi}^{\rm out\,*}_{Lj}(x) \tag{4.27}$$

where $x_A \sim (-\tau, \Omega_A)$ is the point antipodal to x. In odd dimensions this becomes

$$\tilde{\phi}^{\rm in}_{Lj}(x_A) = \tilde{\phi}^{\rm in}_{Lj}{}^{*}(x). \tag{4.28}$$

This implies that in odd dimensions the in vacuum is CPT invariant, whereas in even dimensions CPT interchanges in and out.

4.3. The Euclidean Vacuum

In this subsection we construct the Euclidean vacuum $|E\rangle$ in the basis of spherical modes.

The Lorentzian de Sitter geometry (4.1) can be continued to Euclidean signature by taking τ to run along the imaginary τ axis, from $\tau = -\frac{i\pi}{2}$ to $\tau = \frac{i\pi}{2}$. The resulting geometry is a round d-sphere. We define the upper (lower) Euclidean hemisphere as the portion of this path that lies in the upper (lower) complex τ plane. In particular, the upper (lower) Euclidean pole lies at $\tau = \frac{i\pi}{2}$ ($\tau = -\frac{i\pi}{2}$).

We define positive frequency Euclidean modes to be those that are regular when analytically continued to the lower Euclidean hemisphere. In this subsection we find these modes in global coordinates. The Euclidean vacuum $|E\rangle$ is the state that is annihilated by the positive frequency Euclidean modes.

We may rewrite (4.10) in terms of the variable $z = 1 - \sigma = 1 + e^{2\tau}$, which is well suited to analyzing the behavior of global modes on the Euclidean geometry. Upon substituting

$$y^E_L = \cosh^L \tau \, e^{(L + \frac{d-1}{2} + i\mu)\tau} x, \tag{4.29}$$

we obtain the hypergeometric equation

$$z(1-z)\frac{d^2x}{dz^2} + [\hat{c} - (1 + a + b^*)\sigma]\frac{dx}{dz} - ab^* x = 0, \tag{4.30}$$

with positive integer coefficient

$$\hat{c} = 2L + d - 1. \tag{4.31}$$

We find the general solution

$$x = CU_1 + DU_2 \tag{4.32}$$

where

$$U_1 = F(L + \frac{d-1}{2}, L + \frac{d-1}{2} + i\mu; 2L + d - 1; z). \tag{4.33}$$

The second solution is given by

$$U_2 = z^{2-2L-d} F(1 - L - \frac{d-1}{2}, 1 + i\mu - L - \frac{d-1}{2}; 3 - 2L - d; z) \tag{4.34}$$

if d is odd, and by

$$U_2 = U_1 \ln z + \sum_{k=2-2L-d}^{\infty} Q_k z^k \tag{4.35}$$

if d is even; the coefficients Q_k are found, e.g., in [66].

The Lorentzian geometry lies on the path from $z = 1$ ($\mathcal{I}^-$) along the real z axis to $z = +\infty$ ($\mathcal{I}^+$). On the throat, at $z = 2$, it intersects with the Euclidean geometry, which lies on a unit circle centered at $z = 1$. The lower (upper) hemisphere corresponds to the lower (upper) half-circle. The Euclidean poles are at $z = 0$. The functions (4.32) have a branch cut from $z = 1$ to $z = +\infty$. Hence, they are not analytic on the whole Euclidean sphere. By choosing the Lorentzian path to run just below the real axis ($z \to z - i\epsilon$), we obtain solutions that are analytic on the lower hemisphere and the entire Lorentzian geometry.

The first solution (4.33) is regular in these regions, whereas the second solution, (4.34) or (4.35), becomes singular at the lower Euclidean pole, at $z = 0 - i\epsilon$. Hence we discard the second set of modes and keep the first. The modes can be analytically continued through the branch cut to the upper hemisphere, where they are not expected to be regular.

The normalized Euclidean modes are

$$\phi^E_{Lj}(x) = \frac{1}{f_L\sqrt{e^{2\pi\mu}-1}} y^E_L(\tau) Y_{Lj}(\Omega) \tag{4.36}$$

where

$$\begin{aligned} y^E_L &= \frac{2^{L+d/2-1} i^{-L+\frac{d-1}{2}}}{\sqrt{\mu}} \cosh^L \tau e^{(L+\frac{d-1}{2}+i\mu)\tau} \\ &\qquad F(L+\frac{d-1}{2}, L+\frac{d-1}{2}+i\mu; 2L+d-1; 1+e^{2\tau}) \\ f_L &= \frac{\Gamma(2L+d-1)}{\Gamma(L+\frac{d-1}{2})} \left| \frac{\Gamma(i\mu)}{\Gamma(L+\frac{d-1}{2}-i\mu)} \right| \end{aligned} \tag{4.37}$$

The Euclidean Green function (3.9) is then given by the mode sum

$$G_E(x,x') = \sum_{L,j} \phi^E_{Lj}(x) \phi^{E*}_{Lj}(x'). \tag{4.38}$$

This expression was given in the four-dimensional case in [43].

4.4. The $|E\rangle \to |\text{in}\rangle$ Transformation

In this subsection we show that the Euclidean and in vacua are MA transforms of each other.

Let us again specialize to the case of $2m > (d-1)$. The y^E are then related to the y^{in} by

$$y^E_L = f_L \left((-)^{L+\frac{d-1}{2}} e^{-i\theta_L} y^{\text{in}*}_L + e^{\pi\mu + i\theta_L} y^{\text{in}}_L \right). \tag{4.39}$$

So the Euclidean modes are related to the global modes by

$$\phi^E_{Lj} = \frac{1}{\sqrt{1-e^{-2\pi\mu}}} \left(\tilde{\phi}^{\text{in}}_{Lj} + (-)^{\frac{d-1}{2}} e^{-\pi\mu} \tilde{\phi}^{\text{in}\,*}_{Lj} \right). \tag{4.40}$$

from which it follows, along with (4.28) and (4.26), that

$$\phi^E_{Lj}(x_A) = \phi^{E\,*}_{Lj}(x) \tag{4.41}$$

in any dimension. This implies the Euclidean vacuum is CPT invariant.

Now, (4.40) may be inverted to give

$$\tilde{\phi}^{\rm in}_{Lj} = \frac{1}{\sqrt{1-e^{-2\pi\mu}}}\left(\phi^E_{Lj} + (-)^{\frac{d+1}{2}} e^{-\pi\mu}\phi^{E\,*}_{Lj}\right) \tag{4.42}$$

which is an MA transformation with

$$\alpha = -\pi\mu + i\left(\frac{d+1}{2}\right)\pi. \tag{4.43}$$

We have thus identified the MA transformation relating the $|{\rm in}\rangle$ vacuum and the Euclidean vacuum $|E\rangle$.

5. CFT Interpretation

In this section we interpret the CPT invariant (real α) family of bulk de Sitter invariant vacua as a line of marginal deformations of the boundary CFT. A similar interpretation may extend to the the case of general complex α but we do not pursue it here. In this and later sections we restrict to the case $d = 3$.

5.1. $\mathcal{I}^{\pm}$ Correlators

In this subsection we evaluate the various Green functions appearing on the right hand side of (3.24) for x and x' on $\mathcal{I}^{\pm}$, and then put the results together to see how the boundary values of the correlators depend on α. We use global coordinates (τ, σ), $\sigma = (w, \bar{w})$, where $w = \tan\frac{\theta}{2}e^{i\varphi}$ is the complex coordinate on the 2-sphere, so that

$$ds^2 = -d\tau^2 + 4\cosh^2\tau\frac{dwd\bar{w}}{(1+w\bar{w})^2}. \tag{5.1}$$

The behavior of the correlators at $\mathcal{I}^{\pm}$ follows from the asymptotic form of the hypergeometric functions. As $|z| \to \infty$ one has (see Appendix B)

$$\begin{aligned} F(h_+, h_-; \frac{3}{2}; z) &\to c_+(-z)^{-h_+} + c_-(-z)^{-h_-}, \\ c_\pm &= \frac{\Gamma(\frac{3}{2})\Gamma(h_\mp - h_\pm)}{\Gamma(h_\mp)\Gamma(\frac{3}{2} - h_\pm)}. \end{aligned} \tag{5.2}$$

This expression is not in general real (unless z is real and negative) because the $h_\pm = 1 \pm i\mu$ are not real. In spherical coordinates one finds near $\mathcal{I}^-$

$$\lim_{\tau,\tau'\to-\infty} P(\tau,\sigma;\tau',\sigma') = -\frac{e^{-\tau-\tau'}|w-w'|^2}{2(1+w\bar{w})(1+w'\bar{w}')}. \tag{5.3}$$

For $x = (\tau,\sigma)$ and $x' = (\tau',\sigma')$ both on $\mathcal{I}^-$

$$\lim_{\tau,\tau'\to-\infty} G_E(x,x') = e^{h_+(\tau+\tau')}\Delta_+(\sigma;\sigma') + e^{h_-(\tau+\tau')}\Delta_-(\sigma;\sigma'). \tag{5.4}$$

$\Delta_\pm$ here is proportional to the two point function for a conformal field of dimension $h_\pm$ on the sphere:

$$\Delta_\pm(\sigma;\sigma') = 4^{h_\pm} c_{m,d} c_\pm \Big[\frac{(1+w\bar{w})(1+w'\bar{w}')}{|w-w'|^2}\Big]^{h_\pm}. \tag{5.5}$$

We note that $G_E(x,x') = G_E(x',x)$ on $\mathcal{I}^-$ as the points are spacelike separated. We have assumed here, and in the following expressions (unless explicitly stated) that x and x' are not coincident so that contact terms can be ignored.

Let us now consider the case where x is on $\mathcal{I}^-$ and x' is on $\mathcal{I}^+$. Since the antipodal point to x', namely $x'_A = (-\tau',\sigma'_A) = (-\tau',-\frac{1}{\bar{w}'},-\frac{1}{w'})$, is on $\mathcal{I}^-$ we may use (5.4) and the formula

$$P(x,x') = -P(x,x'_A). \tag{5.6}$$

In continuing (5.4) to positive P we must take care to go above the branch cut, in accord with the $i\epsilon$ presription for the Wightman function with $\tau' > \tau$. We find

$$\lim_{\substack{\tau\to-\infty\\ \tau'\to\infty}} G_E(x,x') = -e^{h_+(\tau-\tau')}e^{-\pi\mu}\Delta_+(\sigma;\sigma'_A) - e^{h_-(\tau-\tau')}e^{\pi\mu}\Delta_-(\sigma;\sigma'_A). \tag{5.7}$$

To evaluate $G_E(x',x)$ we must go under the branch cut, yielding

$$\lim_{\substack{\tau\to-\infty\\ \tau'\to\infty}} G_E(x',x) = -e^{h_+(\tau-\tau')}e^{\pi\mu}\Delta_+(\sigma;\sigma'_A) - e^{h_-(\tau-\tau')}e^{-\pi\mu}\Delta_-(\sigma;\sigma'_A). \tag{5.8}$$

Now we insert these results into formula (3.24) for the Wightman function in the general vacuum state $|\alpha\rangle$. For both points on $\mathcal{I}^-$ one finds

$$\begin{aligned}\lim_{\tau,\tau'\to-\infty} G_\alpha(x,x') = {} & N_\alpha^2(1-e^{\alpha+\pi\mu})(1-e^{\alpha^*-\pi\mu})e^{h_+(\tau+\tau')}\Delta_+(\sigma;\sigma') \\ & + N_\alpha^2(1-e^{\alpha-\pi\mu})(1-e^{\alpha^*+\pi\mu})e^{h_-(\tau+\tau')}\Delta_-(\sigma;\sigma').\end{aligned} \tag{5.9}$$

On the other hand for x on $\mathcal{I}^-$ and x' on $\mathcal{I}^+$ we get

$$\begin{aligned}\lim_{\substack{\tau\to-\infty\\ \tau'\to\infty}} G_\alpha(x,x') = &- N_\alpha^2 e^{-\pi\mu}|1-e^{\alpha+\pi\mu}|^2 e^{h_+(\tau-\tau')}\Delta_+(\sigma;\sigma'_A)\\ &- N_\alpha^2 e^{\pi\mu}|1-e^{\alpha-\pi\mu}|^2 e^{h_-(\tau-\tau')}\Delta_-(\sigma;\sigma'_A).\end{aligned} \tag{5.10}$$

We see that the boundary correlators depend nontrivially on the choice of vacuum. Since we have taken $|P|\to\infty$, these formulae are valid only for non-coincident points on $\mathcal{I}^\pm$ and omit possible contact terms.

Let us now turn to the interesting special case of the in vacuum, which has $\alpha=-\pi\mu$. For both points on $\mathcal{I}^-$ it follows from (5.9) that the correlators vanish! On the other hand, for x on $\mathcal{I}^-$ and x' on $\mathcal{I}^+$ we get

$$\begin{aligned}\lim_{\substack{\tau\to-\infty\\ \tau'\to\infty}} G_{\rm in}(x,x') &= -2\sinh\pi\mu\, e^{h_-(\tau-\tau')}\Delta_-(\sigma;\sigma'_A),\\ \lim_{\substack{\tau\to-\infty\\ \tau'\to\infty}} G_{\rm in}(x',x) &= -2\sinh\pi\mu\, e^{h_+(\tau-\tau')}\Delta_+(\sigma;\sigma'_A).\end{aligned} \tag{5.11}$$

When the points on $\mathcal{I}^-$ coincide there is a contact term which can be easily computed by noting that the Wightman function on $\mathcal{I}^-$ reduces to a mode sum over spherical harmonics. This gives

$$\lim_{\tau,\tau'\to-\infty} G_{\rm in}(x,x') = \frac{2}{\mu} e^{h_-\tau+h_+\tau'}\delta^2(\sigma,\sigma'). \tag{5.12}$$

The situation can be described as follows. As $\mathcal{I}^-$ is approached, the spatial part of the scalar kinetic terms are exponentially supressed relative to the rest of the action. Neighboring points decouple and the theory becomes ultralocal. It reduces to a harmonic oscillator at each point; hence the vanishing of $G_{\rm in}$. However, the map defined by propagation from $\mathcal{I}^-$ to $\mathcal{I}^+$ is not ultralocal on the sphere. It introduces nontrivial correlators when one point is on $\mathcal{I}^-$ and the other is on $\mathcal{I}^+$.

Of course, in other vacua—such as the Euclidean vacuum—there are nontrivial $\mathcal{I}^-$ correlators. As will be seen in the next subsection, the wave functions for these vacua differ from the in vacuum wavefunction by terms which are nonlocal on $\mathcal{I}^-$. These terms are directly responsible for the nontrivial $\mathcal{I}^-$ correlators.

5.2. dS Vacua as Marginal CFT Deformations

Now we argue that the dual interpretation of the one-parameter family of dS_3 vacua is a one-parameter family of marginal deformations of the CFT. It is convenient to define operators on $\mathcal{I}^-$ and $\mathcal{I}^+$ by

$$\begin{aligned}\lim_{\tau\to-\infty}\phi(\tau,\sigma) &= \phi_+^{\rm in}(\sigma)e^{h_+\tau}+\phi_-^{\rm in}(\sigma)e^{h_-\tau},\\ \lim_{\tau\to\infty}\phi(\tau,\sigma_A) &= \phi_+^{\rm out}(\sigma)e^{-h_+\tau}+\phi_-^{\rm out}(\sigma)e^{-h_-\tau}.\end{aligned} \tag{5.13}$$

$\phi_\pm^{\rm out}$ has been defined with an antipodal inversion relative to $\phi_\pm^{\rm in}$ so that they transform the same way under conformal transformations [16]. These are position space versions of the creation operators associated to the spherical modes $\phi^{\rm in}$ and $\phi^{\rm out}$,

$$\begin{aligned}\phi_+^{\rm in}(\sigma) = (\phi_-^{\rm in}(\sigma))^\dagger &= \sqrt{\frac{2}{\mu}}\sum_{Lj} a_{Lj}^{\rm in\,\dagger}\, Y_{Lj}^*(\sigma)\\ \phi_+^{\rm out}(\sigma) = (\phi_-^{\rm out}(\sigma))^\dagger &= \sqrt{\frac{2}{\mu}}\sum_{Lj} a_{Lj}^{\rm out}\, Y_{Lj}(\sigma_A)\end{aligned} \tag{5.14}$$

From the asymptotic Green functions (5.12) and (5.11) we find that the only non-zero commutators are

$$\begin{aligned}[\phi_-^{\rm in}(\sigma),\phi_+^{\rm in}(\sigma')] = [\phi_+^{\rm out}(\sigma),\phi_-^{\rm out}(\sigma')] &= \frac{2}{\mu}\delta^2(\sigma,\sigma'),\\ [\phi_\pm^{\rm in}(\sigma),\phi_\pm^{\rm out}(\sigma')] &= \pm 2\sinh\pi\mu\,\Delta_\pm(\sigma,\sigma').\end{aligned} \tag{5.15}$$

The in and out operators are related by a Bogolyubov transformation and hence are not independent. In this subsection we take $\phi_\pm^{\rm in}$ to be the fundamental operators. At a general point in the bulk ϕ is determined from its value on $\mathcal{I}^-$ via

$$\phi(x) = i\int_{\mathcal{I}^-} d^2x'\sqrt{g}\,G_C(x,x')\overleftrightarrow{\partial}_{\tau'}\phi(x'). \tag{5.16}$$

In particular, taking x to be on $\mathcal{I}^+$ and using the limiting expression for G_C (which does not depend on α) we find

$$\phi_\pm^{\rm out}(\sigma) = -\mu\sinh\pi\mu\int d^2\sigma'\Delta_\pm(\sigma,\sigma')\,\phi_\mp^{\rm in}(\sigma'). \tag{5.17}$$

This is a position-space version of the Bogolyubov transformation (4.21).[10] We see that the absence of mixing between $\phi^{\rm in}$ and $\phi^{\rm out*}$, which seemed so surprising in section 3.2, follows directly from the asymptotic behavior of the Green functions. We note parenthetically that this implies the identity (verified in [67])

$$(\mu \sinh \pi\mu)^2 \int d^2\sigma'' \Delta_-(\sigma,\sigma'')\Delta_+(\sigma'',\sigma') = \delta^2(\sigma,\sigma'). \tag{5.18}$$

The $|{\rm in}\rangle$ vacuum obeys

$$\phi^{\rm in}_-(\sigma)|{\rm in}\rangle = 0. \tag{5.19}$$

The general $|\alpha\rangle$ vacuum state discussed in section 2.2 can be constructed in terms of the in vacuum as

$$|\alpha\rangle = \exp\left\{c(\gamma)\frac{\mu}{2}\int d^2\sigma\, \phi^{\rm in}_+\phi^{\rm out}_- - c(\bar\gamma)\frac{\mu}{2}\int d^2\sigma\, \phi^{\rm in}_-\phi^{\rm out}_+\right\}|{\rm in}\rangle, \tag{5.20}$$

where

$$e^\gamma = \frac{\sinh\frac{\pi\mu+\alpha}{2}}{\sinh\frac{\pi\mu-\alpha}{2}}, \tag{5.21}$$

and the function c is given by (3.19). This equation may be formally rewritten as

$$|\alpha\rangle = C\exp\left(e^{\gamma^*}\frac{\mu}{4}\int d^2\sigma\, \phi^{\rm in}_+\phi^{\rm out}_-\right)|{\rm in}\rangle. \tag{5.22}$$

These vacua obey the manifestly $SL(2,C)$ invariant condition

$$\phi^{\rm in}_-(\sigma)|\alpha\rangle = -e^{\gamma^*}\phi^{\rm out}_-(\sigma)|\alpha\rangle. \tag{5.23}$$

This is most easily seen by applying the representation $\phi^{\rm in}_- = -\frac{2}{\mu}\frac{\delta}{\delta\phi^{\rm in}_+}$ of (5.15) to (5.22). In particular, the Euclidean vacuum has $\alpha = -\infty$ and therefore obeys

$$\phi^{\rm in}_-(\sigma)|E\rangle = e^{-\pi\mu}\phi^{\rm out}_-(\sigma)|E\rangle. \tag{5.24}$$

[10] In fact, expression (5.17) is singular for $\sigma = \sigma'$ and so is really defined by (4.21).

Now we consider the boundary field theory. Consider the two operators $\mathcal{O}_\pm$ dual to $\phi^{\rm in}_\mp$ with conformal weights $h_\pm$. According to the dS/CFT correspondence [16], the dual $\mathcal{O}_\pm$ correlators are determined from the $\phi^{\rm in}_\pm$ correlator (5.9) as

$$\langle\alpha|\mathcal{O}_\pm(\sigma)\mathcal{O}_\pm(\sigma')|\alpha\rangle = -\frac{\mu^2}{4}N_\alpha^2(1-e^{\alpha\pm\pi\mu})(1-e^{\alpha^*\mp\pi\mu})\Delta_\pm(\sigma,\sigma'). \tag{5.25}$$

The commutators (5.15) also imply the contact terms

$$\begin{aligned}\langle\alpha|\mathcal{O}_-(\sigma)\mathcal{O}_+(\sigma')|\alpha\rangle &= \frac{1}{1-e^{\gamma+\gamma^*}}\,\frac{\mu}{2}\delta^2(\sigma,\sigma'),\\ \langle\alpha|\mathcal{O}_+(\sigma)\mathcal{O}_-(\sigma')|\alpha\rangle &= \frac{e^{\gamma+\gamma^*}}{1-e^{\gamma+\gamma^*}}\,\frac{\mu}{2}\delta^2(\sigma,\sigma').\end{aligned} \tag{5.26}$$

From the CFT point of view this is an unusual contact term prescription in that it depends on the operator ordering.

What is the CFT origin of the parameter α? Usually a one-parameter family of correlators corresponds to a line of marginal deformations generated by a dimension $(1,1)$ operator. Indeed, $\mathcal{O}_+\mathcal{O}_-$ is a dimension $(1,1)$ operator. Let us consider adding this operator to the two-dimensional CFT action with real coefficient λ. At linear order this perturbs the correlators according to the formula

$$\begin{aligned}\delta_\lambda\langle\alpha|\mathcal{O}_+(\sigma)\mathcal{O}_+(\sigma')|\alpha\rangle &= -\langle\alpha|\frac{\lambda}{2}\int d\sigma''\,\{\mathcal{O}_+(\sigma'')\mathcal{O}_-(\sigma''),\mathcal{O}_+(\sigma)\mathcal{O}_+(\sigma')\}\,|\alpha\rangle\\ &= -4\mu\lambda\coth\gamma\,\langle\alpha|\mathcal{O}_+(\sigma)\mathcal{O}_+(\sigma')|\alpha\rangle.\end{aligned} \tag{5.27}$$

Let's take α to be real, so that $\langle\alpha|\mathcal{O}_+\mathcal{O}_+|\alpha\rangle$ is a monotonically increasing function of α. Then the variation of the two point function as $\alpha\to\alpha+\epsilon$ is proportional to the deformation (5.27), which may be integrated to determine λ as a function of α.

This strongly suggests that the family of CPT and $SO(d,1)$ invariant vacuum states are marginal deformations of the boundary CFT generated by the $(1,1)$ operator $\mathcal{O}_+\mathcal{O}_-$. The two point functions of these CFTs can all be made equivalent by rescaling operators, except for the special case $\alpha=-\pi\mu$. So in principle from this analysis alone the CFTs with $\alpha\neq\pi\mu$ might all be equivalent. In order to complete

the argument one should check that the three point function is not invariant under such rescalings. This has been shown in [68].[11]

6. $\mathcal{CPT}$ and the Inner Product

In this section we discuss various choices of norm for the Hilbert space of a real scalar field on dS_3, or equivalently the definition of the adjoint. The first naive choice one might make is

$$\phi^\dagger(x) = \phi(x). \tag{6.1}$$

However Witten [20] argues that this choice may not be well-defined for full quantum gravity oustide of perturbation theory. An alternate norm is proposed [20] which involves path integral evolution form $\mathcal{I}^-$ to $\mathcal{I}^+$ together with $\mathcal{CPT}$ conjugation. In this section we will explicitly compute this norm for a free scalar and find, after a slight modification involving the form of $\mathcal{P}$, that it has a very natural boundary interpretation: it yields the Zamolodchikov metric for the boundary CFT.

Before delving into details it is instructive to recall an isomorphic discussion of norms which arises in the standard treatment of Euclidean CFT. Consider the mode expansion for a free boson on the Lorentzian cylinder (ignoring zero modes)

$$X(\sigma^+, \sigma^-) = i \sum_n \big(\frac{\alpha_n}{n} e^{-2\pi i n \sigma^+} + \frac{\bar{\alpha}_n}{n} e^{2\pi i n \sigma^-} \big). \tag{6.2}$$

Using $\alpha_{-n}^\dagger = \alpha_n$ one finds

$$X^\dagger(\sigma^+, \sigma^-) = X(\sigma^+, \sigma^-). \tag{6.3}$$

On the other hand, the standard mode expansion on the complex Euclidean plane is

$$X(z, \bar{z}) = i \sum_n \frac{1}{n} \big(\frac{\alpha_n}{z^n} + \frac{\bar{\alpha}_n}{\bar{z}^n} \big) \tag{6.4}$$

[11] We thank Greg Moore for discussions on this point.

Using $\alpha^\dagger_{-n} = \alpha_n$ one now finds

$$\begin{aligned} X^\dagger(z,\bar{z}) &= -i\sum_n \frac{1}{n}\left(\frac{\alpha_{-n}}{\bar{z}^n} + \frac{\bar{\alpha}_{-n}}{z^n}\right) \\ &= X(\frac{1}{\bar{z}}, \frac{1}{z}). \end{aligned} \tag{6.5}$$

In this case the adjoint relates X at points in the Euclidean plane reflected across the unit circle. In particular the norm of the state created by $X(z,\bar{z})$ or any other operator is just the two point function, and hence is the Zamolodchikov norm.

Returning now to dS_3, the naive adjoint rule (6.1) induces an adjoint in the Euclidean boundary CFT of the form $X^\dagger(z,\bar{z}) = X(z,\bar{z})$. On the other hand we will show that the modified Witten adjoint gives precisely (6.5). We further consider the dS_3 $SL(2,C)$ isometry generators $\mathcal{L}_n$, $\bar{\mathcal{L}}_n$, for $n = 0, \pm 1$. It is shown that $\mathcal{L}_n^\dagger = \bar{\mathcal{L}}_n$ for the naive adjoint, but $\mathcal{L}_n^\dagger = \mathcal{L}_{-n}$ for the modified adjoint.

Although we take $d = 3$, much of the following discussion carries over simply to higher dimensions.

6.1. Continuous and Discrete Symmetries of de Sitter Space

dS_3 can be represented by the hyberboloid

$$X^+X^- + z\bar{z} = \ell^2 \tag{6.6}$$

in flat Minkowski space. The isometries of dS_3 are then inherited from the $SL(2,C)$ Lorentz isometries of Minkowski space. The six generators can be written as combinations $\vec{J} + i\vec{K}$ of rotations and boosts together with their complex conjugates. We denote the associated Killing vectors by ζ_n and $\bar{\zeta}_n$ for $n = 0, \pm 1$. The past and future horizons of an observer worldline at $z = 0$ are located on the hyperboloid at $X^+X^- = 0$. We denote the Killing vectors preserving this horizon as

$$\begin{aligned} \zeta_0 + \bar{\zeta}_0 &= X^+\partial_+ - X^-\partial_-, \\ \zeta_0 - \bar{\zeta}_0 &= \bar{z}\partial_{\bar{z}} - z\partial_z. \end{aligned} \tag{6.7}$$

The four additional Killing vectors are

$$\begin{aligned}
\zeta_1 &= X^+\partial_z - \bar{z}\partial_-, \\
\zeta_{-1} &= X^-\partial_{\bar{z}} - z\partial_+, \\
\bar{\zeta}_1 &= X^+\partial_{\bar{z}} - z\partial_-, \\
\bar{\zeta}_{-1} &= X^-\partial_z - \bar{z}\partial_+.
\end{aligned} \tag{6.8}$$

They obey the Lie bracket relation

$$[\zeta_m, \zeta_n] = (n-m)\zeta_{m+n}. \tag{6.9}$$

In addition, we consider the two discrete symmetries parity and time reversal

$$\begin{aligned}
PX^\pm &= X^\pm, \qquad Pz = -z, \\
TX^\pm &= X^\mp, \qquad Tz = z.
\end{aligned} \tag{6.10}$$

In terms of the global coordinates (τ, Ω), P takes a point $\Omega = (\theta, \varphi)$ on the 2-sphere to the point $P\Omega = (\theta, \pi + \varphi)$ and T takes τ to $-\tau$.

Our choice of parity P in (6.10) reflects all the coordinates about an observer at the south pole. An alternate choice is $Pz = \bar{z}$ which reflects only one coordinate. This is the choice employed in [20], motivated by the fact that the corresponding $\mathcal{CPT}$ operation is known to be an exact field theory symmetry, after taking a flat space limit of dS_3. We shall indicate below how the results are modified if this definition of P is employed.

6.2. $\mathcal{CPT}$

We now compute the action of the discrete symmetries $\mathcal{C}$, $\mathcal{P}$ and $\mathcal{T}$ on the field operators.

We consider a real scalar field so that $\mathcal{C}$ is trivial. We wish to find Hilbert space operators $\mathcal{P}$ and $\mathcal{T}$ that implement (6.10) on $\phi(x)$ as

$$\mathcal{P}\phi(x)\mathcal{P} = \phi(Px), \qquad \mathcal{T}\phi(x)\mathcal{T} = \phi(Tx). \tag{6.11}$$

As usual $\mathcal{T} = UK$ is an antilinear operator which combines a unitary operator U with complex conjugation K of functions.

The mode expansions for ϕ in terms of the $\phi^{\rm in}$ and $\phi^{\rm out}$ modes are

$$\phi(\tau,\sigma) = \sum_{L,j} \big(a^{\rm in}_{Lj} y^{\rm in}_L(\tau) Y_{Lj}(\Omega) + b^{\rm in}_{Lj} y^{\rm in*}_L(\tau) Y^*_{Lj}(\Omega) \big) \tag{6.12}$$

$$\phi(\tau,\sigma) = \sum_{L,j} \big(a^{\rm out}_{Lj} y^{\rm out}_L(\tau) Y_{Lj}(\Omega) + b^{\rm out}_{Lj} y^{\rm out*}_L(\tau) Y^*_{Lj}(\Omega) \big) \tag{6.13}$$

We have written lowering and raising operators as a's and b's, respectively, and are not assuming here that $a^\dagger = b$.

We define the action of $\mathcal{P}$ by

$$\mathcal{P} a^{\rm in}_{Lj} \mathcal{P} = (-)^j a^{\rm in}_{Lj}, \qquad\qquad \mathcal{P} b^{\rm in}_{Lj} \mathcal{P} = (-)^j b^{\rm in}_{Lj} \tag{6.14}$$

and similarly for the out operators. Since $Y_{Lj}(P\Omega) = (-)^j Y_{Lj}(\Omega)$ this definition reproduces (6.11). We define the action of $\mathcal{T}$ by

$$\mathcal{T} a^{\rm in}_{Lj} \mathcal{T} = (-)^L a^{\rm out}_{Lj}, \qquad \mathcal{T} b^{\rm in}_{Lj} \mathcal{T} = (-)^L b^{\rm out}_{Lj}. \tag{6.15}$$

At the same time it acts as complex conjugation on functions. The wave functions appearing in (6.12) transform as

$$\begin{aligned} Y^*_{Lj}(\Omega) &= (-)^L Y_{Lj}(\Omega), \\ y^{\rm in\,*}_L(\tau) &= y^{\rm out}_L(-\tau). \end{aligned} \tag{6.16}$$

Putting this together gives

$$\begin{aligned} \mathcal{T}\phi(\tau,\sigma)\mathcal{T} &= \sum_{L,j} \big(a^{\rm out}_{Lj} y^{\rm out}_L(-\tau) Y_{Lj}(\Omega) + b^{\rm out}_{Lj} y^{\rm out*}_L(-\tau) Y^*_{Lj}(\Omega) \big) \\ &= \phi(-\tau,\sigma), \end{aligned} \tag{6.17}$$

as required.

We wish to consider the action of $\mathcal{CPT}$ on the in and out field operators $\phi^{\rm in}_+$ and $\phi^{\rm out}_+$ defined by (5.13). Using (6.14)–(6.16) these obey

$$\begin{aligned} \mathcal{PT}\phi^{\rm in}_+(\sigma)\mathcal{PT} &= \phi^{\rm out}_-(P\sigma_A) \\ \mathcal{PT}\phi^{\rm out}_+(\sigma)\mathcal{PT} &= \phi^{\rm in}_-(P\sigma_A). \end{aligned} \tag{6.18}$$

6.3. The Witten Inner Product and Modifications

Following Witten [20], we now describe a modified inner product. First we construct a bilinear pairing between states on $\mathcal{I}^-$and states on $\mathcal{I}^+$. We will consider asymptotic states on $\mathcal{I}^\pm$ [12]

$$|\Psi^{\rm in}\rangle = \int \Psi^{\rm in}(\sigma)\phi_+^{\rm in}(\sigma)|{\rm in}\rangle, \qquad |\Psi^{\rm out}\rangle = \int \Psi^{\rm out}(\sigma)\phi_-^{\rm out}(\sigma)|{\rm in}\rangle, \tag{6.19}$$

where $\Psi^{\rm in}(\Omega)$ and $\Psi^{\rm out}(\Omega)$ are functions on the 2-sphere. Using (5.17), the out state can be expressed as a linear combination of in states

$$|\Psi^{\rm out}\rangle = -\mu \sinh \pi\mu \int\int \Psi^{\rm out}(\sigma')\Delta_-(\sigma',\sigma)\phi_+^{\rm in}(\sigma)|{\rm in}\rangle. \tag{6.20}$$

This corresponds to evolving the state $|\Psi^{\rm out}\rangle$ backwards from $\mathcal{I}^+$ to $\mathcal{I}^-$, and defines the bilinear pairing

$$(\Psi^{\rm out}|\Psi^{\rm in}) = -\mu \sinh \pi\mu \int\int \Psi^{\rm out}(\sigma')\Delta_-(\sigma',\sigma)\Psi^{\rm in}(\sigma). \tag{6.21}$$

We now use the pairing to define an inner product on $\mathcal{I}^-$ that is antilinear in the first argument. Note that applying $\mathcal{CPT}$ to a state on $\mathcal{I}^-$ gives us a state on $\mathcal{I}^+$:

$$\mathcal{CPT}|\Psi^{\rm in}\rangle = \int \Psi^{\rm in*}(P\sigma_A)\phi_-^{\rm out}(\sigma)|{\rm in}\rangle \tag{6.22}$$

to which we may apply the pairing (6.21). We find the inner product between two states on $\mathcal{I}^-$

$$\langle\Psi^{\rm in}|\Upsilon^{\rm in}\rangle = -\mu \sinh \pi\mu \int\int \Psi^{\rm in*}(\Omega)\Delta_-(P\Omega_A,\Omega')\Upsilon^{\rm in}(\Omega'). \tag{6.23}$$

For free field theory the norm (6.23) implies the adjoint relations[13]

$$\begin{aligned} \phi^\dagger(x) &= \phi(PTx), \\ \phi_\pm^{\rm in\dagger}(\Omega) &= \phi_\pm^{\rm out}(P\Omega_A). \end{aligned} \tag{6.24}$$

[12] Of course, these states are linear in $b^{\rm in}$ and $b^{\rm out}$. The general asymptotic states will take a more complicated form.

[13] It is intriguing that this adjoint relates degrees of freedom separated by a horizon.

This may look strange at first but is in fact precisely the usual norm employed for a Euclidean CFT. Note that P coupled with the antipodal map is reflection about the equator, so that

$$PA(z,\bar{z}) = (\frac{1}{\bar{z}}, \frac{1}{z}), \tag{6.25}$$

as in (6.5). For states constructed by acting with operators on $\mathcal{I}^-$, it therefore follows that the norm is simply the two point function. Hence (6.23) gives the Zamolodchikov metric on the boundary CFT.

Formula (6.23) in fact remains valid for any choice of P. Using $Pz = \bar{z}$ as in [20], one finds instead of (6.25), $PA(z,\bar{z}) = (-\frac{1}{z}, -\frac{1}{\bar{z}})$. The adjoint then involves rotation by π about $z = \pm i$ rather than reflection across the unit disc.

6.4. Adjoints of the $SL(2,C)$ Generators

The quantum generators of the symmetries (6.7) and (6.8) are as usual given by

$$\begin{aligned} \mathcal{L}_n &= \int_\Sigma d\Sigma^\mu \mathcal{T}_{\mu\nu} \zeta_n^\nu, \\ \bar{\mathcal{L}}_n &= \int_\Sigma d\Sigma^\mu \mathcal{T}_{\mu\nu} \bar{\zeta}_n^\nu, \end{aligned} \tag{6.26}$$

for any complete spacelike slice Σ. We choose Σ to be the throat $X^+ = X^-$ because it is mapped to itself under both P and T. For a massive scalar,

$$\mathcal{T}_{\mu\nu}(x) = \partial_\mu \phi(x) \partial_\nu \phi(x) - \frac{1}{2} g_{\mu\nu} \left[(\nabla \phi(x))^2 + m^2 \phi^2(x) \right]. \tag{6.27}$$

With the ordinary inner product, $\mathcal{T}_{\mu\nu}$ is hermitian, and one finds $\mathcal{L}_n^\dagger = \bar{\mathcal{L}}_n$. With the modified inner product, one has

$$\mathcal{L}_n^\dagger = \int d\Sigma^\mu(x) \mathcal{T}_{\mu\nu}(PTx) \bar{\zeta}_n^\nu(x). \tag{6.28}$$

We then consider a coordinate transformation $x' = PTx$. One finds

$$\mathcal{L}_n^\dagger = \int d\Sigma^\mu(PTx') \mathcal{T}_{\mu\nu}(x') \bar{\zeta}_n^\nu(PTx'). \tag{6.29}$$

Using the relations

$$\begin{aligned} \zeta_n(PTx') &= -\bar{\zeta}_{-n}(x'), \\ d\Sigma^\mu(PTx') &= -d\Sigma^\mu(x'), \end{aligned} \tag{6.30}$$

it follows that

$$\mathcal{L}_n^\dagger = \mathcal{L}_{-n}. \tag{6.31}$$

In [16] the $SL(2,C)$ isometries of dS_3 were conjectured to extend to a full Virasoro symmetry of the full quantum gravity (not just a free scalar). This naturally acted not on closed spacelike slices but on asymptotically flat slices ending on $\mathcal{I}$. It would be interesting to compute the adjoints of these generators.

7. The Cylinder

In this section we study scalar field theory in static coordinates. Again for simplicity we specialize to dS_3, although we expect the higher dimensional cases to be similar. The metric is

$$ds^2 = -(1-r^2)dt^2 + \frac{dr^2}{(1-r^2)} + r^2 d\varphi^2. \tag{7.1}$$

This metric is singular at the horizons $r = 1$, which divides dS_3 into four regions. There are two regions with $0 \leq r < 1$ corresponding to the causal diamonds of observers at the north and south poles. We shall refer to these as the northern and southern diamonds. There are two more regions with $1 < r < \infty$ containing $\mathcal{I}^+$ and $\mathcal{I}^-$ which we shall refer to as the future and past triangles. On $\mathcal{I}^\pm$, where $r \to \infty$, the spatial metric approaches $r^2(dt^2 + d\varphi^2)$ and hence is conformal to the cylinder.

Unlike the global coordinates, static coordinates do not smoothly cover all of dS_d. However, they are well-suited to describing the physics associated to an observer who can access a single causal diamond. The Killing vector $\frac{\partial}{\partial t}$ is manifest in static coordinates, but is future-directed only in the southern diamond; it is past-directed in the northern diamond and space-like in the past and future triangles.

In the following we solve the scalar wave equation in the four regions. Then we patch the solutions together to get a global solution over all of dS_3 by matching at the horizons. We further show explicitly that tracing the Euclidean vacuum over the Hilbert space of the northern modes leads to a thermal density matrix in the southern diamond.

7.1. The Wave Equation

The equation of motion for a scalar field of mass m is $(\nabla^2 - m^2)\phi = 0$. In static coordinates, this becomes

$$\left[-\frac{1}{1-r^2}\partial_t^2 + \frac{1}{r}\partial_r(1-r^2)r\partial_r + \frac{1}{r^2}\partial_\varphi^2 - m^2\right]\phi = 0. \tag{7.2}$$

The equation separates, so that a general solution can be expanded

$$\phi(t,r,\varphi) = \int_0^\infty d\omega \sum_{j=-\infty}^{\infty} a_{\omega j}\phi_{\omega j} + b_{\omega j}\phi^{\omega j} + a^\dagger_{\omega j}\phi^*_{\omega j} + b^\dagger_{\omega j}\phi^{\omega j *}, \tag{7.3}$$

where

$$\phi_{\omega j} = f_{\omega j}(r)e^{-i\omega t + ij\varphi}, \qquad \phi^{\omega j} = f^{\omega j}(r)e^{-i\omega t + ij\varphi}, \tag{7.4}$$

and $f_{\omega j}(r)$, $f^{\omega j}(r)$ are two linearly independent solutions of the radial equation

$$(1-r^2)\frac{d^2 f_{\omega j}}{dr^2} + \left(\frac{1}{r} - 3r\right)\frac{df_{\omega j}}{dr} + \left(\frac{\omega^2}{1-r^2} - \frac{j^2}{r^2} - m^2\right)f_{\omega j} = 0. \tag{7.5}$$

7.2. The Northern and Southern Diamonds

A solution smooth near $r = 0$ is given by

$$\begin{aligned} \phi^S_{\omega j} &= f_{\omega j}(r)e^{-i\omega t + ij\varphi}, \\ f_{\omega j}(r) &\equiv r^{|j|}(1-r^2)^{\frac{i\omega}{2}}F(a,b;c;r^2), \\ a &\equiv \frac{1}{2}(|j| + i\omega + h_+), \\ b &\equiv \frac{1}{2}(|j| + i\omega + h_-), \\ c &\equiv 1 + |j|. \end{aligned} \tag{7.6}$$

We have not normalized this solution, although the necessary factor follows from computations below. The superscript S denotes that this solution is in the southern diamond. One can show from the transformation formulae for hypergeometric functions (see Appendix B) that

$$f^*_{\omega j} = f_{-\omega j} = f_{\omega j}. \tag{7.7}$$

Similarly we may define northern modes

$$\phi^N_{\omega j} = f_{\omega j}(r) e^{-i\omega t + ij\varphi}. \tag{7.8}$$

It is convenient to use the time coordinate t both in the northern and in the southern diamond. Although this coordinate system does not uniquely label points on all of dS_3, there will be no confusion since we denote northern functions with a superscript N. The coordinate t runs forward in the southern diamond and backward in the northern diamond. Hence for $\omega > 0$ the modes (7.6) are positive frequency and (7.8) are negative frequency.

Near the horizon, for $r \to 1$, one can show (see Appendix B for details) that (7.6) becomes:

$$\begin{aligned}\phi^S_{\omega j} \to e^{-i\omega t + ij\varphi}\Gamma(1+|j|)\big[&\frac{\Gamma(-i\omega)}{\Gamma(\frac{1}{2}(|j|-i\omega+h_+))\Gamma(\frac{1}{2}(|j|-i\omega+h_-))}(1-r^2)^{\frac{i\omega}{2}} \\ &+ \frac{\Gamma(i\omega)}{\Gamma(\frac{1}{2}(|j|+i\omega+h_+))\Gamma(\frac{1}{2}(|j|+i\omega+h_-))}(1-r^2)^{-\frac{i\omega}{2}}\big].\end{aligned} \tag{7.9}$$

In order to analyze the flux across the horizons it is useful to introduce Kruskal coordinates

$$\begin{aligned} r &= \frac{1+UV}{1-UV}, \\ t &= \frac{1}{2}\ln(-\frac{U}{V}), \end{aligned} \tag{7.10}$$

in which

$$ds^2 = \frac{1}{(1-UV)^2}\big(-4dUdV + (1+UV)^2 d\varphi^2\big). \tag{7.11}$$

$U > 0$ and $V < 0$ in the southern diamond. The future (past) horizon is at $V = 0$ ($U = 0$). In contrast to the static coordinates, Kruskal coordinates are nonsingular at the horizon.

The modes (7.9) become, for $r \to 1$ ($UV \to 0$):

$$\phi^S_{\omega j} \to e^{ij\varphi}\left[\alpha_{\omega j}(-V)^{i\omega} + \alpha^*_{\omega j}U^{-i\omega}\right], \tag{7.12}$$

where we define the complex constants

$$\alpha_{\omega j} \equiv \frac{\Gamma(1+|j|)\Gamma(-i\omega)2^{i\omega}}{\Gamma(\frac{1}{2}(|j|-i\omega+h_+))\Gamma(\frac{1}{2}(|j|-i\omega+h_-))} = \alpha^*_{-\omega j}. \tag{7.13}$$

The first term in (7.12) is incoming flux across the past horizon, while the second is outgoing flux across the future horizon. A similar analysis in the northern diamond with $U < 0,\ V > 0$ gives for $r \to 1$:

$$\phi^N_{\omega j} \to e^{ij\varphi}\left[\alpha_{\omega j}V^{i\omega} + \alpha^*_{\omega j}(-U)^{-i\omega}\right]. \tag{7.14}$$

The northern and southern modes are simply related by

$$\phi^S_{\omega j}(-U,-V) = \phi^N_{\omega j}(U,V). \tag{7.15}$$

The second family of solutions is given by

$$\phi^{\omega j} = \ln(r^2)\phi_{\omega j} + e^{-i\omega t+ij\varphi}r^{|j|}(1-r^2)^{\frac{i\omega}{2}}\sum_{n=-|j|}^{\infty}A_n r^{2n}, \tag{7.16}$$

where the coefficients A_n are given in, e.g., equation 15.5.19 of [69]. These modes are singular at r=0 for all j and hence are excluded.

7.3. The Past and Future Triangles

Let us analyze the behavior of the modes in the past triangle (which includes $\mathcal{I}^-$ but not $\mathcal{I}^+$) where $r^2 > 1$. A complex solution of (7.2) is

$$\begin{aligned}\phi^{\text{in}+}_{\omega j} &= f^+_{\omega j}(r)e^{-i\omega t+ij\varphi},\\ f^+_{\omega j}(r) &\equiv r^{-h_+}(1-\frac{1}{r^2})^{\frac{i\omega}{2}}F(a,1-a^*;h_+;\frac{1}{r^2}).\end{aligned} \tag{7.17}$$

Using properties of the hypergeometric functions one finds that $f^+_{\omega j}$ is invariant under $\omega \to -\omega$, but is not real. Therefore the second solution of (7.2) is obtained by complex conjugation:

$$\phi^{\text{in}-}_{\omega j} = (f^+_{\omega j}(r))^* e^{-i\omega t + ij\varphi}. \tag{7.18}$$

This is equivalent to replacing h_+ with h_- in (7.17). Near $\mathcal{I}^-$ we find

$$\phi^{\text{in}\pm}_{\omega j} \sim r^{-h_\pm}. \tag{7.19}$$

In the past triangle the coordinate r is timelike and past-directed, so that the $\phi^{\text{in}-}$ are positive frequency for $m^2 > 1$.

Near the horizon, for $r \to 1$, we find

$$\begin{aligned}\phi^{\text{in}+}_{\omega j} \to e^{-i\omega t + ij\varphi}\Gamma(h_+)\big[&\frac{\Gamma(-i\omega)}{\Gamma(\frac{1}{2}(|j| - i\omega + h_+))\Gamma(\frac{1}{2}(-|j| - i\omega + h_+))}(r^2-1)^{\frac{i\omega}{2}} \\ &+ \frac{\Gamma(i\omega)}{\Gamma(\frac{1}{2}(-|j| + i\omega + h_+))\Gamma(\frac{1}{2}(|j| + i\omega + h_+))}(r^2-1)^{-\frac{i\omega}{2}}\big].\end{aligned} \tag{7.20}$$

The relation between static and Kruskal coordinates in the past triangle is

$$\begin{aligned} r &= \frac{1+UV}{1-UV}, \\ t &= \frac{1}{2}\ln(\frac{U}{V}). \end{aligned} \tag{7.21}$$

U and V are both negative in this region. The boundary with the northern (southern) diamond is at $V = 0$ ($U = 0$). The near horizon behavior (7.20) becomes

$$\phi^{\text{in}+}_{\omega j} \to e^{ij\varphi}\big[\beta_{\omega j}(-V)^{i\omega} + \beta_{-\omega j}(-U)^{-i\omega}\big], \tag{7.22}$$

where

$$\beta_{\omega j} \equiv \frac{\Gamma(h_+)\Gamma(-i\omega)2^{i\omega}}{\Gamma(\frac{1}{2}(|j| - i\omega + h_+))\Gamma(\frac{1}{2}(-|j| - i\omega + h_+))}. \tag{7.23}$$

Similarly one finds near $r = 1$ that

$$\phi^{\text{in}-}_{\omega j} \to e^{ij\varphi}\big[\beta^*_{-\omega j}(-V)^{i\omega} + \beta^*_{\omega j}(-U)^{-i\omega}\big]. \tag{7.24}$$

One may also define modes in the future triangle by

$$\begin{aligned}\phi^{\text{out}+}_{\omega j} &= f^{+}_{\omega j}(r)e^{-i\omega t+ij\varphi},\\ \phi^{\text{out}-}_{\omega j} &= (f^{+}_{\omega j}(r))^{*}e^{-i\omega t+ij\varphi}.\end{aligned} \tag{7.25}$$

Near $\mathcal{I}^+$ we find

$$\phi^{\text{out}\pm}_{\omega j} \sim r^{-h_\pm}. \tag{7.26}$$

In the future triangle the coordinate r is future-directed, so that the $\phi^{\text{out}+}$ are positive frequency.

The relation between static and Kruskal coordinates in the future triangle is again given by (7.21), which means that t increases to the south (north) in the future (past) triangle. U and V are both positive in this region. The boundary of the future triangle with the northern (southern) diamond is at $U = 0$ ($V = 0$). Near the horizons ($UV = 0$) the ϕ^{out} modes obey

$$\begin{aligned}\phi^{\text{out}+}_{\omega j} &= e^{ij\varphi}\left[\beta_{\omega j}V^{i\omega} + \beta_{-\omega j}U^{-i\omega}\right],\\ \phi^{\text{out}-}_{\omega j} &= e^{ij\varphi}\left[\beta^{*}_{-\omega j}V^{i\omega} + \beta^{*}_{\omega j}U^{-i\omega}\right].\end{aligned} \tag{7.27}$$

The past and future modes are simply related by

$$\phi^{\text{out}\pm}_{\omega j}(U,V) = \phi^{\text{in}\pm}_{\omega j}(-U,-V). \tag{7.28}$$

7.4. Matching Across the Horizon.

In the previous two subsections we have described solutions in the past and future triangles as well as the northern and southern diamonds. By matching fluxes across the horizon, these may be extended to global solutions over all of dS_3. For example the $(-V)^{i\omega}$ ($(-U)^{-i\omega}$) terms in the past modes (7.22) and (7.24) carry flux into the southern (northern) diamond. The continuation of (7.22) and (7.24) into these regions is obtained by matching to (7.12) along $U = 0$ and to (7.14) along $V = 0$. Matching across the horizon again then yields the future mode.

Henceforth we shall use the symbol $\phi^{\text{in}\pm}$ to denote the global solution so constructed. Similarly, $\phi^{\text{out}\pm}$ will denote the global solution agreeing with (7.27) in the future triangle. We may also construct global solutions ϕ^S (ϕ^N) that agree with the modes (7.6) ((7.8)) in the southern (northern) diamond—these solutions vanish in the northern (southern) diamond.

From the matching procedure outlined above we find that these modes obey

$$\begin{pmatrix} \phi^S_{\omega j} \\ \\ \phi^N_{\omega j} \end{pmatrix} = \mathbf{A}_{\omega j} \begin{pmatrix} \phi^{\text{in}+}_{\omega j} \\ \\ \phi^{\text{in}-}_{\omega j} \end{pmatrix} = \mathbf{A}^*_{\omega j} \begin{pmatrix} \phi^{\text{out}-}_{\omega j} \\ \\ \phi^{\text{out}+}_{\omega j} \end{pmatrix}, \tag{7.29}$$

where

$$N_{\omega j}\mathbf{A}_{\omega j} = \begin{pmatrix} \alpha_{\omega j}\beta^*_{\omega j} & -\alpha_{\omega j}\beta_{-\omega j} \\ \\ -\alpha^*_{\omega j}\beta^*_{-\omega j} & \alpha^*_{\omega j}\beta_{\omega j} \end{pmatrix} \tag{7.30}$$

and

$$N_{\omega j} \equiv (\beta_{\omega j}\beta^*_{\omega j} - \beta_{-\omega j}\beta^*_{-\omega j}) = -\frac{\mu}{\omega}. \tag{7.31}$$

Reversing the signs of U and V and using $\sigma_x \mathbf{A} \sigma_x = \mathbf{A}^*$, one finds that the second equation in (7.29) follows from the first. The Bogolyubov transformation from $\mathcal{I}^-$ to $\mathcal{I}^+$ then follows from (7.29) as

$$\begin{pmatrix} \phi^{\text{out}-}_{\omega j} \\ \\ \phi^{\text{out}+}_{\omega j} \end{pmatrix} = \mathbf{B}_{\omega j} \begin{pmatrix} \phi^{\text{in}+}_{\omega j} \\ \\ \phi^{\text{in}-}_{\omega j} \end{pmatrix}, \tag{7.32}$$

where

$$\mathbf{B}_{\omega j} = \sigma_x \mathbf{A}^{-1}_{\omega j} \sigma_x \mathbf{A}_{\omega j} = \begin{pmatrix} \dfrac{\alpha_{\omega j}\beta^*_{\omega j}}{\alpha^*_{\omega j}\beta_{\omega j}} & 0 \\ \\ 0 & \dfrac{\alpha^*_{\omega j}\beta_{\omega j}}{\alpha_{\omega j}\beta^*_{\omega j}} \end{pmatrix}. \tag{7.33}$$

As with the spherical modes of section 3.2, the Bogolyubov transformation (7.32) is trivial. The vacuum $|\text{in}\rangle$ defined by the modes ϕ^{in} is identical to the vacuum $|\text{out}\rangle$ defined by the ϕ^{out}.

7.5. Euclidean Modes on the Cylinder

In this subsection, following [70] we write the Euclidean modes as linear combinations of northern and southern modes.

In Kruskal coordinates the southern modes (7.6) in the southern diamond are of the form

$$\phi^S_{\omega j} = f_{\omega j}(UV)e^{ij\varphi}(-\frac{V}{U})^{\frac{i\omega}{2}} \tag{7.34}$$

for $U > 0, V < 0$, and vanish for $U < 0, V > 0$. The northern modes in the northern diamond are of the same form

$$\phi^N_{\omega j} = f_{\omega j}(UV)e^{ij\varphi}(-\frac{V}{U})^{\frac{i\omega}{2}}, \tag{7.35}$$

but have support for $U < 0, V > 0$ instead of $U > 0, V < 0$. We wish to find a linear combination of (7.34) and (7.35) which is analytic in the lower complex U and V planes.[14] This can be accomplished by analytically continuing the southern modes (7.34) to the northern diamond along the contour

$$U \to e^{-i\gamma}U, \qquad V \to e^{i\gamma}V, \tag{7.36}$$

taking γ from 0 to π. Notice that the product UV is independent of γ, so that the continuation of the southern mode (7.34) is

$$e^{-\pi\omega}f_{\omega j}(UV)e^{ij\varphi}(-\frac{V}{U})^{\frac{i\omega}{2}}. \tag{7.37}$$

Comparing with (7.35) we see that the linear combination

$$\phi^E_{\omega j} = \phi^S_{\omega j} + e^{-\pi\omega}\phi^N_{\omega j} \tag{7.38}$$

[14] Euclidean modes were defined earlier to be regular on the lower Euclidean hemisphere ($\tau^{\rm Re} = 0$, $-\frac{\pi}{2} \le \tau^{\rm Im} \le 0$). Explicit transformation of coordinates shows that sgn $U^{\rm Im}$ = sgn $V^{\rm Im}$ = sgn $\tau^{\rm Im}$. The lower pole, $\tau = -i\frac{\pi}{2}$, maps to a single point, $U = V = -i$, independently of θ. Smooth curves through this pole remain smooth in the U and V planes. Thus, modes that are analytic and bounded in the lower half U and V planes will be regular on the lower Euclidean hemisphere.

is analytic in the lower half of the complex U and V planes. Since t runs backwards in the northern diamond, this is a linear combination of positive and negative frequency modes. A second linear combination

$$\phi^{E\prime}_{\omega j} = (\phi^N_{\omega j})^* + e^{-\pi\omega}(\phi^S_{\omega j})^* \tag{7.39}$$

is also analytic in the lower half plane. Both ϕ^E and $\phi^{E\prime}$ are positive frequency for $\omega > 0$.

7.6. MA Transform to Euclidean Modes

In this subsection we will show that the $|\text{in}\rangle$ vacuum on the cylinder is the same as the $|\text{in}\rangle$ vacuum on the sphere by showing that it is an MA transform of the Euclidean vacuum with $\alpha = -\pi\mu$. This result is anticipated by the fact that the dual CFTs should be simply related by the conformal transformation from the sphere to the cylinder. Nevertheless, it provides a useful check on our constructions.

The first step is to redefine $\phi^{\text{in}\pm}$ in order to simplify the expression for $\mathbf{A}$ in (7.29). Let

$$\begin{aligned} \tilde\phi^{\text{in}+}_{\omega j} &= i^j \frac{\alpha_{\omega j}\beta^*_{\omega j}}{N_{\omega j}} \phi^{\text{in}+}_{\omega j}, \\ \tilde\phi^{\text{in}-}_{\omega j} &= (-i)^j \frac{\alpha^*_{\omega j}\beta_{\omega j}}{N_{\omega j}} \phi^{\text{in}-}_{\omega j}. \end{aligned} \tag{7.40}$$

Then (7.29) becomes

$$\begin{pmatrix} \phi^S_{\omega j} \\ \\ \phi^N_{\omega j} \end{pmatrix} = (-i)^j \begin{pmatrix} 1 & q \\ \\ (-)^j q & (-)^j \end{pmatrix} \begin{pmatrix} \tilde\phi^{\text{in}+}_{\omega j} \\ \\ \tilde\phi^{\text{in}-}_{\omega j} \end{pmatrix}, \tag{7.41}$$

with

$$q \equiv (-)^{j+1} \frac{\alpha_{\omega j}\beta_{-\omega j}}{\alpha^*_{\omega j}\beta_{\omega j}} = -\frac{(-)^j + e^{\pi(\omega+\mu)}}{e^{\pi\omega} + (-)^j e^{\pi\mu}} \tag{7.42}$$

It follows that the Euclidean modes obey

$$\begin{aligned} \phi^E_{\omega j} &= \phi^S_{\omega j} + e^{-\pi\omega}\phi^N_{\omega j} \\ &= (-i)^j \frac{e^{\pi\omega} - e^{-\pi\omega}}{e^{\pi\omega} + (-)^j e^{\pi\mu}} \big(\tilde\phi^{\text{in}+}_{\omega j} - e^{\pi\mu}\tilde\phi^{\text{in}-}_{\omega j}\big). \end{aligned} \tag{7.43}$$

Inverting this relation, one recovers $\alpha = -\pi\mu$.

Let us summarize the southern and northern mode expansions:

$$\begin{aligned}\phi^S(t,r,\varphi) &= \int_0^\infty d\omega \sum_{j=-\infty}^{\infty} a^S_{\omega j}\phi^S_{\omega j} + (a^S_{\omega j})^\dagger(\phi^S_{\omega j})^* \\ \phi^N(t,r,\varphi) &= \int_0^\infty d\omega \sum_{j=-\infty}^{\infty} a^N_{\omega j}\phi^N_{\omega j} + (a^N_{\omega j})^\dagger(\phi^N_{\omega j})^*.\end{aligned} \tag{7.44}$$

Here we take the modes ϕ^S and ϕ^N to be normalized with respect to the Klein-Gordon inner product (3.7). The Fock space in the southern diamond is constructed with lowering operators $a^S_{\omega j}$ and raising operators $(a^S_{\omega j})^\dagger$. The Fock space in the northern diamond is constructed with lowering operators $(a^N_{\omega j})^\dagger$ and raising operators $a^N_{\omega j}$.

The modes (7.38) and (7.39) annihilate the Euclidean vacuum, $|E\rangle$. This allows us to express $|E\rangle$ as a superposition of states in the northern and southern Fock spaces [71]:

$$\begin{aligned}|E\rangle &= \prod_{\omega=0}^{\infty}\prod_{j=-\infty}^{\infty} \left(1-e^{-2\pi\omega}\right)^{\frac{1}{2}} \exp\left[e^{-\pi\omega}(a^S_{\omega j})^\dagger a^N_{\omega j}\right]|S\rangle\otimes|N\rangle \\ &= \prod_{\omega,j}\left(1-e^{-2\pi\omega}\right)^{\frac{1}{2}} \sum_{n_{\omega j}=0}^{\infty} e^{-\pi\omega n_{\omega j}}|n_{\omega j},S\rangle\otimes|n_{\omega j},N\rangle.\end{aligned} \tag{7.45}$$

Here $|S\rangle$ and $|N\rangle$ are the southern and northern vacua, and

$$\begin{aligned}|n_{\omega j},S\rangle &= (n_{\omega j}!)^{-\frac{1}{2}}[(a^S_{\omega j})^\dagger]^{n_{\omega j}}|S\rangle, \\ |n_{\omega j},N\rangle &= (n_{\omega j}!)^{-\frac{1}{2}}[a^N_{\omega j}]^{n_{\omega j}}|N\rangle.\end{aligned} \tag{7.46}$$

Only the southern diamond is causally accessible to an observer at the south pole. The quantum state in this region is described by a density matrix ρ^S, which is obtained from a global state by tracing over the field modes in the northern diamond. For the Euclidean vacuum (7.45) we obtain

$$\rho^S_E = \mathrm{tr}_N|E\rangle\langle E| = \prod_{\omega,j}\left[\left(1-e^{-2\pi\omega}\right)\sum_{n_{\omega j}} e^{-2\pi\omega n_{\omega j}}|n_{\omega j},S\rangle\langle n_{\omega j},S|\right]. \tag{7.47}$$

Recall that the Killing vector $\xi^\mu \partial_\mu = \partial_t$ is everywhere time-like and future directed in the southern diamond. Neglecting gravitational back-reaction of the field modes, this allows us to define a Hamiltonian for the southern modes:

$$\mathcal{M} = \int_{\Sigma^S} d\Sigma^\mu \mathcal{T}_{\mu\nu} \xi^\nu = \int_0^\infty d\omega \sum_{j=-\infty}^{\infty} (a^S_{\omega j})^\dagger a^S_{\omega j} \; \omega, \tag{7.48}$$

where $\mathcal{T}$ is the stress tensor of the scalar field. Here Σ^S is a $t =$ constant Cauchy surface in the southern diamond with normal vector is $n^\mu_\Sigma \partial_\mu = (1 - r^2)^{-\frac{1}{2}} \partial_t$. This definition of energy is natural for the observer at the south pole. For later use, we also define the angular momentum $\mathcal{J}$ as the conserved charge associated with the Killing vector $v^\mu \partial_\mu = -\partial_\varphi$:

$$\mathcal{J} = \int_{\Sigma^S} d\Sigma^\mu \mathcal{T}_{\mu\nu} v^\nu = \int_0^\infty d\omega \sum_{j=-\infty}^{\infty} (a^S_{\omega j})^\dagger a^S_{\omega j} \; j. \tag{7.49}$$

With respect to the Hamiltonian $\mathcal{M}$, the southern state (7.47) becomes a thermal density matrix

$$\rho^S_E = C \exp\left(-\frac{\mathcal{M}}{T}\right) \tag{7.50}$$

with temperature $T = \frac{1}{2\pi}$; $C = \prod(1 - e^{-2\pi\omega})$ is a normalization factor.

8. Kerr-de Sitter

In this section we generalize the discussion of the previous sections to the three-dimensional Kerr-de Sitter solution, which represents a spinning point mass in dS_3.

8.1. Static Coordinates

The Kerr-de Sitter metric describes the gravitational field of a point particle whose mass and spin are parametrized by $1 - M$ and J:

$$ds^2 = -N^2 dt^2 + N^{-2} dr^2 + r^2 \left(d\varphi + N^\varphi dt\right)^2. \tag{8.1}$$

The lapse and shift functions are

$$N^2 = M - r^2 + \frac{16G^2J^2}{r^2}, \qquad N^\varphi = -\frac{4GJ}{r^2}. \tag{8.2}$$

The lapse function vanishes for one positive value of r:

$$r_+ = \frac{1}{2}\left(\sqrt{\tau} + \sqrt{\bar{\tau}}\right). \tag{8.3}$$

where

$$\tau \equiv M + i(8GJ). \tag{8.4}$$

This is the cosmological event horizon surrounding an observer at $r = 0$. It has a Bekenstein-Hawking entropy [72,73] of

$$S = \frac{\pi r_+}{2G} = \frac{\pi}{4G}\left(\sqrt{\tau} + \sqrt{\bar{\tau}}\right). \tag{8.5}$$

8.2. Kerr-dS_3 as a Quotient of dS_3

In 2+1 dimensions, there is no black hole horizon for Kerr-de Sitter because the "black hole" degenerates to a conical singularity at the origin. This is best seen by writing the metric as an identification of de Sitter [74]. Let us define $\mu = r_+$ and $\alpha = 4GJ/r_+$, so that

$$M = \mu^2 - \alpha^2, \quad J = \frac{\mu\alpha}{4G}. \tag{8.6}$$

The coordinate transformation

$$\begin{aligned} \tilde{t} &= \mu t + \alpha\varphi, \\ \tilde{\varphi} &= \mu\varphi - \alpha t, \\ \tilde{r} &= \sqrt{\frac{r^2 + \alpha^2}{\mu^2 + \alpha^2}} \end{aligned} \tag{8.7}$$

changes the Kerr-de Sitter metric to the vacuum form

$$ds^2 = -\left(1 - \tilde{r}^2\right) d\tilde{t}^2 + \frac{d\tilde{r}^2}{1 - \tilde{r}^2} + \tilde{r}^2 d\tilde{\varphi}^2, \tag{8.8}$$

but with a non-standard coordinate identification. In empty de Sitter space, $(\tilde{t},\ \tilde{r},\ \tilde{\varphi}+2\pi n)$ labels the same point for all integer n. In the presence of a particle, the points

$$(\tilde{t},\ \tilde{r},\ \tilde{\varphi}) + 2\pi n(\alpha,\ 0,\ \mu) \tag{8.9}$$

are identified instead.

8.3. Kerr-dS_3 Temperature and Angular Potential

In this subsection we consider a scalar field in Kerr-dS_3. The cylinder mode solutions found for de Sitter in Section 6 are also solutions in Kerr-de Sitter, after the substitutions $t \to \tilde{t}$, $r \to \tilde{r}$ and $\varphi \to \tilde{\varphi}$ are performed. For the modes to remain single-valued, the angular momentum j must be non-integer:

$$j = \frac{n + \omega\alpha}{\mu}, \qquad n \text{ integer}. \tag{8.10}$$

The mode analysis carries over trivially. In particular, the Euclidean modes (7.38) and (7.39) take the same form in Kerr-de Sitter.

Analogues of (7.48) and (7.49) define conserved charges associated with the Killing vectors $\tilde{\xi}^\mu\partial_\mu = \partial_{\tilde{t}}$ and $\tilde{v}^\mu\partial_\mu = -\partial_{\tilde{\varphi}}$:

$$\begin{aligned} \tilde{\mathcal{M}} &= \int_{\Sigma^S} d\Sigma^\mu \mathcal{T}_{\mu\nu}\tilde{\xi}^\nu = \int_0^\infty d\omega \sum_{j=-\infty}^{\infty} (a^S_{\omega j})^\dagger a^S_{\omega j}\ \omega, \\ \tilde{\mathcal{J}} &= \int_{\Sigma^S} d\Sigma^\mu \mathcal{T}_{\mu\nu}\tilde{v}^\nu = \int_0^\infty d\omega \sum_{j=-\infty}^{\infty} (a^S_{\omega j})^\dagger a^S_{\omega j}\ j, \end{aligned} \tag{8.11}$$

where $\mathcal{T}_{\mu\nu}$ is the matter stress tensor. Here the hypersurface Σ^S is defined, for example, by the normal vector

$$n^\mu_{\Sigma^S}\partial_\mu = \frac{\tilde{r}}{\sqrt{1-\tilde{r}^2}}\frac{\mu}{r}\partial_{\tilde{t}} + \frac{\sqrt{1-\tilde{r}^2}}{\tilde{r}}\frac{\alpha}{r}\partial_{\tilde{\phi}}. \tag{8.12}$$

(For $\alpha > 0$, Σ^S is not a space-like surface near the origin; this does not affect the definition of conserved quantities.) The expressions for $\tilde{\mathcal{M}}$ and $\tilde{\mathcal{J}}$ nevertheless take

the same form as $\mathcal{M}$ and $\mathcal{J}$ in de Sitter space. The Euclidean state, restricted to the southern diamond ($\tilde{r} < 1$), is a density matrix

$$\rho_E^S = C \exp\left(-2\pi\tilde{\mathcal{M}}\right). \tag{8.13}$$

In the (t, r, φ) coordinates, the asymptotic metric of Kerr-de Sitter space takes a standard form near $\mathcal{I}$ (detailed in section 7.4 below). In order to compare conserved quantities of different space-times, we must use the Killing vectors ∂_t and ∂_φ to measure energy and angular momentum.[15] The corresponding conserved charges are related to $\tilde{\mathcal{M}}$ and $\tilde{\mathcal{J}}$ by a linear transformation. Using (8.7) one finds

$$\tilde{\mathcal{M}} = \frac{\mu}{\mu^2 + \alpha^2}\mathcal{M} + \frac{\alpha}{\mu^2 + \alpha^2}\mathcal{J}. \tag{8.14}$$

Thus we obtain a density matrix

$$\rho_E^S = C \exp\left(-\frac{\mathcal{M} + \Omega\mathcal{J}}{T}\right), \tag{8.15}$$

at temperature and angular potential

$$T = \frac{\mu^2 + \alpha^2}{2\pi\mu}, \qquad \Omega = \frac{\alpha}{\mu}. \tag{8.16}$$

For later convenience it is useful to rewrite the the density matrix (8.15) in terms of the complex inverse temperature

$$\beta \equiv \frac{1 + i\Omega}{T} = \frac{2\pi}{\sqrt{\bar{\tau}}}, \tag{8.17}$$

and the complex charges

$$\mathcal{L}_0 = \frac{1}{2}(\mathcal{M} - i\mathcal{J}), \qquad \bar{\mathcal{L}}_0 = \frac{1}{2}(\mathcal{M} + i\mathcal{J}). \tag{8.18}$$

These charges are constructed from the complex Killing vector fields

$$\zeta_0 = \frac{1}{2}(\partial_t + i\partial_\varphi), \qquad \bar{\zeta}_0 = \frac{1}{2}(\partial_t - i\partial_\varphi). \tag{8.19}$$

Then the density matrix of the scalar field in the southern diamond takes the form

$$\rho_E^S = C \exp\left(-\beta\mathcal{L}_0 - \bar{\beta}\bar{\mathcal{L}}_0\right). \tag{8.20}$$

[15] We are choosing the normalization of the time-like Killing vector to be fixed at $\mathcal{I}$, as is appropriate for a CFT description. By normalizing at $\tilde{r} = 0$ instead, one would obtain the apparent temperature seen by a local observer [75].

8.4. The Boundary Stress Tensor and Virasoro Charges

In this subsection we define, compute and interpret the Brown-York boundary stress tensor in static coordinates, following [45].

In the static coordinates $\mathcal{I}^{\pm}$ is at $r \to \infty$. The metric takes the asymptotic form

$$ds^2 = -\frac{dr^2}{r^2} + (r^2 - \frac{M}{2})dwd\bar{w} + \frac{\tau}{4}dw^2 + \frac{\bar{\tau}}{4}d\bar{w}^2 + \mathcal{O}(\frac{1}{r^4}), \tag{8.21}$$

with

$$w \equiv \varphi + it. \tag{8.22}$$

Since $w \sim w + 2\pi$, the boundary is a cylinder with conformal metric

$$ds^2_{\text{conf}} = dwd\bar{w}. \tag{8.23}$$

dS_3 has an infinite number of asymptotic symmetries, whose associated bulk vector fields ζ generate the conformal group on $\hat{\mathcal{I}}^-$[16]. With each of these symmetries there is an associated charge. A general procedure for constructing such charges for spacelike slices ending on a boundary was given in [76], adapted to AdS in [77], and adapted to dS in [16]. For dS_3 in planar coordinates, $\mathcal{I}^-$ is a plane and the charges are

$$\begin{aligned} L_n &= \frac{1}{2\pi i}\oint dz\, T_{zz} z^{n+1}, \\ \bar{L}_n &= -\frac{1}{2\pi i}\oint d\bar{z}\, T_{\bar{z}\bar{z}} \bar{z}^{n+1}, \end{aligned} \tag{8.24}$$

where T_{zz} is the boundary stress tensor given by [76,77,16]

$$T_{\mu\nu} = \frac{1}{4G}\big[K_{\mu\nu} - (K+1)\gamma_{\mu\nu}\big]. \tag{8.25}$$

Here $\gamma_{\mu\nu}$ is the induced metric on the boundary, and the extrinsic curvature is defined by $K_{\mu\nu} = \frac{1}{2}\mathcal{L}_n\gamma_{\mu\nu}$ with n^μ the future-directed unit normal. The contour integral is over the S^1 boundary of $\mathcal{I}^-$ in planar coordinates at $|z| = \infty$. The AD

mass [78] is proportional to $L_0 + \bar{L}_0$. The complex coordinates on the boundary cylinder in (8.21) are related to those of the plane by

$$z = e^{-iw}. \tag{8.26}$$

In the previous section charges $\mathcal{L}_0$ and $\bar{\mathcal{L}}_0$ were constructed for weak scalar field excitations on a fixed de Sitter background. These can be related to the weak field limit of L_0 and $\bar{L}_0$ by using the conservation equation [76]

$$\frac{1}{2\pi}\nabla^\mu T_{\mu\nu} = n^\mu \mathcal{T}_{\mu\nu}, \tag{8.27}$$

which states that the failure of $T_{\mu\nu}$ to be conserved is given by the matter flux across the boundary. Contracting both sides of (8.27) with a Killing vector ζ and integrating over a disc Σ_C spanning a contour C on $\mathcal{I}^-$ yields

$$\frac{1}{2\pi}\int_C d\sigma^\mu T_{\mu\nu}\zeta^\nu = \int_{\Sigma_C} d\Sigma^\mu \mathcal{T}_{\mu\nu}\zeta^\nu, \tag{8.28}$$

where $d\sigma^\mu$ is the normal boundary volume element normal to the curve C. Comparing with (8.11), (8.18), and (8.19), we see that integrand on the right hand side of this expression for L_0 ($\bar{L}_0$) agrees with that in the expression for $\mathcal{L}_0$ ($\bar{\mathcal{L}}_0$). [16] Of course when the fields are not weak there are gravitational corrections to the bulk expressions.

The cylinder charges corresponding to (8.24) are [17]

$$H_n = -\frac{1}{2\pi}\int_0^{2\pi} dw\, T_{ww} e^{-inw} \tag{8.29}$$

[16] Our sign convention in (8.24) was chosen so that in the weak field limit $\mathcal{H}$ reduces to the integral of the scalar stress energy density, without a relative minus sign. This convention agrees with [16,45,65], but differs by a sign from [49,50].

[17] A minus sign arises in this expression from the relative orientation of the z and w contours.

and its complex conjugate. We have used the symbol H_n rather than L_n because on the cylinder (8.29) includes a Casimir energy contribution for H_0. We will be interested in H_0, which is the charge associated to the vector field

$$\zeta_0 = \frac{1}{2}\left(\partial_t + i\partial_\varphi\right). \tag{8.30}$$

For $r \to \infty$ one finds

$$T_{ww} = \frac{1}{4G}\gamma_{ww} = \frac{\tau}{16G}. \tag{8.31}$$

Integrating around the cylinder then gives

$$H_0 = -\frac{1}{2\pi}\int_0^{2\pi} d\varphi\, T_{ww} = -\frac{c}{24}\tau, \tag{8.32}$$

and similarly

$$\bar{H}_0 = -\frac{c}{24}\bar{\tau}. \tag{8.33}$$

For later convenience we have written these expressions in terms of the dS_3 central charge

$$c = \frac{3\ell}{2G}, \tag{8.34}$$

where we have restored the factor of the de Sitter radius ℓ. However, so far our discussions have been purely classical.

We note for pure de Sitter space ($M = 1$ and $J = 0$) $H_0 = -\frac{c}{24}$. This has a nice interpretation in the dual field theory on the boundary, as discussed in [45].[18] According to [16], the bulk gravity state on the slice $t = \infty$ in planar coordinates is dual to a CFT state on the S^1 boundary of $\mathcal{I}^-$ (i.e., where the slice $t = \infty$ intersects $\mathcal{I}^-$) at $z = \infty$. This state is the wave functional produced by fixing boundary conditions on the S^1 and then doing the CFT path integral over the disc. This should give the $SL(2,C)$ invariant ground state of the CFT. Transforming from planar to static coordinates in the bulk is then dual to the conformal mapping

[18] An alternate interpretation was given in [49].

from the plane to the cylinder. This mapping should produce, via the Schwarzian in the stress tensor transformation law, the Casimir energy $-\frac{c}{24}$ for a CFT with central charge c on a circle of radius 1. Indeed this agrees beautifully with the fact that the boundary stress tensor vanishes in planar coordinates but gives $H_0 = -\frac{c}{24}$ in static coordinates.

We note for future reference that the state so constructed on $\mathcal{I}^-$ is a pure state with no entropy.

The agreement with the CFT picture persists for general τ. (8.32) is then precisely the Casimir energy from conformal mapping from the plane to a cone. We note also that as M decreases, the energy H_0 increases, in accord with the expectation that a positive deficit angle has a positive mass.

9. Entropy

In this section we discuss the conditions under which the entropy (8.5) might be microscopically derived from a 2D CFT. Related discussions have appeared in [11,48,49].

Consider the canonical partition function of a 2D CFT with complex potential β,

$$Z = \int dL_0\, d\bar{L}_0\, \rho(L_0, \bar{L}_0)\, e^{-\beta L_0 - \bar{\beta}\bar{L}_0}, \tag{9.1}$$

where ρ is the density of states. We wish to evaluate this in the saddle point approximation. Let us assume that we are in a regime where the thermodynamic approximation is valid, and we can use Cardy's formula [79] for the density of states[19]

$$\rho(L_0, \bar{L}_0) = \exp\left[2\pi\sqrt{\frac{c}{6}(L_0 - \frac{c}{24})} + 2\pi\sqrt{\frac{c}{6}(\bar{L}_0 - \frac{c}{24})}\right], \tag{9.2}$$

[19] Since we are working in the canonical, rather than microcanonical picture, the final formula for the entropy is unaffected by the shift of L_0 in the exponent.

When β is complex, (9.1) has a complex saddle point at $L_0 = \frac{\pi^2 c}{6\beta^2} + \frac{c}{24}$.[20] Evaluating the integral at the saddle point and using $S = (1 - \beta\partial_\beta - \bar{\beta}\partial_{\bar{\beta}}) \ln Z$ gives

$$S = \frac{\pi^2 c}{3\beta} + \frac{\pi^2 c}{3\bar{\beta}}. \tag{9.3}$$

If we now use the formula

$$c = \frac{3\ell}{2G}, \tag{9.4}$$

for the central charge of the boundary CFT, together with the formula

$$\beta = \frac{2\pi}{\sqrt{M - i(8GJ)}}, \tag{9.5}$$

derived in section 6.3 for the complex temperature of Kerr-dS$_3$, the microscopic formula (9.3) reproduces exactly the macroscopic formula (8.5) for the Bekenstein-Hawking entropy of Kerr-dS$_3$.

This yields a two-parameter fit relating the area of the Kerr-dS$_3$ horizon to the number of microstates of a 2D CFT. However with our current understanding, this should be regarded as highly suggestive numerology rather than a derivation of the entropy. One problem is that the dual CFT is not unitary, and hence is not obligated to obey Cardy's formula. A second problem is that we have not specified where the CFT density matrix resides whose entropy is being computed. In most discussions—including ours—the quantum state on global de Sitter is in a pure state. Furthermore its dual—as discussed at the end of the previous section—is the $SL(2, C)$ invariant CFT vacuum. A density matrix arises only after tracing over a correlated but unobservable sector. We saw in section 6.3 that for a scalar field in the (pure) Euclidean vacuum state, a thermal density matrix arises after a northern trace over the Hilbert space in the unobservable northern diamond. One might expect that the quantum state of the boundary CFT would also become

[20] For pure dS$_3$ this is $L_0 = \frac{c}{12}$, as in [11].

thermal after performing a similar trace. However it is not clear to us exactly what a northern trace corresponds to in the boundary CFT on $\mathcal{I}^{\pm}$.

It appears that de Sitter entropy arises when attention is restricted to the true observables in the theory. The boundary CFT includes information about correlators at acausal separations that do not directly correspond to observable data. It is a challenging and important problem to understand what are the true observables in the language of the of the boundary CFT.

Acknowledgements

We are grateful to M. Aganagic, T. Banks, M. Headrick, G. Horowitz, A. Karch, G. Moore, M. Spradlin, N. Toumbas, A. Volovich and E. Witten for useful conversations. This work was supported in part by DOE grant DE-FG02-91ER40654, an NSF Graduate Fellowship, and by the National Science Foundation under Grant No. PHY99-07949.

Appendix A. Alternate Forms of Green Functions on dS_d

In this Appendix we present several alternate expressions for the Green functions.

First, let us consider a de Sitter invariant vacuum $|\Omega\rangle$, so that the wave equation for $G_\Omega(x, x')$ becomes

$$(1 - P^2)\partial_P^2 G - dP\partial_P G - m^2 G = 0, \tag{A.1}$$

where P is related to the geodesic distance $\theta(x, x')$ by

$$P = \cos\theta. \tag{A.2}$$

Note that if G_{d,m^2} solves (A.1) in d dimensions for mass-squared m^2, then $\partial_P G_{d,m^2}$ solves (A.1) in $d+2$ dimensions with mass-squared $m^2 + d$. This gives an iterative

procedure for constructing Green's functions in all dimensions. We find

$$\begin{aligned} G_{3+2n,m^2} &= \partial_P^n G_{3,m^2+1-(n+1)^2} \\ G_{2+2n,m^2} &= \partial_P^n G_{2,m^2-n(n+1)} \end{aligned} \tag{A.3}$$

where n is a positive integer.

Let us first consider odd d. For $d = 3$, if we let

$$G_{3,m^2} = \frac{\chi}{\sin\theta} \tag{A.4}$$

then χ satisfies

$$\partial_\theta^2 \chi + (1 - m^2)\chi = 0. \tag{A.5}$$

So the general solution in 3 dimensions is

$$G_{3,m^2} = \frac{A \sinh \mu(\pi - \theta) + B \sinh \mu\theta}{\sin\theta} \tag{A.6}$$

where $\mu = \sqrt{m^2 - 1}$ and A and B are arbitrary constants. The first term gives the usual short distance singularity for the Euclidean vacuum—with the correct normalization, it gives the usual expression (3.9). The second term is present for the transformed vacuum states $|\alpha\rangle$, and has the antipodal singularities mentioned in section 2.2. From (A.3) we can obtain an expression for the Green functions in higher dimensions,

$$\begin{aligned} G_{d,m^2} = \sum_{m=0}^{n} \binom{n}{m} \frac{\Gamma(n - m + 2i\mu)}{\Gamma(m + 1 + 2i\mu)} \sin^{2-d}\theta \\ (A \sinh(2\mu - in + 2im)(\pi - \theta) + B \sinh(2\mu - in + 2im)\theta) \end{aligned} \tag{A.7}$$

where $n = \frac{1}{2}(d - 3)$ and

$$\mu = \sqrt{m^2 - \left(\frac{d-1}{2}\right)^2}. \tag{A.8}$$

We have absorbed an overall normalization into the constants A and B. As a function of θ, G has isolated singularities but no branch cuts. However, $\theta = \cos^{-1} P$

has a branch cut from $P = 1$ to ∞ along the real axis, across which $\theta(P)$ changes sign. When expressed as a function of P, G will likewise have a branch cut.

For even d, we start with the $d = 2$ solution in terms of Legendre functions

$$G_{2,m^2} = AP_\nu(\cos\theta) + BQ_\nu(\cos\theta) \tag{A.9}$$

where $\nu(\nu+1) = -m^2$. So

$$G_{d,m^2} = AP_\nu^{(n)}(\cos\theta) + BQ_\nu^{(n)}(\cos\theta) \tag{A.10}$$

where $n = \frac{1}{2}(d-2)$ and $\nu(\nu+1) = n(n+1) - m^2$. Here, $P_\nu^{(n)}$ is an associated Legendre function, the n^{th} derivative of the Legendre function.

Appendix B. Properties of Hypergeometric Functions

We collect a few relevant facts about hypergeometric functions. More details may be found in, e.g., [69].

The formula

$$F(a,b;c;z) = (1-z)^{c-a-b}F(c-a,c-b;c;z) \tag{B.1}$$

relates hypergeometric functions of z with different values of parameters, as in (7.7). To relate hypergeometric functions of different variables we use

$$\begin{aligned} F(a,b;c;z) &= \frac{\Gamma(c)\Gamma(b-a)}{\Gamma(c-a)\Gamma(b)}(-z)^{-a}F(a,a+1-c;a+1-b;\frac{1}{z}) \\ &\qquad + \frac{\Gamma(c)\Gamma(a-b)}{\Gamma(a)\Gamma(c-b)}(-z)^{-b}F(b,b+1-c;b+1-a;\frac{1}{z}) \\ &= \frac{\Gamma(c)\Gamma(c-a-b)}{\Gamma(c-a)\Gamma(c-b)}F(a,b;1+a+b-c;1-z) \\ &\qquad + \frac{\Gamma(c)\Gamma(a+b-c)}{\Gamma(a)\Gamma(b)}(1-z)^{c-a-b}F(c-a,c-b;c-a-b+1;1-z). \end{aligned} \tag{B.2}$$

These give us the Bogolyubov relations (4.21) and (4.39), respectively. Since $F(a,b;c;0) = 1$ these equations also fix the behavior of $F(a,b;c;z)$ as $z \to \infty$ and $z \to 1$, as in (5.2), (7.9) and (7.20).

Chapter 3

de Sitter Space in Non-Critical String Theory [21]

10. Introduction

Recent progress in string theory has led to deep conceptual insights into the quantum nature of a number of spacetime geometries, including black holes and AdS. dS (de Sitter) has so far been largely left out of the fun. A key reason for this is that so far no fully satisfactory dS solution of string theory has been found.[22] The problem is intrinsically difficult because there can be no unbroken supersymmetry in dS [85]. Hence the solutions are likely to be isolated with no massless scalars or moduli.

A recent approach [86] employs supercritical superstring theory. Although they do not have flat space as a solution, noncritical string theories are of intrinsic interest for a wide variety of reasons. They are implicated in tachyon decay processes in compact closed string backgrounds [87], and in attempts to obtain the QCD string [88]. Their precise place in the M-theory duality web remains an outstanding question. New cosmological solutions (with a strongly coupled singularity) of supercritical string theory were discussed in [89]. The recent application to de Sitter space [86] utilizes an asymmetric orientifold construction in non-critical 12-dimensional string theory which has no moduli. The supercriticality introduces a leading-order cosmological term (dilaton potential) which aids in fixing the dilaton. By turning on RR fluxes it is possible to arrange for the dilaton to have a nontrivial minimum with a positive cosmological constant. The string coupling at the minimum is numerically, but not parametrically, small. However, as stressed in [86], the

[21] This chapter is based on the paper [2], with E. Silverstein and A. Strominger.

[22] However there are a number of interesting constructions which may not have been fully exploited [80-84].

true expansion parameter about the minimum – and the nature of string perturbation theory about a minimum which balances dilaton tadpoles from noncriticality against RR fluxes – are not understood. For both of these reasons the existence of a string perturbation expansion about the minimum is in question, and strong coupling effects could in principle eliminate the dS solution. A second issue in this model is that the dS minimum is unstable to decay to flat space. This implies that not every point on the asymptotic boundary of the space is dS. One of the recent lessons of string theory is that the nature of the boundary can be quite important, so a theory which asymptotically decays to flat space may be very different from a "stable" dS.

In this paper we report on work in progress which improves on this construction. A generalized asymmetric orientifold construction is introduced with a new parameter: the number of dimensions D. By making the number of dimensions large and employing the Bousso-Polchinski mechanism [90] with the RR fluxes we are able to make the cosmological constant at the minimum parametrically small, the higher-dimensional string coupling parametrically weak, and the effective barrier to the linear dilaton regime parametrically large. Despite this improvement we have not understood the true expansion parameter about the minimum, which could therefore in principle be eliminated by strong coupling effects.

In particular, as a function of the dimensionality D, the number of RR fields is $n_{RR} = 2^D$, which dominates the spectrum at large D. This is potentially both a liability and an asset: on the one hand, the 2^D RR species threaten to render the effective coupling uncontrollably large; on the other hand, the large number of RR fluxes facilitate the construction of vacua with small cosmological constant and weak D-dimensional string coupling. As one increases D, the naive number of degrees of freedom increases, and as we will see one can obtain a larger and larger de Sitter space. It is tempting to speculate that the 2^D RR degrees of freedom pertain

to the entropy; this will be interesting to explore in the future. In particular, since a large de Sitter space requires a large number of states (to account for the large entropy), the large number of degrees of freedom intrinsic to supercritical string theory may play a natural role.

We also consider, in a more general setting, the issue of the decay of dS space to flat space. When the barrier is small such decays clearly occur via flat space bubble nucleation and are described by gravitational instantons. However, the required bubble size grows with the barrier height, and eventually the bubble wall crosses the horizon. We will argue that the inclusion of such superhorizon processes has bizarre consequences. Causality and unitarity appear to be violated, and for very large height the process describes the tunneling of the entire universe to a planckian region! The proper rules for dS quantum gravity are not well understood, and this casts doubt on the assertion that such instantons should be included in the first place. We further note that the tunneling time exceeds the Poincare recurrence time for dS [91] for exactly the same parameter range that the instanton becomes superhorizon sized. (It also exceeds the (shorter) time for all of de Sitter space to tunnel into a maximal black hole [92].) Hence both the observable significance and the validity of the semiclassical approximation are in question for the superhorizon decay processes.[23] If the superhorizon instantons are excluded, a "false" dS vacuum may be stable against decay to flat space (or to the linear dilaton regime in the case of the supercritical models), or equivalently the decay time may become so long as to be meaningless.

In the supercritical models, one can in this way potentially forbid decays from a large range of dS minima to the linear dilaton regime, since as we will see the

[23] As discussed in section 3.4 and alluded to in [93], this is a de Sitter analog of the breakdown of the semiclassical approximation for black holes discussed in [94]. Related discussions can be found in [95,96].

domain wall tension is too large for a sub-horizon size bubble. However, we also find decays between different flux vacua proceeding via nucleation of D-branes (as in [97,90,93]), including transitions from dS to AdS. The model thus is a stringy construction sharing features with those studied in [98,97,90,93] exhibiting a dynamical relaxation of the cosmological constant. Among the different flux vacua, there are many more choices of flux configuration yielding larger values of the cosmological constant than smaller values, and in our system there are large degeneracies among different flux vacua due to the highly symmetric structure of the internal dimensions.

This paper is organized as follows. Section 2.1 presents the asymmetric orientifold construction. 2.2 describes the de Sitter minima, and 2.3 discusses the lower limit on the cosmological constant implied by flux quantization. 3.1 reviews the instantons which describe the tunneling from de Sitter to flat space. 3.2 questions the conventional wisdom that this tunneling occurs (or is even well-defined) for arbitrarily high barriers. 3.3 relates this to Poincare recurrence and the breakdown of the semiclassical approximation. Finally in section 3.4 we address the stability of the asymmetric orientifold models.

11. de Sitter Compactifications of Super-Critical String Theory

In this section we generalize the construction of [86] to large numbers D of dimensions and describe de Sitter solutions of the low energy action. We compute the contributions to the dilaton potential from noncriticality, orientifold planes and RR fluxes. We demonstrate that by taking the number of dimensions to be large, one can find potentials having minima at a parametrically small value of the D-dimensional string coupling. Finally, we consider flux quantization and show that at large D the cosmological constant can be made parametrically small.

11.1. Asymmetric Orientifolds in Non-Critical String Theory

In D (more than 10) dimensions, we start with the string frame low energy effective theory for the graviton, dilaton and Ramond-Ramond fields

$$S_D = \frac{1}{2\kappa_D^2}\int d^D x\sqrt{-G}\left(e^{-2\phi}\left(R - \frac{2(D-10)}{3\alpha'} + 4\nabla_\mu\phi\nabla^\mu\phi\right) - \frac{1}{2}\sum_p (F_p)^2\right) \tag{11.1}$$

where the sum runs over the various RR fields F_p in the theory.

We will be interested in asymmetric orientifold models obtained from this D-dimensional theory in which the dilaton is fixed. Let us begin by noting a few salient points regarding the spectrum in these relatively unfamiliar theories. Note from the action (11.1) (and as discussed in [99] and reviewed in [86]), the graviton, dilaton, and RR fields in D dimensions are massless. However, if one calculates using free field theory the putative zero-point energy of these fields in flat (string-frame) space, i.e. in the linear dilaton background, one finds in the NS sector a vacuum energy of $-(D-2)/16$. As explained in [99], this reflects the effective tachyonic behavior of the fields in the linear dilaton background (obtained from (11.1) by expanding in small fluctuations about the linear dilaton solution). In order to obtain the effective mass squared of the fields in the Lagrangian expanded around a putative extremum with constant dilaton (such as those we are studying in this paper) one must therefore cancel the contribution from the linear dilaton from the zero point energy. This amounts to the statement that in the NS sector, the effective vacuum energy E is off from the free field result E_0 by

$$E = E_0 + \frac{D-10}{16}. \tag{11.2}$$

Let us now proceed to the models of interest here, which are compactifications from D down to $d = D - r$ dimensions. We will eventually be interested in the case of large D with d held fixed, and in particular how various quantities depend on D.

Because as we will see the quantities relevant to our conclusions scale exponentially with D, some numerical factors which are order one will not be explicitly computed.

We begin with a self-dual torus T^r. The zero modes on the torus are given by

$$\begin{aligned} p_L^i &= \frac{1}{\sqrt{\alpha'}}(m^i + n^i) \\ p_R^i &= \frac{1}{\sqrt{\alpha'}}(m^i - n^i) \end{aligned} \tag{11.3}$$

and the dimensions of the corresponding worldsheet operators are $(\frac{\alpha'}{4}p_L^2, \frac{\alpha'}{4}p_R^2)$. Mod out by the orientifold group generated by

$$g_1 \equiv (0, s^2)_{d+1} \dots (0, s^2)_{d+r} \tag{11.4}$$

$$g_2 \equiv (-1, 1)_{d+1} \dots (-1, 1)_{d+r} \tag{11.5}$$

$$g_3 \equiv \Omega I_r \tag{11.6}$$

$$g_4 \equiv (-1)^F (s, s)_{d+1} \dots (s, s)_{d+r} \tag{11.7}$$

As in [86], we adopt the following notation. $(0, s^2)_i$ is an asymmetric shift on the i^{th} coordinate, and acts as $(-1)^{n^i+m^i}$. $(s, s)_i$ is a geometric shift on the i^{th} coordinate by half the circle radius, and acts as $(-1)^{m^i}$. Ω is an orientation reversal, I_r a reflection on all r coordinates of the T^r. $(-1, 1)_i$ is a reflection on the i^{th} left-moving coordinate only, and is at the heart of the moduli-fixing effect of this model, since it projects out all the untwisted NS NS moduli.

In order to check level-matching (for modular invariance) and to check for twisted moduli, we must compute the vacuum energy in all inequivalent sectors, taking into account (11.2). Let us start with the shifts. In the $(0, s^2)^r$ twisted sector, the momentum and winding lattice (11.3) is shifted so that $(m, n) \to (m + 1/2, n + 1/2)$, while in the (s, s) sector it is shifted by $(m, n) \to (m, n + 1/2)$. Each $(0, s^2)$ shift (per direction) has a right-moving energy of $1/4$, while each (s, s)

shift (per direction) gives left and right moving energies of 1/16. For the element $g_2 = (-1,1)^r$, we have ground state energies

$$(E_L = \frac{r}{8} - \frac{1}{2}, E_R = -\frac{1}{2}) \tag{11.8}$$

This level-matches if $r = 4k$ for integer k. In order to avoid any massless modes (potential moduli) in this sector, we must take $k > 1$. For the element $g_2 g_4$ we have

$$(E_L = \frac{r}{8} - \frac{1}{2} = \frac{k-1}{2}, E_R = \frac{r}{16} - \frac{1}{2} = \frac{k-2}{4}), \tag{11.9}$$

requiring that $k \equiv 2N$ be even for level-matching. As discussed in [99], in order to have a standard GSO projection, one requires $D = d + r \equiv 8j + 2$ for integer j. Altogether, in order to have a consistent orientifold group we need

$$r = 8N \tag{11.10}$$

for integer $N \geq 1$, and to have an ordinary GSO projection we need

$$d = D - 8N = 8j + 2 - 8N. \tag{11.11}$$

This model has two sets of orientifold planes – O-$(d-1)$-planes generated by the element g_3 and spacefilling O-$(D-1)$-planes generated by the T-dual element $g_2 g_3 g_2 = \Omega$. We also have anti-orientifold planes, which are necessary to cancel the RR tadpoles – these are generated by the elements $g_3 g_4$ and $g_2 g_3 g_4 g_2$. The total contribution to the action due to these orientifold planes is

$$S_{\text{Orientifold}} = \sum_i T_{O_i} \int d^{p_i+1} x \sqrt{-G} e^{-\phi} \tag{11.12}$$

where i runs over the orientifolds – here the orientifold group acting on the r dimensions of our torus introduces 2^{r-1} O-$(d-1)$ planes, 2^{r-1} $\bar{O}$-$(d-1)$ planes, as well as the T-dual objects, an O-$(D-1)$ plane, and an $\bar{O}$-$(D-1)$ plane. These

T-dual pairs are identified under the action of g_2, so (11.12) is just 2^r times the action for a single O_{d-1} plane:

$$\begin{aligned} S_{\text{Orientifold}} &= 2^r T_{O_{d-1}} \int d^d x \sqrt{-G} e^{-\phi} \\ &= -\frac{2^{7/2+D/4}\pi^{1/2}}{\kappa_D \ell_s^{1-D/2+d}} \int d^d x \sqrt{-G_d} e^{-\phi}. \end{aligned} \tag{11.13}$$

Here we have defined the string length

$$\ell_s = 2\pi\sqrt{\alpha'} \tag{11.14}$$

and are using the generalized formula for the tension of an orientifold p-plane in D dimensions derived in [86] with the assumptions listed there (which consist essentially of the procedure (11.2) for the closed-string channel modes applied to the annulus diagram),

$$2^{D-(p+1)} T_{O_p} = -\frac{2^{7/2+D/4}\pi^{1/2}}{\kappa_D \ell_s^{p+2-D/2}}. \tag{11.15}$$

The action of the orientifold group projects out the NS-NS moduli of the T^r, so the d-dimensional action for the untwisted NS-NS sector reduces to

$$S_{\text{NS}} = \frac{1}{2\kappa_d^2} \int d^d x \sqrt{-G_d} e^{-2\phi} \left(R_d - \frac{2(D-10)}{3\alpha'} + 4\nabla_\mu \phi \nabla^\mu \phi \right) \tag{11.16}$$

where the d-dimensional gravitational coupling is

$$\kappa_d^2 = \frac{\kappa_D^2}{v \ell_s^r} = v^{-1} \ell_s^{d-2}. \tag{11.17}$$

v here is the dimensionless effective volume of the compactification space given by

$$\left(\int_{T^r} d^{4m} x \sqrt{-G_r} \right)_{eff} = v \ell_s^r, \tag{11.18}$$

and is of order one. We have taken the D-dimensional coupling to be $\kappa_D^2 = \ell_s^{D-2}$.[24]

[24] In making this choice, we are tacitly assuming that high order terms in the perturbation series will be $\leq$ order one with respect to this choice of coupling. See the discussion in [86] for more details.

Note that one could also consider multiple copies of this orientifold group acting on subtori of T^r. Each ΩI_p action reduces the RR spectrum by half, so this has the virtue of reducing the number of species which contribute to the effective coupling. However, there is a danger of also reducing the effective volume and thus v in (11.18), thereby increasing the effective coupling. It would be interesting to determine the winner of the competition between these two effects, but for now we will stick to a single copy of the orientifold group (11.4)-(11.7).

We now turn on some RR fluxes along the compact directions (see, e.g. [100–106]). In D dimensions, a p-form field strength wrapped on a cycle of volume V_p will be quantized as

$$\frac{1}{2\kappa_D}\int_{V_p} F_p = \sqrt{\pi}\ell_s^{\frac{2p-D}{2}} Q \tag{11.19}$$

where Q is an integer. Let us use a basis of cycles given by the square subtori $\subset T^r$. We will label these by $i = 1, \ldots, 2^r$. Turning on RR fluxes adds a dilaton independent piece to the d dimensional string frame action. Before orientifolding, there are $\binom{r}{k}$ possible k-form fluxes to choose from, for a total of 2^r. Although some of the internal fluxes will be projected out by the orientifold action, certain flux configurations will be left invariant. These invariant combinations of fluxes from the untwisted sector of the orbifold, which involve fluxes of different rank related to each other by T-duality, will also be subject to the quantization condition inherited from the parent theory. Because our orbifold is of finite order independent of r, the number of invariant fluxes still scales like 2^r for large r after taking into account the reduction in the RR spectrum effected by the orientifold action. Chern-Simons couplings among the many RR fields at large D may also affect the spectrum in a given flux background, and the set of consistent choices of flux configuration; this would be interesting to work out in detail.

Going to d-dimensional Einstein frame

$$G_{d\mu\nu} \to \tilde{G}_{\mu\nu} = G_{d\mu\nu} e^{\frac{4\phi}{2-d}} \tag{11.20}$$

the low energy action becomes

$$S = \frac{1}{2\kappa_d^2} \int d^d x \sqrt{-\tilde{G}} \left(\tilde{R} - \left(\frac{4}{(d-2)} \right) \partial_\mu \phi \partial^\mu \phi - \frac{1}{v \ell_s^2} U(\phi) \right). \tag{11.21}$$

The Einstein frame dilaton potential is

$$U(\phi) = e^{\frac{4}{d-2}\phi} (a - b e^{\phi} + c e^{2\phi}) \tag{11.22}$$

where

$$\begin{aligned} a &= v 4\pi^2 \left(\frac{2(D-10)}{3} \right) \\ b &= 2\ 2^{7/2 + D/4} \pi^{1/2} v_O \\ c &= \sum_{i=1} \frac{\pi}{v_{p_i}} Q_i^2 \ell_s^{2p_i - D} + \Lambda_1 \equiv \pi \sum_{i=1} \tilde{Q}_i^2 + \Lambda_1. \end{aligned} \tag{11.23}$$

Here in the expression for b, v_O is a dimensionless volume associated with the orientifold planes on our orbifold similar to v; again this is of order 1 in our model and we will not keep track of such factors in our analysis. In the expression for c, i labels the fluxes in the square basis discussed above, and we consider only invariant combinations of these basic fluxes. p_i is the degree of the field strengh and v_{p_i} is an order one dimensionless volume associated to the i^{th} flux. (Before the orientifolding, these volumes are self-dual, but as in (11.21)the effective volumes may be reduced by the action of the orientifold group.)

Λ_1 is the one-loop dilaton potential. It will be proportional to $n_{RR} \sim 2^D$ times $\xi(D)$ where $\xi(D)$ is an unknown D-dependent constant, which is related to the effective loop-counting parameter in our theory. (For some insight into the scaling of loop effects in gravitational field theory as a function of dimension D, see [107], where factors of $1/D!$ appear with additional loops, providing enhanced control at large D.) Because the 2^D RR bosons dominate the spectrum, Λ_1 is likely to be negative in the string theoretically regulated theory, similarly to the situation in for example Scherk-Schwarz compactifications [108] and many other non-supersymmetric orbifold examples that have been analyzed in critical string

theory, in which one finds the sign of Λ_1 to be the same as that of the difference between the number of massless fermions and bosons in the tree-level spectrum. Below, we will analyze the potential assuming conservatively that $\Lambda_1 \sim -2^D$ for definiteness, but as will become clear the qualitative results apply for a large range of possible values of Λ_1 including those with smaller magnitude.

In principle, we should also include a renormalization of Newton's constant at the same order; this will not affect the perturbative stabilization in what follows in this section, but nonperturbatively may adjust the instanton actions in §3.

11.2. de Sitter Solutions

Let us write the potential as

$$U(\phi) = \left(a - be^{\phi} + \frac{b^2}{4a}(1+\delta)e^{2\phi}\right)e^{\frac{4\phi}{d-2}}. \tag{11.24}$$

There is a de Sitter solution if $U(\phi)$ has a stable minimum at positive energy. This requires that the solutions of $U'(\phi) = 0$

$$e^{\phi_\pm} = \frac{a}{db}\left(\frac{d+2 \pm \sqrt{(d-2)^2 - 8d\delta}}{1+\delta}\right) \tag{11.25}$$

are real – here $\phi_\pm$ is the local minimum (maximum). In addition the effective cosmological constant

$$\Lambda = U(\phi_+), \tag{11.26}$$

should be greater than zero. These two conditions require that

$$0 < \delta < \frac{(d-2)^2}{8d}. \tag{11.27}$$

As δ increases from the lower bound to the upper bound, $U(\phi_+)$ increases from 0 to $\frac{a^{\frac{d+2}{d-2}} 8^{\frac{4}{d-2}} (d-2)^2}{b^{\frac{4}{d-2}} d(d+2)^{\frac{d+2}{d-2}}}$. and the string coupling decreases from $\frac{2a}{b}$ to $\frac{8a}{b(d+2)}$. Near $\delta = 0$, the cosmological constant goes like

$$U(\phi_+) = a(\frac{2a}{b})^{\frac{4}{d-2}}\delta + \mathcal{O}(\delta^2). \tag{11.28}$$

If we wish to minimize the string coupling we must take $\delta \sim \frac{(d-2)^2}{8d}$. For example, in the original scenario of [86] ($D = 12$, $d = 4$) this gives

$$a = \frac{8\pi^2}{3}, \qquad b = \pi^{1/2}2^{15/2}, \qquad \Lambda \sim \frac{1}{(2\pi\alpha^{1/2})^4}(0.05), \qquad e^{\phi_+} \sim 0.11. \quad (11.29)$$

This has the disadvantage that Λ is only a couple orders of magnitude above string scale. Also, the potential barrier seperating the local minimum from the global minimum at $\phi \to -\infty$ is small, so the vacuum is not very stable against tunneling effects. Let us instead try to minimize Λ by taking $\delta \to 0$. We find that (modulo issues of flux quantization, which we will consider in the next section) we can make Λ as small as we like, with

$$\Lambda \sim 0, \qquad e^{\phi_+} \sim 0.16. \quad (11.30)$$

We have found that Λ can be made arbitrarily small, at the cost of a small increase in the string coupling. In addition, this solution is much more stable, since the potential barrier is high.

A solution with small D-dimensional string coupling is found by taking $a/b \to 0$. From the expressions (11.23) it is clear that this can always be accomplished by taking D large. However, it is not clear that this implies a small true effective string coupling after compactification. The latter may for example be enhanced by the enormous multiplicity ($\sim 2^D$) of RR fields. (On the other hand, if things work as in [107], there may in fact be overcompensating loop-suppression factors as a function of D that preserve the smallness of the effective coupling.)

11.3. Solutions With Small Λ

In order to get a small cosmological constant we must take $\delta \to 0$. However, flux quantization constrains how small we can get δ, and thus how small we can get Λ. We see from §2.2 that for $\Lambda \sim 0$ and large D, c approaches a large value

$$c = \pi \sum_i \tilde{Q}_i^2 + \Lambda_1 \to \frac{b^2}{4a} \sim \frac{2^{D/2}}{4a} \quad (11.31)$$

For example, this is $\frac{3072}{\pi}$ in the scenario in [86]. Since $\Lambda_1 \sim -2^D$, we have

$$\pi \sum_i \tilde{Q}_i^2 \sim 2^D. \tag{11.32}$$

By taking linear combinations of many different fluxes we can tune c quite accurately – this is similar to the mechanism of Bousso and Polchinski [90], though in our case we have large degeneracies in the set of flux configurations. The allowed charges Q_i lie on a $q \sim 2^r \sim 2^D$-dimensional lattice. Because of the flux quantization condition, the smallest jumps we can have in c are of order 1. Because of (11.32) and the fact that we have 2^D independent fluxes $\tilde{Q}_i$ to pick, there will always be some $\tilde{Q}_i$ which are of order 1 (or smaller), so order 1 jumps are indeed possible. Using (11.28), this gives for the scale of the lowest-lying de Sitter minima

$$\begin{aligned} \Delta c &\sim \frac{b^2}{4a}\delta \sim 1 \\ \Lambda = U(\phi_+) &\sim \left(\frac{a}{b}\right)^{\frac{2d}{d-2}} \sim 2^{-\frac{Dd}{2(d-2)}} \end{aligned} \tag{11.33}$$

Since $b \sim 2^{D/4}$, this vacuum energy is exponentially small for large D.

12. Metastability of the de Sitter Vacuum

In addition to the de Sitter minimum, the dilaton potential (11.22) has a global minimum with vanishing cosmological constant at $\phi \to -\infty$. Our system also has a multitude of different dS and AdS vacua obtained from different configurations of flux in the internal space. This raises the issue of whether or not the de Sitter minimum is only metastable. This question arises generically in any string construction of a de Sitter solution involving a potential which vanishes at weak coupling, and/or containing many flux vacua.

Instantons have been described [109,97] which might be related to this tunneling. However, as we will see in this section, when the barrier between the minima is sufficiently large, the instanton degenerates and no longer describes tunneling of a

de Sitter horizon volume to a comparably sized-region of flat space. The instanton describes a rather unphysical process in which the visible universe disappears altogether. Such "super-horizon" instantons occur in the parameter range for which the bubble wall lies behind the horizon.

Whether or not such processes actually occur, and whether or not such de Sitter vacua can be stable, are questions which cannot be definitively settled with our present understanding of quantum gravity in de Sitter space. In ordinary field theory, instantons provide saddle point approximation to a functional integral with fixed boundary conditions. The instantons which describe the decay/disappearance of de Sitter space have no boundary at all, and so it is not clear if they should be included. We will argue that the super-horizon instantons in a sense violate both causality and unitarity and should be omitted altogether. We will also discuss other potential mechanisms for mediating vacuum decay.

12.1. The Instantons

For simplicity we work in the thin wall approximation, in which case the relevant instanton solutions are rather simple. They have been described in detail in [97] and will now be reviewed.

The euclidean solutions are characterized by the tension T of the bubble wall and the dS cosmological constant Λ. The solutions are determined by simply matching the extrinsic curvatures on the two sides of the bubble wall to the tension T in accord with the Israel junction condition. The instanton looks like a portion of a round sphere glued to a portion of flat space. The spherical portion is

$$ds^2 = R_{dS}^2\big(d\theta^2 + sin^2\theta d\Omega_3^2\big), \qquad 0 \leq \theta \leq \arcsin\frac{R_B}{R_{dS}}, \tag{12.1}$$

where $d\Omega_3^2$ is the metric on the unit three sphere, $R_{dS} = \sqrt{3/\Lambda}$ is the dS radius, and R_B is the radius of the S^3 boundary. The flat space portion is

$$ds^2 = dr^2 + r^2 d\Omega_3^2, \qquad 0 \leq r \leq R_B. \tag{12.2}$$

The full instanton is then obtained by gluing together (12.1) and (12.2) along the S^3 bubble wall at radius R_B. This is depicted in figure 1a-c. The Israel junction condition

$$\frac{1}{R_B^2} = \frac{1}{R_{dS}^2} + \big(\frac{1}{TR_{dS}^2\kappa^2} - \frac{T\kappa^2}{4}\big)^2 \tag{12.3}$$

where M_P the Planck mass, determines R_B in terms of T. Note that R_B increases with T for small T but then decreases for T greater than the critical value

$$T_C = \frac{2}{\kappa^2 R_{dS}}. \tag{12.4}$$

R_B approaches zero for very large T.

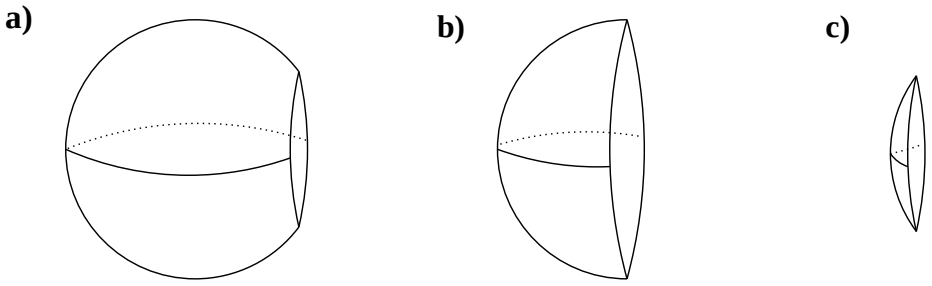

Fig. 1: The Euclidean instanton solutions matching the sphere (Euclidean de Sitter) to flat space. The cases $T < T_C$, $T = T_C$ and $T > T_C$ are shown in figures **a)**, **b)** and **c)** respectively.

It is straightforward to generalize these euclidean solutions to the dS→dS and dS→AdS cases. In general dimension d, the relation (12.3) becomes [97]

$$\frac{1}{R_B^2} = \frac{2\Lambda_o}{(d-2)(d-1)} + \left(\frac{\kappa_d^2 T}{2(d-2)} + \frac{\Lambda_i - \Lambda_o}{(d-1)T\kappa_d^2}\right)^2. \tag{12.5}$$

Here, Λ_o is the initial dS cosmological constant (outside the bubble) and Λ_i is the final cosmological constant Λ_i (inside the bubble). In general dimension d, the critical tension is

$$T_C^2 = \frac{2(\Lambda_o - \Lambda_i)(d-2)}{(d-1)\kappa_d^4}. \tag{12.6}$$

The instanton purportedly describes tunneling from one classical geometry to another. We are interested in an initial dS geometry. The final geometry is then

given by the analytic continuation of the instanton, which describes an expanding bubble of flat space inside dS. The two geometries are glued together along the moment of time symmetry. This is depicted in figure 2a-c. The tunneling rate is purportedly given by the action of the instanton minus the background action of Euclidean dS without a bubble. This is

$$\Delta S = 2\pi^2 R_B^3 T + \frac{2\pi^2}{R_{dS}^2 \kappa^2}\left[2R_{dS}^4 \mp \left\{3R_{dS}^3(R_{dS}^2 - R_B^2)^{1/2} - R_{dS}(R_{dS}^2 - R_B^2)^{3/2}\right\}\right]. \tag{12.7}$$

The upper and lower signs correspond to $T < T_C$ and $T > T_C$, respectively. Again, the expression for general d was worked out in [97] (equations (6.4)-(6.7)).

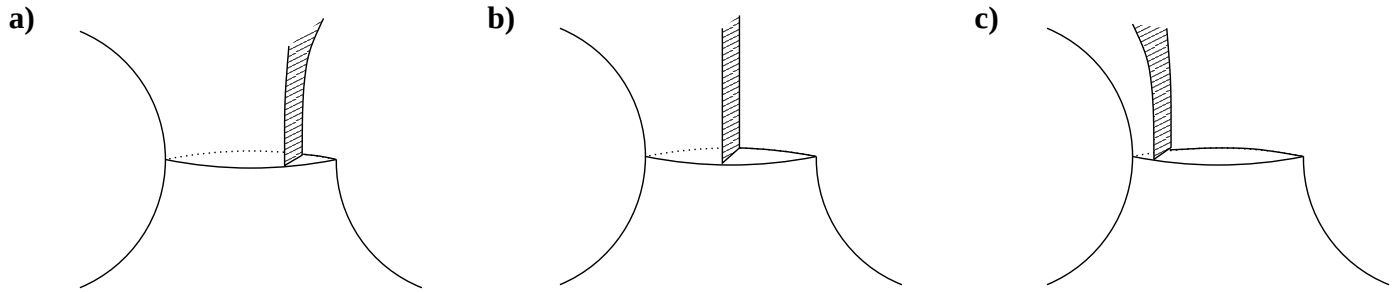

Fig. 2: The Lorentzian instanton geometry describing the nucleation of a bubble of flat space (the shaded region) inside de Sitter space. The cases $T < T_C$, $T = T_C$ and $T > T_C$ are shown in figures **a)**, **b)** and **c)** respectively.

12.2. Causality

The tunneling process depicted for small tensions in figure 2a approaches the usual flat space false vacuum decay in the limit $M_P \to \infty$ with T held fixed. The rate according to (12.7) also approaches the correct flat space value. The instanton of figure 1a surely describes this tunneling process for sufficiently small but finite $\frac{T}{M_P^3}$.

The process depicted in figure 1c on the other hand has a bizarre interpretation. The entire universe tunnels to a small dime, with one flat and one dS face! Furthermore for $T \to \infty$ the rate from (12.7) approaches a constant. Hence the tunneling

rate can be enhanced by adding a large number of ultra-planckian domain walls. In fact, the action (12.7) is not monotonically increasing in the regime $T > T_C$; for certain ranges of paramaters, the tunneling rate *increases* as the tension increases! This conflicts with the notion of decoupling in low-energy field theory, as well as the general fact that tunneling effects are supressed as the size of the barrier increases.

This process also appears in conflict with causality. An observer in dS should be insensitive to any physics behind the horizon. In particular there should be no consequences of placing boundary conditions on the fields along a timelike surface behind the horizon. It is easy to find boundary conditions that forbid the super-horizon instanton. Therefore the observer can learn about physics behind the horizon by waiting to see whether or not the tunneling occurs.

There is also an issue with unitarity. In the benign process of figure 2a, an observer at the south pole finds him or herself, after the tunneling, in the middle of a bubble of flat space. However for the superhorizon case of figure 2c, his or her entire southern causal diamond - the entire observable universe - disappears. It has been advocated by many (see for example [6] and the contribution [110] to these proceedings) that the causal diamond should be viewed as a closed unitary system (whose microstates compute the entropy). Surely this process - in which the diamond disappears altogether- violates unitarity in the worst possible manner!

Based on these observations, our conclusion is that when the tension T exceeds T_C, the superhorizon instantons simply should not be included in the semiclassical description of dS. At the same time we wish to stress that, with our current level of understanding of dS quantum gravity, no such conclusions can be drawn with certainty.

The above arguments apply equally well to tunneling from de Sitter to de Sitter or Anti-de Sitter, with the critical tension given by (12.6). We should note that the

criterion

$$T > T_C \tag{12.8}$$

in the case $\Lambda_o = 0$, $\Lambda_i < 0$ reproduces the well known Coleman and DeLuccia condition for the stability of flat space against tunneling to Anti de Sitter [109]. We may thus regard the stability criterion (12.8) as a generalization of the Coleman - DeLuccia mechanism.

Even if such instantons are not to be included, there may be other processes which mediate the decay of the dS to flat space when the barrier is very high. For example if de Sitter space is viewed as a thermal ensemble[25], thermal fluctuations could eventually push the value of ϕ over the top (see e.g. [111][112] for a discussion of this mechanism). This however is also not obviously possible. There appears to be a maximum energy allowed in dS given by the largest black hole which can fit inside the observer horizon. If the energy required to cross the barrier to flat space exceeds this value, it may be suppressed. Furthermore if the appealing notion [113,114,115] that dS has a finite number of states given by the area law is accepted, there must be a highest energy state. Again if this is less than the barrier height decay to flat space is suppressed.

12.3. Breakdown of the Semiclassical Approximation

There is yet another way to interpret the condition $T^2 > T_C^2 \sim \Lambda$, which involves a further assumption about de Sitter quantum gravity. Following [113], we assume that de Sitter gravity has a finite number of degrees of freedom which determine the de Sitter quantum entropy. Imagine in this context a detector sitting on a timelike geodesic for a very long time. The detector must be built out of a subset of the finite number of degrees of freedom, all of which will eventually be

[25] with temperature conjugate to the energy defined by the timelike Killing vector which preserves the causal diamond

thermalized by de Sitter radiation from the horizon. This thermalization process sets a maximum timescale in de Sitter space, intervals longer than which can never be measured by a geodesic observer. (See also [95,96].) The precise value of the thermalization time depends on the structure of the detector, but it is certainly less than the Poincare recurrence time, which is a timescale on which *all* degrees of freedom have been thermalized. This recurrence time is related to the de Sitter entropy by [91] [26]

$$t_{\rm recurrence} \sim \exp\{S\} = \exp\left\{\frac{8\pi^2 R_{dS}^2}{\kappa^2}\right\}. \tag{12.9}$$

Another time scale in de Sitter is the typical time for the entire space to tunnel to a maximal sized black hole. This has been estimated using instantons in [92] as

$$t_{\rm blackhole} \sim \ (t_{\rm recurrence})^{1/3}. \tag{12.10}$$

Hence the entire space tunnels into a maximal black hole exponentially many times before the Poincare recurrence time.

We wish to compare these times to the expected lifetime of de Sitter space due to vacuum decay. When the tension equals the critical value T_C, the lifetime for the putative instanton decay is (omitting a prefactor which is polynomial in R_{dS})

$$t_{\rm decay} \sim \exp\{\Delta S\} = \exp\left\{\frac{8\pi^2 R_{dS}^2}{\kappa^2}\right\}. \tag{12.11}$$

This is precisely the Poincare recurrence time! Thus as T approaches the critical value T_C the lifetime becomes comparable to the recurrence time, and no observer will ever live long enough to see the vacuum decay. [27] Moreover, at $T = T_C$ the

[26] The authors of [91] considered several different types of recurrence phenomena. Here we quote the timescale for two point fluctuations proportional the thermal background value of the Green function – so called "relative" fluctuations – as opposed to fluctuations of some fixed size independent of S.

[27] Given that the action (12.7) *decreases* at $T >> T_C$ one might worry that naively applying the instanton methods for very large tensions would lead to decay timescales shorter than the recurrence time. This turns out not to be the case: as $T \to \infty$ the decay time precisely approaches (12.11).

lifetime is much longer than the time (12.10)

$$\begin{aligned} t_{\text{decay}} &\sim t_{\text{recurrence}} \\ &\sim t^3_{\text{black hole}}. \end{aligned} \tag{12.12}$$

Hence in order to observe the decay of de Sitter space when $T = T_C$ one needs a detector capable of passing through a black hole exponentially many times. We regard the existence of such detectors doubtful!

Let us state this in yet another way. The semiclassical approximation describes the de Sitter horizon as a hot wall in contact with a heat reservoir with $infinite$ heat capacity. In this approximation no correlations ever appear in the radiation emitted from the horizon. In the exact theory, it is plausible that the horizon has a finite heat capacity as determined from the finite de Sitter entropy. This means that if we watch long enough correlations will be seen in the radiation.[28] A typical time required to see those correlations is the Poincare recurrence time. Hence this time scale signals the breakdown of the semiclassical approximation. A semiclassical instanton which involves a longer time scale therefore cannot be trusted.

Phrased in this way, our argument parallels a similar one give for black holes in [94], and alluded to in the de Sitter context in [93]. In [94], it was argued that the semiclassical approximation for near-extremal black holes breaks down as the temperature goes to zero very near extremality. The breakdown occurs when the energy of a typical thermal Hawking quantum exceeds the excitation energy of the black hole above extremality. Clearly the Hawking emission cannot proceed under these circumstances because it would leave a subextremal black hole with a naked singularity.

This is a close analogy to the situation we have described in the de Sitter context. The hot horizon emits a thermal spectrum of bubbles of flat space. When the

[28] Of course, as mentioned above, no one can live that long. However this only underscores the unphysical nature of a tunneling process which takes such a long time.

energy of these bubbles (as determined in part by the tension of the bubble walls) exceeds the energy of de Sitter space above flat space, the semiclassical approximation breaks down.

In the black hole case, it was eventually quantitatively understood [116] in the context of string theory that this breakdown of the semiclassical approximation signals the appearance of a gap. Presumably similarly interesting and yet-to-be understood phenomena appear in the de Sitter context.

In conclusion, superhorizon tunneling processes from dS to flat space do not appear to be meaningful or consistent. The stability and correct quantum description of a dS vacuum separated by a very high barrier from flat space is an open question.

12.4. Instantons in the Orientifold Model

In the asymmetric orientifold model the tension of the domain wall separating the de Sitter from the flat vacuum at $\phi \to -\infty$ is determined by the shape of $U(\phi)$; for example in $d = 4$ it is roughly

$$T \sim \frac{a^{3/2}}{b}. \tag{12.13}$$

Using the criterion of the previous subsection, we conclude that many of the de Sitter minima discussed in section 2 are stable against decay to the linear dilaton regime. [29] The maximum-energy de Sitter minimum stable under this decay is at $c \sim \frac{b^2}{4a} + \mathcal{O}(b^2)$, i.e. at $\delta \sim 1$. (Here we are only keeping track of exponential dependence on D, i.e. factors of b but not a.) This corresponds to an energy of the order

$$U_+^{max} \sim \frac{1}{b^2} \sim 2^{-D/2} \tag{12.14}$$

[29] We should note that when D is large, the thin wall approximation breaks down for the potentials (11.22); in this limit the width of the domain wall interpolating between the de Sitter and flat vacua scales as T^{-1}. However, this subtlety does not affect the causality considerations of Section 3.2.

The minimum-energy de Sitter minima possible with our quantization condition on the charges and thus on c (which are of course also stable under this decay) have $c \sim \frac{b^2}{4a} + \mathcal{O}(1)$, i.e. at $\delta \sim \frac{a}{b^2}$. This corresponds to an energy of the order

$$U_+^{min} \sim \frac{1}{b^4} \sim 2^{-D}. \tag{12.15}$$

In addition to the instanton decays to the linear dilaton regime discussed above, there is also the possibility of transitions among the different flux vacua, as in [97][90][93][117]. D-branes extended along $d-1$ of the d de Sitter dimensions constitute domain walls separating vacua with different flux configurations. More specifically, D-branes of charge Q connect vacua of flux Q_1 and $Q_1 - Q$ on the dual cycle to the D-brane on the compactification. In order to determine the (in)stability of our solutions, we must apply the results reviewed in §3.1 to such D-brane induced decays in addition to the dilatonic domain wall we considered above.

At our de Sitter minima for $d = 4$, the string coupling is

$$g_s \sim 1/b \tag{12.16}$$

and the energy is

$$U_+ \sim (a^4/b^4)(c - (b^2/4a)) \tag{12.17}$$

As we just discussed, the lowest-lying dS vacua have c tuned to cancel $b^2/(4a)$ to within order 1, so that

$$U_+^{min} \sim 1/b^4 \tag{12.18}$$

The highest-lying dS minima that are stable against decay to the linear dilaton background have, from our earlier calculation, c tuned such that $c - (b^2/4a) \sim b^2$, i.e.

$$U_+^{max} \sim a^2/b^2 \tag{12.19}$$

Recall from (12.6) that

$$T_C^2 \sim \Lambda_o - \Lambda_i. \tag{12.20}$$

The D-brane tension is, in Einstein frame, from [86] and the above scaling of g_s at the minimum,

$$T \sim (1/b^2)2^{-D/4}. \tag{12.21}$$

This formula will apply for a transition in which the bubble wall is a single D-brane; the tension of multiple D-branes will be subject to appropriate binding energy contributions.

If we allow the instanton, i.e. if $T < T_C$, then its action B is given by equation (6.4) in [97]. One should keep in mind that the renormalization of Newton's constant may affect the overall scaling of the action. In addition to the contribution of exp(-action) to the probability for decay, there will also be significant degeneracy factors from the large multiplicity of vacua in our large-D system. Here we will confine ourselves to checking whether the transitions occur at all according to the criterion we have developed in this paper, assuming that the semiclassical instanton analysis applies (i.e. that the action is large enough in renormalized Planck units).

For example, consider decays from $U_+^{max} \to U_+^{max} - a^4/b^4$. This occurs if $c \sim \sum(\tilde{Q}_i)^2$ changes by order 1, and in particular can proceed via a bubble consisting of a single D-brane . In this case, the D-brane tension is

$$T_{(i)} \sim 2^{-D/4}(1/b^2), \tag{12.22}$$

while the critical tension in this case is

$$T_{C(i)} \sim 1/b^2. \tag{12.23}$$

So $T_{(i)} << T_{C(i)}$, and the decay proceeds according to our criterion developed above.

Similarly, there are decays from dS to AdS. Consider for example a transition $U_+^{min} \to -U_+^{min}$. Here again

$$T_{(iii)} \sim 2^{-D/4}1/b^2 \tag{12.24}$$

and

$$T_{C(iii)} \sim 1/b^2 \tag{12.25}$$

so the decay is again allowed.

As we mentioned above, there will be large factors in the transition rates associated with the relative multiplicity of different decay endpoints. In particular, the smaller the value of $\sum \tilde{Q}_i^2 \equiv R^2$ coming into the coefficient c, the fewer choices of flux configuration there are in the window between R and $R + \Delta R$ for a fixed ΔR. So although decays to AdS are possible, it is reassuring that this degeneracy factor prefers the less negative Λ_i values. (In fact these factors also prefer higher dS vacua to lower ones, which may act to suppress the decays depending on the scaling of the renormalized instanton action.)

Acknowledgements

We are grateful to M. Aganagic, T. Banks, R. Bousso, S. Kachru, A. Karch, A. Linde, S. Minwalla, L. Motl, L. Susskind, N. Toumbas and A. Vilenkin for useful conversations. This work was supported in part by DOE grant DE-FG02-91ER40654 and under contract DE-AC03-76SF00515 and by the A.P. Sloan Foundation.

Chapter 4

S-Brane Thermodynamics [30]

13. Introduction

A spacelike brane, or s-brane, is much like an ordinary brane except that one of its transverse dimensions includes time. S-branes arise as time-dependent, soliton-like configurations in a variety of field theories. In string theory, the potential for the open string tachyon field leads to s-branes [118] in a time-dependent version of the construction [119] of D-branes as solitons of the open string tachyon. These s-branes can be thought of as the creation and subsequent decay of an unstable brane. They are of interest as relatively simple examples of time-dependent string backgrounds. Some of the recent investigations can be found in [120-135] and related earlier work is in [136,137].

An elegant worldsheet construction of a family of s-branes was given in the classical $g_s = 0$ limit by Sen [120]. This construction employs an analytic continuation of the conformally-invariant boundary Sine-Gordon model. It describes the tachyon field on an unstable bosonic D-brane by the boundary interaction on the string worldsheet

$$S_{boundary} = \lambda \int d\tau \cosh \frac{X^0(\tau)}{\sqrt{\alpha'}}, \tag{13.1}$$

where X^0 is the time coordinate. Qualitatively similar constructions were also given for the superstring [121]. In this paper we will describe some surprising and intriguing properties of these s-branes.

A salient feature of time-dependent backgrounds is that there is in general no preferred vacuum and particle production is unavoidable. We study the open string

[30] This chapter is based on the paper [3], with A. Strominger and X. Yin.

vacua on an s-brane and find that they have somewhat mysterious thermal properties reminiscent of black hole or de Sitter vacua. For the case (13.1) there is open string pair production with a strength characterized by the Hagedorn temperature [129,134]

$$T_H = \frac{1}{4\pi\sqrt{\alpha'}}. \tag{13.2}$$

Mathematically, the temperature arises from the periodicity of the boundary interaction (13.1) in imaginary time. Physically, we show that (for the quantum state of a brane created with no incoming string excitations) an Unruh detector will see a thermal bath. We further show that at late times the exact Green function approaches the thermal Green function plus asymptotically vanishing corrections.

The appearance of the Hagedorn temperature signals a breakdown of string perturbation theory [129,131,138,139]. Describing the mechanism which cuts off this divergence is an interesting problem which we will not address in this paper.[31] Herein we simply avoid the problem by working at $g_s = 0$. Interestingly, we find that the Hagedorn problem disappears in the $\lambda = \frac{1}{2}$ sD-brane case discussed below.[32]

In addition to the pure vacuum states mentioned above, we construct a series of mixed thermal states with temperatures

$$T = \frac{1}{2\pi n\sqrt{\alpha'}} \tag{13.3}$$

for positive integer n. Ordinarily it makes no sense to discuss a thermal state in a highly time-dependent background. However, because of the Euclidean time periodicity of the interaction (13.1), we can construct mixed states whose Green functions have exact thermal periodicity at all times. Physically, it is natural to

[31] The divergence might be controlled by lowering the s-brane temperature either with the addition of an electric field [140,141] or a null linear dilaton (4.12).

[32] This can be seen both from the absence of on-shell open strings and the vanishing of the projection of the boundary state onto the massless winding state in the closed string channel associated to the Hagedorn divergence.

expect open strings on an s-brane to be in a mixed state, since they are correlated with the closed string modes whose energy was needed to create the s-brane in the first place.

Ordinary branes are usefully characterized at long distances by a long-distance effective field theory. It is rather subtle to define such an effective theory for an s-brane because there is no time-translation invariant ground state around which to define and expand the low-lying excitations. One may try to define a long-distance effective field theory as the Euclidean theory which reproduces the long-distance equal time correlators on the s-brane. In general these correlators depend strongly on the quantum state of the fields on the s-brane, and will not behave like those of any Euclidean field theory whose dimension is that of the s-brane. However, we show that the thermal state of the s-brane gives an effective field theory which is essentially a (twisted) compactification of the unstable brane whose creation/decay comprises the s-brane. Ultimately, this Euclidean effective field theory may play an interesting role in timelike holographic duality.

The thermal s-brane states can be succinctly characterized by a CFT boundary state. The thermal boundary state at temperature $T = \frac{1}{2\pi n\sqrt{\alpha'}}$ differs from the zero-temperature boundary state of [120] by a periodic identification $\phi \sim \phi + 2\pi n$ of the Euclidean timelike scalar $\phi = -iX^0$. The thermal s-brane boundary state contains closed strings with winding in the ϕ direction. These thermal boundary states enable efficient evaluation of various worldsheet string diagrams.

At the special value of the coupling $\lambda = \frac{1}{2}$ appearing in (13.1), a dramatic simplification occurs. For any λ the boundary interaction (13.1) generates a right-moving rotation by $2\pi\lambda$ in the SU(2) level one current algebra generated by ∂X^0, $\cosh X^0$ and $i \sinh X^0$. When $\lambda = \frac{1}{2}$ the rotation is by π, which simply transforms the Neumann boundary state into a Dirichlet boundary state. The s-brane then degenerates into a periodic array of sD-branes (i.e. D-branes with a Dirichlet

boundary condition on the time coordinate) located on the imaginary time axis at $\phi = m\pi$ for odd integer m. This gives the precise relation between the Dirichlet type boundary states discussed in [118] and the Sine-Gordon type boundary states discussed in [120].[33] In this $\lambda = \frac{1}{2}$ limit there are no on-shell open string states[34], but the on-shell closed string states determined from the boundary state remain. This remaining closed string configuration has the unusual property that its total energy is of order $\frac{1}{g_s}$ and its behavior can be determined from open string calculations on the sD-brane. The annulus diagram connecting one (bosonic) D-brane and one s-brane is computed for arbitrary λ using the boundary state. At $\lambda = \frac{1}{2}$, the long-distance force between a D-brane and an sD-brane is shown to be $\frac{11}{12}$ times the force between two D-branes (which corresponds to $\lambda = 0$).[35]

This paper is organized as follows. Section 2 describes various s-brane vacua and their properties in a minisuperspace approximation which treats the open strings as quantum fields with a time-dependent $\cosh t$ or $e^{\pm t}$ mass. Most of the important behavior follows from the Euclidean periodicity of the interaction, which is an exact property of the worldsheet CFT. In section 2.1 we review the "half s-brane" corresponding to brane decay, which is described by a (in some respects simpler) boundary interaction $\int e^{X^0} d\tau$ instead of (13.1). We recall that open string

[33] Reference [118] only considered sD-branes on the real time axis. As discussed therein, these have problems both with the dominant energy condition and the existence of a well-defined string perturbation expansion. Both of these problems seem to be resolved by moving the sD-brane to imaginary time. In [131] it was shown that, for the bosonic string, the theory with $\lambda = -\frac{1}{2}$ has an sD-brane at real time.

[34] Off-shell open string states still appear in the Euclidean effective field theory.

[35] This might appear to contradict the claim [120] that $\lambda = \frac{1}{2}$ is the trivial closed string vacuum. The interesting resolution of this apparent conflict, discussed in section 6.1 in some detail, is that when there is time-dependence, the boundary state does not uniquely determine the closed string fields. The implicit prescription adopted in [120] differs from the one used herein, which latter amounts to the use of the Feynman propagators obtained by analytic continuation from Euclidean space.

pair creation is characterized by the Hagedorn temperature $T_H = \frac{1}{4\pi\sqrt{\alpha'}}$ [129]. In section 2.2 we consider the time-reverse process of brane creation, for which a natural state is one with no incoming open strings. In section 2.3 we move on to the full s-brane (13.1), whose linearized solutions are Mathieu functions. We use these solutions in section 2.4 to describe two vacua of the full s-brane with no particles in the far past and the far future, respectively. In 2.5 a time-reversal invariant s-brane vacuum is defined by the condition that there is no particle flux in the middle of the s-brane at $t = 0$. The resulting positive frequency modes are found to be bounded in the lower half plane $t \to -i\infty$. This vacuum can therefore be obtained by analytic continuation from Euclidean space. Other possible vacua are described in 2.6.

In section 3 we discuss the thermal properties of s-branes. In 3.1 it is shown that thermal Green functions at temperature $T = \frac{1}{2\pi n\sqrt{\alpha'}}$ can be obtained by analytic continuation from a periodically identified Euclidean section. The Minkowskian mixed thermal state (or density matrix) which reproduces these Green functions is explicitly constructed. Thermal properties of certain pure vacuum states arising from the imaginary-time periodicity of (13.1) are also demonstrated. For example, in 3.2 it is shown that an Unruh detector in the vacuum with no incoming particles measures a temperature T_H during brane creation. Furthermore, in 3.3 it is found that at late times the correlators in the pure state approach thermal correlators plus asymptotically vanishing corrections. This suggests that branes are naturally produced in something close to a thermal state.

Section 4 defines the notion of long-distance effective field theory for an s-brane. This effective theory is determined as the Euclideanization and time compactification, with twisted fermion boundary conditions and a periodic boundary tachyon interaction on the worldsheet, of the theory on the unstable brane whose creation/decay describes the s-brane. Long-distance modes are related to zero modes of this compactified theory.

In section 5.1 the boundary states which generate the finite-temperature string correlators on an s-brane are constructed. They differ from the usual expression by a periodic identification of Euclidean time, which allows for winding modes in the closed string channel. The superstring is discussed in 5.2, and the allowed temperatures are shown to be

$$T = \frac{1}{2\pi n\sqrt{2\alpha'}}. \tag{13.4}$$

In section 6 we turn to the special case of $\lambda = \frac{1}{2}$, in which the boundary interaction becomes an $SU(2)$ rotation by π. In this case the s-brane collapses to an array of sD-branes on the imaginary time axis at $t = m\pi i$ for odd integer m. In section 6.1 we explain an ambiguity in the propagator used to obtain the spacetime closed string fields from the boundary state, which is due to the appearance of on-shell states in the boundary state. It is shown that the analytic continuation of the Feynman propagator gives a non-zero answer even when the support of the boundary state moves off the real time axis. The summation over the sD-branes m is performed in a simple example to give a closed-form expression for a massless closed string field. In 6.2 we compute the RR field emanating from an sD-brane and integrate it over a transverse spacelike surface to find the s-charge. Long range dilaton/graviton fields are computed in 6.3. In section 6.4 we compute the annulus diagram connecting an ordinary D-brane to an s-brane for general λ, using old results on the boundary Sine-Gordon model [142]. We find that the long distance force between a D-brane and an s-brane has a coefficient of $23+\cos(2\pi\lambda)$, indicating that the force between an sDp-brane ($\lambda = \frac{1}{2}$) and a D-brane is $\frac{11}{12}$ times the force between two ordinary D-branes. In 6.5 we extend the annulus computation to finite temperature. In 6.6 we discuss the relation between sD-branes and D-instantons. Finally, we conclude in section 7 with speculations on timelike holography.

Results overlapping with those of this paper will appear in [138].

14. Quantum vacuum states

We wish to understand the dynamics of the open string worldsheet theory with a time-dependent tachyon

$$S = -\frac{1}{4\pi}\int_{\Sigma_2} d^2\sigma \partial^a X^\mu \partial_a X_\mu + \int_{\partial\Sigma_2} d\tau\ m^2(X^0), \tag{14.1}$$

where here and henceforth we set $\alpha' = 1$. For the open bosonic string $m^2 = T$ where T is the spacetime tachyon, while for the open superstring $m^2 \sim T^2$ after integrating out worldsheet fermions. We use the symbol m^2 to denote the interaction because the coupling (among other effects) imparts a mass to the open string states. We consider three interesting cases described by the marginal interactions [120,129,134,143][36]

$$m_+^2(X^0) = \frac{\lambda}{2}e^{X^0} \tag{14.2}$$

$$m_-^2(X^0) = \frac{\lambda}{2}e^{-X^0} \tag{14.3}$$

$$m_s^2(X^0) = \lambda\cosh X^0. \tag{14.4}$$

The first case m_+^2 describes the process of brane decay, in which an unstable brane decays via tachyon condensation. The second case describes the time-reverse process of brane creation, in which an unstable brane emerges from the vacuum. The final case describes an s-brane, which is the process of brane creation followed by brane decay. Brane decay (14.2) (creation (14.3)) can be thought of as the future (past) half of an s-brane, i.e. as the limiting case where the middle of the s-brane is pushed into the infinite past (future).

[36] For the bosonic string one could also consider a $\sinh X^0$ interaction, although we do not do so here. In the bosonic theory $\cosh X^0$ describes a process in which a tachyon rolls up the barrier and then back down the same side, while $\sinh X^0$ describes the tachyon rolling over the barrier. The bosonic $\sinh X^0$ interaction is challenging because it ventures into the unbounded side of the tachyon potential. The superstring potential is always positive, so there is no analog of a $\sinh X^0$ type interaction.

An exact CFT analysis of these s-brane theories should be possible [120,129,134,143], and some exact results are given in sections 5 and 6. However in this and the next section we shall confine ourselves to the minisuperspace analysis [129] in which the effect of the interaction is simply to give a time-dependent shift (given by (14.2)-(14.4)) to the masses of all the open string states. The range of validity of the minisuperspace approximation is unclear, although some evidence in favor of its validity at high frequencies was found in [134]. However, most of the results of the next two sections follow from the periodicity in imaginary time, which is an exact property of the CFTs defined by (14.2)-(14.4), so we expect our conclusions to be qualitatively correct.

In the minisuperspace approximation only the zero-mode dependence of the interaction $m^2(X^0)$ is considered. In this case we can plug in the usual mode solution for the free open string with oscillator number N to get an effective action for the zero modes

$$S = \int d\tau \left[-\frac{1}{4}\dot{x}^\mu \dot{x}_\mu + (N-1) + 2m^2(x^0) \right]. \tag{14.5}$$

This is the action of a point particle with a time dependent mass. Here $x^\mu(\tau)$ is the zero mode part of $X^\mu(\sigma,\tau)$, and the second term in (14.5) is an effective contribution from the oscillators, including the usual normal ordering constant. From (14.5) we can write down the Klein-Gordon equation for the open string wave function $\phi(t,\vec{x})$,

$$\left(\partial^\mu\partial_\mu - 2m^2(t) - (N-1)\right)\phi(t,\vec{x}) = 0, \tag{14.6}$$

where $(t,\vec{x})$ are the spacetime coordinates corresponding to the worldsheet fields $(X^0,\vec{X})$. This is the equation of motion for a scalar field with time-dependent mass.

At this point, we should make a few remarks about field theories with time dependent mass. Time translation invariance has been broken, so energy is not

conserved and there is no preferred set of positive frequency modes. This is a familiar circumstance in the study of quantum field theories in time-dependent backgrounds which leads to particle creation. The probability current $j_\mu = i(\phi^* \partial_\mu \phi - \partial_\mu \phi^* \phi)$ is conserved, allowing us to define the Klein-Gordon inner product

$$\langle f|g\rangle = i \int_\Sigma d\Sigma^\mu (f^* \partial_\mu g - \partial_\mu f^* g) \tag{14.7}$$

where Σ is a spacelike slice. This norm does not depend on the choice of Σ if f and g solve the wave equation. Normalized positive frequency modes are chosen to have $\langle f|f\rangle = 1$. Negative frequency modes are complex conjugates of positive frequency modes, with $\langle f^*|f^*\rangle = -1$. There is a set raising and lowering operators associated to each choice of mode decomposition – these operators obey the usual oscillator algebra if the corresponding modes are normalized with respect to (14.7). We also define a vacuum state associated to each mode decomposition – it is the state annihilated by the corresponding lowering operators.

14.1. The $|in\rangle_+$ vacuum for brane decay

In this section we review some results of [129] on a scalar field with mass

$$m_+^2(t) = \frac{\lambda}{2} e^t, \tag{14.8}$$

describing open strings on a decaying brane. A natural vacuum in this case is that with no particles present in the far past: we shall denote this state $|in\rangle_+$.

Expanding ϕ in plane waves

$$\phi(t, \vec{x}) = e^{i\vec{p}\cdot\vec{x}} u(t) \tag{14.9}$$

the wave equation becomes

$$(\partial_t^2 + \lambda e^t + \omega^2) u = 0, \qquad \omega^2 = p^2 + N - 1. \tag{14.10}$$

This is a form of Bessel's equation. It has normalized, positive frequency solutions [37]

$$u_+^{in} = \lambda^{i\omega} \frac{\Gamma(1-2i\omega)}{\sqrt{2\omega}} J_{-2i\omega}(2\sqrt{\lambda}e^{t/2}) \tag{14.11}$$

These solutions have been chosen because they approach flat space positive frequency plane waves in the far past $t \to -\infty$,

$$u_+^{in} \sim \frac{1}{\sqrt{2\omega}} e^{-i\omega t}. \tag{14.12}$$

We will also consider the wave functions

$$u_+^{out} = \sqrt{\frac{\pi}{2}} (ie^{2\pi\omega})^{-1/2} H^{(2)}_{-2i\omega}(2\sqrt{\lambda}e^{t/2}) \tag{14.13}$$

that are purely positive frequency in the far future $t \to +\infty$,

$$u_+^{out} \sim \frac{\lambda^{-1/4}}{\sqrt{2}} \exp\left\{-t/4 - 2i\sqrt{\lambda}e^{t/2}\right\}. \tag{14.14}$$

These are related to the previous set of wave functions by a Bogolubov transformation

$$u_+^{out} = a u_+^{in} + b u_+^{in\,*} \tag{14.15}$$

whose coefficients

$$a = e^{2\pi\omega + \pi i/2} b^* = \sqrt{\omega\pi} e^{\pi\omega - \pi i/4} \left(\frac{\lambda^{-i\omega}}{\sinh 2\pi\omega \Gamma(1-2i\omega)} \right) \tag{14.16}$$

obey the usual unitarity relation $|a|^2 - |b|^2 = 1$. All solutions of the wave equation during brane decay vanish exponentially in the far future (but not in the far past) because the mass is growing exponentially.

---

[37] A $+$ $(-)$ subscript on a wave function denotes solutions with $m^2 = m_+^2$ $(m^2 = m_-^2)$ during brane decay (creation). A wave function without a subscript refers to solutions for full s-brane $m^2 = m_s^2$. A superscript *in*, *out* and 0 on a wave function denotes solutions that are purely positive frequency when $t \to -\infty$, $t \to +\infty$ or $t = 0$. The wave functions u depend on $\vec{p}$ as well, although we will typically suppress momentum indices.

The relation (14.15) between in and out modes implies as usual the relation between in and out creation and annihilation operators

$$a^{in} = aa^{out} + b^*(a^{out})^\dagger. \tag{14.17}$$

From this, the condition that $a^{in}|in\rangle = 0$ implies that $|in\rangle$ is a squeezed state

$$|in\rangle_+ = \Pi_{\vec{p}}(1-|\gamma|^2)^{1/4} \exp\left\{-\frac{1}{2}\gamma(a^{out\,\dagger}_{\vec{p}})^2\right\}|out\rangle_+, \qquad \gamma = b^*/a. \tag{14.18}$$

Physically, this is the statement that particles are produced during brane decay: if we start in a state with no particles at $t \to -\infty$, there will be many particles at time $t \to +\infty$. We should emphasize here that γ is a function of $\vec{p}$

$$\gamma = b^*/a = -ie^{-2\pi\omega} \tag{14.19}$$

that decreases exponentially as the energy ω increases. In particular, this implies that the $|in\rangle_+$ and $|out\rangle_+$ vacua become identical at very short distances. The density of particles with momentum $\vec{p}$ is

$$n_{\vec{p}} = |\gamma|^2 = e^{-4\pi\omega}. \tag{14.20}$$

Despite the fact that (14.18) is a pure state, this is precisely the Boltzmann density of states at temperature $T_H = 1/4\pi$. In string units, T_H is the Hagedorn temperature. The fact that this "temperature" is so high means that g_s corrections are likely qualitatively important even for $g_s \to 0$ [129], but we do not consider these here.

The appearance of the temperature T_H here is ultimately due to the Euclidean periodicity of the interactions (14.2)-(14.4). This will lead to other thermal properties as described in the next section. Since the thermal periodicity is an exact property of the worldsheet CFT (14.1), we expect this behavior to persist beyond the minisuperspace approximation considered here.

14.2. The $|in\rangle_-$ vacuum for brane creation

Solutions u_- of the wave equation during brane creation are related to those (u_+) during brane decay by time reversal. In particular,

$$u_-^{out}(t) = u_+^{in}(-t)^* \tag{14.21}$$

becomes a plane wave in the far future $t \to +\infty$, and

$$u_-^{in}(t) = u_+^{out}(-t)^* = \sqrt{\frac{\pi}{2}}(ie^{2\pi\omega})^{1/2} H^{(1)}_{-2i\omega}(2\sqrt{\lambda}e^{-t/2}) \tag{14.22}$$

becomes purely positive frequency in the far past $t \to -\infty$

$$u_-^{in} \sim \frac{\lambda^{-1/4}}{\sqrt{2}} \exp\left\{t/4 + 2i\sqrt{\lambda}e^{-t/2}\right\}. \tag{14.23}$$

These two solutions are related by the Bogolubov transformation

$$u_-^{in} = a^* u_-^{out} + b^* u_-^{out*}, \tag{14.24}$$

where a and b are given by (14.16). Wave functions during brane creation vanish exponentially in the far past but not in the far future, because the masses are infinite in the far past.

The natural vacuum state during brane creation is not, however, the time reverse $\mathcal{T}$ of the in state for brane decay $\mathcal{T}|in\rangle_+$. The latter state has particles present in the far past with infinite masses. Indeed it would cost an infinite amount of energy to prepare such an initial state. Rather, the natural in state $|in\rangle_-$ for brane creation has no particles in the far past and is the time reverse $\mathcal{T}|out\rangle_+$ of the out vacuum for brane decay. We can write $|in\rangle_-$ in terms of the free out operators as

$$|in\rangle_- = \Pi_{\vec{p}}(1-|\gamma|^2)^{1/4} \exp\left\{\frac{1}{2}\gamma^*(a_{\vec{p}}^{out\,\dagger})^2\right\}|out\rangle_- \tag{14.25}$$

where γ is given by (14.19). The spectrum in the region $t \to +\infty$ is just the free spectrum of the unstable D-brane, and (14.25) is a pure state of open string excitations. Despite this fact we shall see in section 3 that (14.25) closely resembles

a thermal state at temperature T_H. Indeed we shall see that the results of measurements done after brane creation differ from thermal results by asymptotically vanishing amounts.

14.3. Full s-brane modes

For the full s-brane potential (14.4), the Klein-Gordon equation is

$$(\partial_t^2 + 2\lambda \cosh t + \omega^2)u = 0. \tag{14.26}$$

This is a form of Mathieu's equation. We will now summarize a few useful properties of the solutions – see e.g. [66–145] for more detail. The solutions are generalized Mathieu functions, which can be written as [38]

$$u = Ae^{-i\tilde{\omega}t}P(t) + Be^{i\tilde{\omega}t}P(-t) \tag{14.27}$$

where the function

$$P(t) = \sum_{r=-\infty}^{\infty} c_{2r}e^{rt} \tag{14.28}$$

is periodic in imaginary time $P(t) = P(t + 2\pi i)$. The constants $\tilde{\omega}$ and c_{2r} obey complicated recursive formulae and are typically computed numerically. Although it is not obvious from (14.27), all solutions u vanish exponentially in the far past and the far future. This is because open string modes get very massive far from the interior of the brane.

Solutions to Mathieu's equation are typically classified by their behavior with respect to imaginary time $\tau = it$. A solution is bounded on the τ axis only if $\tilde{\omega}$ is purely imaginary. In this case the solution is called *stable* - otherwise it is *unstable*. Solutions are stable only for certain regions of the (ω^2, λ) plane. For large positive

[38] This form for u differs from the standard convention for Mathieu functions. Our $\tilde{\omega}$ is related to the standard characteristic exponent (often denoted ν in the literature) by $\nu = -2i\tilde{\omega}$.

ω^2 – the case of interest – $\tilde{\omega}$ is real and all solutions are unbounded on the real τ axis. However, there is a unique solution that vanishes as $\tau \to +\infty$ – this is the solution with $B = 0$. We will see later that this solution is naturally associated to the state with no particles in the interior of the s-brane at $t = 0$.

It is useful to assemble Mathieu functions in the form [145] analogous to Bessel functions

$$\begin{aligned} J(-2i\tilde{\omega}, t/2) =& \equiv e^{-i\tilde{\omega}t} P(t) = \sum_{n=-\infty}^{\infty} \phi\left(n - i\tilde{\omega}\right) e^{(n-i\tilde{\omega})t}, \\ H^{(1)}(-2i\tilde{\omega}, t/2) \equiv& \frac{J(2i\tilde{\omega}, t/2) - e^{-2\pi\tilde{\omega}} J(-2i\tilde{\omega}, t/2)}{\sinh 2\pi\tilde{\omega}}, \\ H^{(2)}(-2i\tilde{\omega}, t/2) \equiv& \frac{J(2i\tilde{\omega}, t/2) - e^{2\pi\tilde{\omega}} J(-2i\tilde{\omega}, t/2)}{-\sinh 2\pi\tilde{\omega}}. \end{aligned} \tag{14.29}$$

They have asymptotic behavior

$$\left.\begin{aligned} H^{(1)}(-2i\tilde{\omega}, t/2) &\to \frac{\lambda^{-1/4}}{\sqrt{\pi}} e^{-\pi\tilde{\omega}} \exp\left(-\frac{t}{4} + 2i\sqrt{\lambda} e^{t/2} - i\frac{\pi}{4}\right) \\ H^{(2)}(-2i\tilde{\omega}, t/2) &\to \frac{\lambda^{-1/4}}{\sqrt{\pi}} e^{\pi\tilde{\omega}} \exp\left(-\frac{t}{4} - 2i\sqrt{\lambda} e^{t/2} + i\frac{\pi}{4}\right) \end{aligned}\right\} \quad \text{as} \quad t \to +\infty. \tag{14.30}$$

Mathieu's equation is invariant under $t \to -t$, so $J(-2i\tilde{\omega}, -t/2)$ is also a solution. Under $t \to t + 2\pi i$, $J(-2i\tilde{\omega}, -t/2)$ picks up the phase $e^{-2\pi\tilde{\omega}}$, so it must be proportional to $J(2i\tilde{\omega}, t/2)$

$$J(2i\tilde{\omega}, t/2) = \chi J(-2i\tilde{\omega}, -t/2) \tag{14.31}$$

where the proportionality factor χ is related to ϕ by

$$\chi = \frac{\phi(n + i\tilde{\omega})}{\phi(-n - i\tilde{\omega})} = \frac{\phi(i\tilde{\omega})}{\phi(-i\tilde{\omega})}. \tag{14.32}$$

The coefficients $\phi(\tau)$ can be computed using the formula

$$\begin{aligned}
\phi(\tau) &= \frac{1}{\Gamma(1+\tau+i\omega)\Gamma(1+\tau-i\omega)} \sum_{n=0}^{\infty} (-1)^n \lambda^{2n+\tau} A_\tau^{(n)}, \\
A_\tau^{(0)} &= 1, \\
A_\tau^{(\lambda)} &= \sum_{p_1=0}^{\infty} \sum_{p_2=0}^{\infty} \cdots \sum_{p_\lambda=0}^{\infty} a_{\tau+p_1} a_{\tau+p_1+p_2} \cdots a_{\tau+p_1+\cdots+p_\lambda}, \\
a_\tau &= \frac{1}{(1+\tau+i\omega)(1+\tau-i\omega)(2+\tau+i\omega)(2+\tau-i\omega)}.
\end{aligned} \tag{14.33}$$

One can analyze the behavior of $H^{(i)}(-2i\tilde{\omega}, t/2)$ as $t \to -\infty$ using the relation

$$\begin{aligned}
H^{(1)}(-2i\tilde{\omega}, t/2) =& \frac{1}{2\sinh 2\pi\tilde{\omega}} \\
& \left[\left(\chi - \frac{1}{\chi} \right) H^{(1)}(-2i\tilde{\omega}, -t/2) + \left(\chi - \frac{e^{-4\pi\tilde{\omega}}}{\chi} \right) H^{(2)}(-2i\tilde{\omega}, -t/2) \right].
\end{aligned} \tag{14.34}$$

When λ is small, we can use the expansion

$$\omega^2 = \tilde{\omega}^2 + \frac{2\lambda^2}{4\tilde{\omega}^2+1} + \frac{(20\tilde{\omega}^2-7)\lambda^4}{2(4\tilde{\omega}^2+1)^3(\tilde{\omega}^2+1)} + \cdots$$

to compute $\tilde{\omega}$.

14.4. $|in\rangle_s$ and $|out\rangle_s$ s-brane vacua

For our full s-brane, the incoming and outgoing positive frequency wave functions are normalized as

$$\begin{aligned}
u^{in}(t) &= \sqrt{\frac{\pi}{2}} (ie^{2\pi\tilde{\omega}})^{1/2} H^{(1)}(-2i\tilde{\omega}, -t/2), \\
u^{out}(t) &= \sqrt{\frac{\pi}{2}} (ie^{2\pi\tilde{\omega}})^{-1/2} H^{(2)}(-2i\tilde{\omega}, t/2).
\end{aligned} \tag{14.35}$$

The in (out) vacuum, which has no incoming (outgoing) particles, is defined by the condition

$$a^{in}|in\rangle_s = 0 = a^{out}|out\rangle_s. \tag{14.36}$$

The relation between in and out modes is determined from (14.34) to be

$$\begin{aligned} u^{in}(t) &= \frac{1}{2\sinh 2\pi\tilde{\omega}}\left[i\left(e^{2\pi\tilde{\omega}}\chi - \frac{e^{-2\pi\tilde{\omega}}}{\chi}\right)u^{out}(t) + \left(\chi - \frac{1}{\chi}\right)u^{out*}(t)\right] \\ &= \alpha u^{out}(t) + \beta u^{out*}(t), \end{aligned} \tag{14.37}$$

where α, β are the Bogolubov coefficients

$$\alpha = \frac{i}{2\sinh 2\pi\tilde{\omega}}\left(e^{2\pi\tilde{\omega}}\chi - \frac{e^{-2\pi\tilde{\omega}}}{\chi}\right), \qquad \beta = \frac{1}{2\sinh 2\pi\tilde{\omega}}\left(\chi - \frac{1}{\chi}\right). \tag{14.38}$$

Although the dependence of $\tilde{\omega}, \chi$ on ω, λ is in general quite complicated, it is known that either $e^{2\pi\tilde{\omega}}$ is real and χ is of unit modulus, or χ is real and $e^{2\pi\tilde{\omega}}$ is of unit modulus. It follows that the Bogolubov coefficients satisfy the unitarity condition $|\alpha|^2 - |\beta|^2 = 1$. In the case of interest, ω is large and $\lambda \ll \omega$, we have

$$\tilde{\omega} = \omega\left[1 + O(\lambda^2/\omega^4)\right]. \tag{14.39}$$

Using (14.32) and (14.33), we obtain the expansion for χ

$$\chi = \frac{\Gamma(1-2i\omega)}{\Gamma(1+2i\omega)}\lambda^{2i\omega}\left[1 + O(\lambda^2/\omega^2)\right]. \tag{14.40}$$

To leading order in $O(\lambda^2/\omega^2)$, the Bogolubov coefficients are

$$\alpha = \frac{\sin(\theta + 2\pi i\omega)}{\sinh 2\pi\omega}, \qquad \beta = -i\frac{\sin\theta}{\sinh 2\pi\omega}, \qquad e^{i\theta} = \lambda^{-2i\omega}\frac{\Gamma(1+2i\omega)}{\Gamma(1-2i\omega)}. \tag{14.41}$$

Sub-leading terms can be computed order by order in $1/\omega^2$ using the methods of [145], although we shall not need them here.

14.5. The $|0\rangle_s$ Euclidean s-brane vacuum

If we take $\lambda \to 0$ there is a long region around $t = 0$, of duration $\ln\lambda$, in which the interaction can be neglected and we just have an ordinary unstable brane. There is then a natural $|0\rangle_s$ vacuum in which there are no particles present at $t = 0$.

This will later be identified with a vacuum obtained by analytic continuation from Euclidean space. It is associated with the wave functions

$$u^0(t) = \sqrt{\frac{4\pi\chi}{\sinh 2\pi\tilde{\omega}}} J(-2i\tilde{\omega}, t/2). \tag{14.42}$$

Using the relation $J = \frac{1}{2}[H^{(1)} + H^{(2)}]$, $u^0(t)$ can be expressed in terms of $u^{out}(t)$ as

$$\begin{aligned} u^0(t) &= \sqrt{\frac{\chi}{2\sinh 2\pi\tilde{\omega}}} \left[e^{\pi\tilde{\omega}+i\frac{\pi}{4}} u^{out}(t) + e^{-\pi\tilde{\omega}-i\frac{\pi}{4}} u^{out*}(t)\right] \\ &= a^* u^{out}(t) - b u^{out*}(t) \end{aligned} \tag{14.43}$$

and in terms of $u^{in}(t)$ as

$$\begin{aligned} u^0(t) &= \frac{1}{\sqrt{2\chi\sinh 2\pi\tilde{\omega}}} \left[e^{\pi\tilde{\omega}-i\frac{\pi}{4}} u^{in}(t) + e^{-\pi\tilde{\omega}+i\frac{\pi}{4}} u^{in*}(t)\right] \\ &= a u^{in}(t) - b^* u^{in*}(t). \end{aligned} \tag{14.44}$$

The Bogolubov coefficients relating the $|0\rangle_s$ vacuum to the $|in\rangle_s$ and $|out\rangle_s$ vacua are given by

$$a = \frac{e^{\pi\tilde{\omega}-i\frac{\pi}{4}}}{\sqrt{2\chi\sinh 2\pi\tilde{\omega}}}, \qquad b = -e^{-\pi\tilde{\omega}-i\frac{\pi}{4}} \sqrt{\frac{\chi}{2\sinh 2\pi\tilde{\omega}}}. \tag{14.45}$$

In the limit $\omega, \omega/\lambda \gg 1$, the s-brane wave functions may be understood in terms of a flux matching procedure. [39] In this limit the Klein-Gordon equation (14.26) describes brane creation (14.10) in the far past and brane decay in the far future, separated by a long region near $t = 0$ where the interaction is negligible. Approximate solutions to (14.26) may be found by matching wave functions of brane creation with wave functions of brane decay across the region $t \sim 0$. In particular, u^{in} and u^{out} look like the half s-brane solutions u^{in}_- and u^{out}_+ in the past and future, respectively. The wave function u^0 looks like an ordinary plane wave solution in the interior of the s-brane, u^{out}_- in the far past and u^{in}_+ in far future. This may be

[39] A similar procedure was used to study scattering of scalar fields by a D3 brane in [146].

verified by noting that to lowest order in $1/\omega^2$ the Bogolubov coefficients (14.45) are given by (14.16).

For transitions to and from the $|0\rangle_s$ vacuum, we find that the particle creation rate is governed by the "thermal" factors :

$$\begin{aligned} \gamma_{0\to in} &= b/a^* = ie^{-2\pi\tilde{\omega}}, & \gamma_{in\to 0} &= -b/a = e^{-2\pi\tilde{\omega}-i\tilde{\theta}} \\ \gamma_{0\to out} &= b^*/a = -ie^{-2\pi\tilde{\omega}}, & \gamma_{out\to 0} &= -b^*/a^* = e^{-2\pi\tilde{\omega}+i\tilde{\theta}}, \end{aligned} \tag{14.46}$$

where $e^{-i\tilde{\theta}} = \chi$. In the limit of large ω and $\omega/\lambda \gg 1$, $\tilde{\omega}, \tilde{\theta} \to \omega, \theta$ and we find the same particle creation rates as for the half s-branes. We see that the particle occupation numbers in the far past and future are both thermal at temperature $T = 1/4\pi$. The $|0\rangle_s$ vacuum is special in this respect.

The $|0\rangle_s$ state is also special because it is time reversal invariant and is the natural state defined by analytic continuation from Euclidean space. This latter property can be readily seen from the fact that it is the unique state whose modes are bounded on the positive Euclidean axis, as described in section 2.2. It is also the only state whose positive and negative frequency modes do not mix under imaginary time translation $t \to t + 2\pi i$. A general solution of the wave equation has the form

$$u = AJ(-2i\tilde{\omega}, t/2) + BJ(-2i\tilde{\omega}, -t/2). \tag{14.47}$$

For the $|0\rangle$ vacuum B vanishes, and the solution transforms as

$$u^0(t + 2\pi i) = e^{2\pi\tilde{\omega}}\ u^0(t) \tag{14.48}$$

under imaginary time translation. In all other states both A and B are non-zero, so this procedure mixes u with u^*. When ω is large and $\omega/\lambda \gg 1$, $\tilde{\omega}$ approaches ω and (14.48) is the usual imaginary time translation condition exhibited by plane waves in flat space. Moreover, in our choice of solutions (14.42) we have chosen the phase of A so that u^0 has the usual time reversal behavior

$$u^0(-t) = u^{0*}(t). \tag{14.49}$$

14.6. More vacua

The wave equation (14.26) is second order, so for any given momentum $\vec{p}$ there is a one complex parameter family of normalized, positive frequency solutions $u(t)$. We can write these solutions as linear combinations

$$u^\alpha = \frac{1}{\sqrt{1 - e^{\alpha+\alpha^*}}} \left(u^0 + e^\alpha u^{0*}\right) \tag{14.50}$$

where α is a function of $\vec{p}$ with negative real part. This choice of modes defines a state $|\alpha\rangle$ for every such function $\alpha(\vec{p})$. The state is invariant under spatial translations when α is a function of p only. This is a very large family of vacua, which includes the $|in\rangle_s$, $|0\rangle_s$ and $|out\rangle_s$ states. Of course, one can define families of vacua for brane creation and brane decay as well.

In order to constrain α further, one needs to demand some other symmetry. One such symmetry is time reversal invariance – this restricts us to states such as $|0\rangle_s$ and $\frac{1}{2}(|in\rangle_s + |out\rangle_s)$. It is also natural to demand that the short distance structure of the vacuum be the same as the $|0\rangle_s$ vacuum. This restricts $\alpha(p)$ to vanish sufficiently quickly at large p.

15. S-brane thermodynamics

In this section we study the thermal properties of s-branes. In the first subsection we will consider the response of a monopole Unruh detector coupled to ϕ. We will show that in the $|in\rangle_-$ and $|out\rangle_+$ vacua the detector response is thermal, but that in other states the detector response is non-thermal. Next, we will demonstrate that in the $|in\rangle_-$ vacuum the correlators of the theory become exactly thermal up to corrections that vanish in the far future. Likewise, the $|out\rangle_+$ vacuum looks thermal in the far past. Similar results pertain to the full s-brane, but we will not work out the details here.

15.1. S-branes at finite temperature

The s-branes described by (14.2)-(14.4) are highly time-dependent configurations. Temperature is an equilibrium (or at best adiabatic) concept, so it usually does not make sense to put a time dependent configuration at finite temperature unless the inverse temperature is much lower than the scale of time variation. Thus it would seem to be impossible to study s-branes at string-scale temperatures. However, certain special properties of s-branes make this possible, as we will now demonstrate for a scalar field obeying (14.6). In section 5 we will see that the finite temperature states in string theory have a natural boundary state description.

Let us first consider the construction of Green functions by analytic continuation from Euclidean space. In Euclidean space, parameterized by $\tau = it$, the formulae (14.2)-(14.4) for $m^2(\tau)$ have the special property that they are periodic under $\tau \to \tau + 2\pi$. It is therefore possible to identify Euclidean space so that $\tau = \tau + 2\pi n$ for any integer n, and compute the Green function on the identified space. After continuing back to Minkowski space, the resulting Green function $G_{2\pi n}(\vec{x}, t; \vec{x}', t')$ will be periodic under $t \to t + 2\pi i n$ and $t' \to t' + 2\pi i n$. This is a thermal Green function at temperature $T = \frac{1}{2\pi n}$.

The thermal Green function so obtained can also be understood as a two point function in a certain mixed state. We will consider the case of brane decay, although a similar discussion will apply to brane creation and to the full s-brane. For $t, t' \to -\infty$, $G_{2\pi n}(\vec{x}, t; \vec{x}', t')$ is clearly the usual thermal Feynman Green function which is given by (suppressing the time-ordering)

$$\begin{aligned} G_{2\pi n}(\vec{x}, t; \vec{x}', t') &= \sum_j e^{-2\pi n E_j} \langle E_j | \phi(\vec{x}', t') \phi(\vec{x}, t) | E_j \rangle \\ &= \mathrm{Tr} \rho_n \phi(\vec{x}', t') \phi(\vec{x}, t). \end{aligned} \tag{15.1}$$

Here we have defined the density matrix

$$\rho_n = C_n e^{-2\pi n H(-\infty)} \tag{15.2}$$

where C_n is a normalization constant and the time dependent Hamiltonian is

$$H(t) = \int_\Sigma d^d x \big((\dot{\phi})^2 + (\nabla \phi)^2 + e^{2t} \phi^2 \big) + N. \tag{15.3}$$

In this expression, N is a (time-independent) normal ordering constant and ϕ is to be expanded in terms of time-independent creation and annihilation operators as

$$\phi = \sum_{\vec{p}} \big(\psi^{in}_{\vec{p}} a^{in}_{\vec{p}} + \psi^{in*}_{\vec{p}} a^{in\dagger}_{\vec{p}} \big) = \sum_{\vec{p}} \big(\psi^{out}_{\vec{p}} a^{out}_{\vec{p}} + \psi^{out*}_{\vec{p}} a^{out\dagger}_{\vec{p}} \big). \tag{15.4}$$

The Hamiltonian $H(t)$ obeys

$$i[H(t), \phi(t)] = \partial_t \phi(t), \qquad i[H(t), \partial_t \phi(t)] = \partial_t^2 \phi(t) \tag{15.5}$$

so that the path-ordered operator

$$U(t_2, t_1) = P\big[e^{i \int_{t_1}^{t_2} H(t) dt} \big] \tag{15.6}$$

generates time evolution on ϕ

$$\phi(\vec{x}, t_2) = U(t_2, t_1) \phi(\vec{x}, t_1) U(t_1, t_2). \tag{15.7}$$

However, because of the explicit time dependence in (15.3), U does not generate evolution of $H(t)$.

In fact (15.1) turns out to be the desired Green function even for finite t, t', and (15.2) can be viewed as the exact Heisenberg-picture density matrix. First, it can be shown from properties of Bessel functions that

$$\phi(\vec{x}, t + 2\pi i n) = e^{-2\pi n H(-\infty)} \phi(\vec{x}, t) e^{2\pi n H(-\infty)}, \tag{15.8}$$

$$\partial_t \phi(\vec{x}, t + 2\pi i n) = e^{-2\pi n H(-\infty)} \partial_t \phi(\vec{x}, t) e^{2\pi n H(-\infty)}. \tag{15.9}$$

Note that shifts in $t \to t + 2\pi i$ are generated by $H(-\infty)$ for *any* t. This implies

$$U(t, t + 2\pi i n) = U(-\infty, -\infty + 2\pi i n) = \frac{\rho_n}{C_n}. \tag{15.10}$$

It then follows that (15.1) obeys

$$G_{2\pi n}(\vec{x}, t + 2\pi i n; \vec{x}', t') = G_{2\pi n}(\vec{x}, t; \vec{x}', t' - 2\pi i n) = G_{2\pi n}(\vec{x}', t'; \vec{x}, t), \qquad (15.11)$$

as expected for a thermal Green function.

It is possible to define a time-dependent Schroedinger picture density matrix

$$\rho_n(t) = C_n U(-\infty, t + 2\pi i n) U(t, -\infty). \qquad (15.12)$$

One can then compute correlators at equal (finite) times by inserting the Schroedinger-picture operators $\phi(\vec{x}, -\infty)$:

$$G_{2\pi n}(\vec{x}, t; \vec{x}', t) = \mathrm{Tr}\rho_n(t)\phi(\vec{x}, -\infty)\phi(\vec{x}', -\infty). \qquad (15.13)$$

The Heisenberg density matrix is related to the Schrodinger density matrix by

$$\rho_n = \rho_n(-\infty). \qquad (15.14)$$

We note that the thermal density matrix ρ_n can not be exactly identified with any of the vacua of the preceding section, all of which are pure states by construction. Despite this fact we will see below that in some cases it becomes difficult to distinguish pure and mixed states.

To summarize, we have seen that, despite the time dependence of the background, it is mathematically possible to define mixed states which approaches the standard thermal vacuum at past infinity while retaining the thermal periodicity at all times.

15.2. Unruh detection

In the previous subsection, a sequence of mixed thermal states were described with temperatures $T = \frac{1}{2\pi n}$. On the other hand, in the previous section we saw that various s-brane vacua – despite being pure states – have some mysterious "thermal"

behavior. In this subsection we will clarify this by showing that a particle detector in these vacua will respond as if it is in a mixed thermal state with temperature $T = \frac{1}{4\pi}$. In the next subsection we will show that the pure state correlators can asymptotically approach those of the thermal state.

Let us imagine coupling some detector to the field ϕ via a monopole interaction term $\int dt\, O(t)\phi(t)$. Here $O(t)$ is a hermitian operator that acts on the Hilbert space of the detector, which we will assume is spanned by some discrete, non-degenerate set of energy eigenstates $|E_i\rangle$. We also assume that the detector is stationary and that the detector Hamiltonian is time independent. We can now calculate the probability that the detector will jump from a state with energy E_i to one with energy E_j. To first order in perturbation theory it is (a recent discussion appears in section 3.2 of [147])

$$P_{i\to j} = |\langle E_i|O(0)|E_j\rangle|^2 \int dt \int dt' e^{-i\Delta E(t-t')} G(t,t') \tag{15.15}$$

where $\Delta E = E_i - E_j$ and $G(t,t')$ is the Wightman two point function of the scalar field in a particular vacuum state. The detector response is thermal at temperature T if the probability amplitudes (15.15) obey the detailed balance condition

$$\frac{P_{i\to j}}{P_{j\to i}} = e^{-\Delta E/T}. \tag{15.16}$$

For time translation invariant theories the green function depends only on $t-t'$ and the double integral (15.15) is infinite. One can then factor out the $\int d(t+t')$ to get a finite expression for the transition rate per unit time $\dot{P}_{i\to j}$. For s-branes the Green function $G(t,t')$ is not time translation invariant and the calculation is more complicated.

In fact, for the full s-brane expression (15.15) – the *total* probability integrated over all time – is finite. This is because the Green function $G(x,y)$ solves the wave equation in both arguments, so that as $t \to \pm\infty$, $G(t,t') \sim e^{\mp t/4}$ vanishes rapidly.

This holds for both t and t', so the double integral (15.15) converges. This is true for any vacuum state of the full s-brane. This behavior has a natural physical interpretation: in the far past and far future the open string states become very massive and cannot couple to the detector.

For brane creation, the Green function $G(t,t')$ does not fall off exponentially as $t \to +\infty$, so that the integrated probability amplitudes (15.15) are infinite. At this point one approach is to consider the transition rates $\dot{P}_{i\to j}(t)$, which are finite and time dependent. We will take a different point of view, however, and show directly that the ratio (15.16) converges to a finite (and interesting) answer.

In order to evaluate (15.15), we rewrite the Green function in a particular vacuum as

$$\begin{aligned} G(x^0,\vec{x};y^0,\vec{y}) &= \langle|\phi(x^0,\vec{x})\phi(y^0,\vec{y})|\rangle \\ &= \int d^{d-1}p\ e^{-i\vec{p}\cdot(\vec{x}-\vec{y})}u^*(x^0)u(y^0) \end{aligned} \tag{15.17}$$

where u are the (p-dependent) positive frequency modes. Then (15.15) becomes

$$P_{i\to j} = \int d^{d-1}\vec{p}\ |\tilde{u}(E_i - E_j)|^2 \tag{15.18}$$

where $\tilde{u}$ are the Fourier transformed modes. For the $|out\rangle_+$ vacuum of brane decay we can evaluate the Fourier integral [40]

$$\begin{aligned} \tilde{u}_+^{out}(E) &= \int e^{-iEt}u_+^{out}(t)\ dt \\ &= \sqrt{\frac{i}{8\pi}}e^{-\pi E}\lambda^{iE}\Gamma(-i(\omega+E))\Gamma(i(\omega-E)). \end{aligned} \tag{15.19}$$

This has the form

$$\tilde{u}_+^{out}(E) = i^{1/2}e^{-\pi E}x(E) \tag{15.20}$$

where $x(-E) = x^*(E)$. The norm is

$$|\tilde{u}_+^{out}(E)|^2 = e^{-2\pi E}\left[xx^*\right], \tag{15.21}$$

[40] As usual, the integral converges only after we deform the contour to give E a small positive imaginary part, $E \to E + i\epsilon$.

where the term in the square brackets is invariant under $E \to -E$. From this fact and expression (15.18) it follows that the transition probabilities in the $|out\rangle_+$ vacuum satisfy the detailed balance condition (15.16) with characteristic temperature $T_H = \frac{1}{4\pi}$. [41] The $|in\rangle_-$ vacuum for brane creation is related to the $|out\rangle_+$ vacuum for brane decay by time reversal, so it has identical transition probabilities $P_{i\to j}$ and thermal detector response.

In fact, the $|in\rangle_-$ and $|out\rangle_+$ vacua are very special in this respect. For example, we could calculate the transition probabilities in the $|in\rangle_+$ vacuum by inverting the Bogolubov relation (14.15). This gives

$$\begin{aligned} \tilde{u}_p^0(E) &= c^* \tilde{u}_p^{out}(E) - d\tilde{u}_p^{out\,*}(-E) \\ &= -2i^{3/2} d e^{\pi\omega} \cosh \pi(\omega - E) x. \end{aligned} \tag{15.22}$$

The norm is

$$|\tilde{u}_p^0(E)|^2 = \cosh^2 \pi(\omega - E) \left[4|d|^2 e^{2\pi\omega} x x^*\right] \tag{15.23}$$

where again the quantity in the square brackets is invariant under $E \to -E$. In this case it is clear that the transition probabilities are not thermal. It seems likely that for *any* vacuum state that is not $|out\rangle_+$ or $|in\rangle_-$, the Bogolubov transformation will give terms proportional to $e^{\pi E}$ so that the detector response is non-thermal.

15.3. Thermal correlators

We will now demonstrate that the correlators of the $|in\rangle_-$ vacuum are asymptotically thermal in the far future. The theory is free, so it suffices to consider the two point function $G(x, y)$. For brane creation, we have

$$u_-^{in} = a(u_-^{out} - e^{-2\pi\omega + i\theta} u_-^{out\,*}) \tag{15.24}$$

[41] As mentioned above, these transition probabilities are infinite, so in evaluating (15.15) it is necessary to regulate the divergent momentum integrals by, e.g. imposing some cutoff. In evaluating the ratio (15.16) one can safely take this regulator to infinity.

so the $|in\rangle_-$ Green function is

$$\begin{aligned} G^{in}_-(x,y) &= \int d^{d-1}\vec{p}\; u^{in}(x)u^{in\,*}(y) \\ &= \int \frac{d^{d-1}\vec{p}}{1-e^{-4\pi\omega}} e^{i\vec{p}\cdot(\vec{x}-\vec{y})} \left[(u_0(t)u_0^*(t') + e^{-4\pi\omega}u_0^*(t)u_0(t')) \right. \\ &\qquad \left. + e^{-2\pi\omega}(e^{i\theta}u_0(t)u_0(t') + c.c.)\right]. \end{aligned} \tag{15.25}$$

In the far future, u^{out}_- approaches a positive frequency plane wave plus corrections exponentially small in $t+t'$. In this limit the term on the second line of (15.25) becomes a function of $t-t'$ only, and approaches the usual (constant mass) thermal Green function at temperature $T_H = \frac{1}{4\pi}$

$$G^T(x,y) = \int \frac{d^{d-1}\vec{p}}{2\omega}\left(\frac{e^{i\vec{p}\cdot(\vec{x}-\vec{y})-i\omega(t-t')}}{1-e^{-4\pi\omega}} - \frac{e^{i\vec{p}\cdot(\vec{x}-\vec{y})+i\omega(t-t')}}{1-e^{4\pi\omega}}\right). \tag{15.26}$$

In the far future the third line of (15.25) depends on $t+t'$ rather than $t-t'$, and gives a contribution to the Green function

$$\int \frac{d^{d-1}\vec{p}}{2\omega}\frac{2}{\sinh 2\pi\omega}\left(e^{i\theta}e^{i\vec{p}\cdot(\vec{x}-\vec{y})-i\omega(t+t')} + c.c.\right) \tag{15.27}$$

plus exponentially small corrections. In the limit $t,t' \to +\infty$ this contribution vanishes as $(t+t')^{-(d-1)/2}$. In fact, when $\omega^2 = p^2$ (i.e. the field becomes massless in the far future) the integral (15.27) can be converted into a contour integral and shown to vanish exponentially in $t+t'$.

We conclude that in the far future the pure state $|in\rangle_-$ correlators become thermal plus asymptotically vanishing corrections. Likewise the $|out\rangle_+$ correlators become thermal in the far past.

16. Long-distance s-brane effective field theory

The dynamics of ordinary D-branes are described at low energies by a long-distance effective field theory. This field theory is of much interest in the understanding of holographic bulk-brane duality. One would like to know if there is a

similar long-distance field theory for s-branes, which would be a candidate holographic dual for an appropriate bulk string cosmology.

The first task is to define the notion of an effective field theory for branes with a spacelike orientation. This is best understood in terms of correlators. We define the long-distance effective field theory on the p+1-dimensional sp-brane as the p+1-dimensional Euclidean field theory that reproduces the long-distance correlators. To be specific, let us consider an s2-brane which is real codimension one in four spacetime dimensions. A massless field confined to the s2-brane should have a correlator that falls off like $\frac{1}{r}$. This is quite distinct from massless correlators at spacelike-separated points in the ambient four-dimensional spacetime, which fall off like $\frac{1}{r^2}$.

Consider a scalar on the full s2-brane with four-dimensional wave equation:

$$\partial^\mu \partial_\mu \phi - (2\lambda \cosh t + \omega^2)\phi = 0, \tag{16.1}$$

as in (14.26). In the far future and far past, ϕ is very massive, and correlators fall off exponentially with the spatial separation. Hence if there are any massless excitations they will be confined to the s2-brane world-volume near $t = 0$ where ϕ is light.

In trying to compute the equal-time correlators near $t = 0$, we immediately encounter a puzzle. Such correlators depend on the choice of quantum state for the field ϕ. Indeed, given any set of equal time correlators $\Delta(\vec{x}, \vec{y})$ there exists a quantum state $\Psi[\phi] = exp[-\frac{1}{4}\int\int \phi(\vec{x})\Delta^{-1}(\vec{x}, \vec{y})\phi(\vec{y})]$ that reproduces them.

In order to determine the long-distance effective field theory we must therefore first specify a quantum state. One possibility is to take the $|0\rangle_s$ state which has no particle flux at $t = 0$. Spacelike correlators at $t = 0$ in this state fall off exactly as they would in Minkowski space, *i.e.* as $\frac{1}{r^2}$. So this does not lead to a low energy effective field theory confined to the s-brane world-volume. As we have seen, a natural state for an s-brane is the thermal state at temperature $T = \frac{1}{2\pi n}$. Such thermal

states plausibly approximate the quantum states of open strings on an s-brane created from incoming closed string excitations. The $t = 0$ correlators in these states indeed fall off as $\frac{1}{r}$, indicating massless modes are confined to the s-brane. This can be most easily seen from the Euclidean construction of the correlators on $R^3 \times S^1$. At distances large compared to the radius of the S^1 (i.e. large compared to the inverse temperature) there is an effective compactification from four to three (Euclidean) dimensions, and so the effective correlators are three-dimensional. Massless modes of the three dimensional effective theory arise as usual from compactification zero modes. From the Minkowskian perspective, the mixed thermal state has excited components which carry more spatial correlations than the vacuum.

The Euclidean zero mode equation following from (16.1) is

$$\partial_\tau^2 \phi - (2\lambda \cos \tau + \omega^2)\phi = 0, \tag{16.2}$$

where $\tau \sim \tau + 2\pi n$. Whether or not there is a zero mode for a given temperature depends on the precise value of the mass parameter ω^2 (16.2), which has to be fine-tuned to get an exact zero mode. This special value might arise as a consequence of Goldstone's theorem or other symmetry considerations.

In conclusion, the s2-brane has a naturally associated three-dimensional Euclidean effective field theory given roughly by the high-temperature limit of the theory on the four-dimensional unstable brane. The full determination of such an effective theory for stringy s-branes is beyond the scope of the present work, although a few preliminary comments are made in our concluding discussion.

17. Thermal boundary states

We have seen that natural quantum states for s-branes are mixed thermal states at temperature $T = \frac{1}{2\pi n}$. In this section we will construct the exact CFT boundary state whose worldsheet correlators give the thermal spacetime Green functions,

generalizing the zero-temperature construction of [120]. Ghost and spacelike components of the boundary state are suppressed, but are similar to those in [120].

17.1. Zero modes and winding sectors

The boundary state $|B\rangle$ for the conformally invariant boundary Sine-Gordon theory

$$S = \frac{1}{2\pi}\int_\Sigma \partial\phi\bar{\partial}\phi + \frac{\lambda}{2}\int_{\partial\Sigma}\left(e^{i\phi}+e^{-i\phi}\right) \tag{17.1}$$

was found using the bulk $SU(2)$ current algebra in [142] (see also [148,149,150]). Here ϕ is Euclidean time, which will later be analytically continued to the Lorentzian world sheet field $X^0 = i\phi$. The boundary state corresponding to temperature $T = \frac{1}{2\pi n}$ arises when one identifies

$$\phi \sim \phi + 2\pi n. \tag{17.2}$$

This identification restricts the left and right moving momenta to be

$$(p_L, p_R) = (\frac{p}{n} + wn, \frac{p}{n} - wn) \tag{17.3}$$

where p and w are integers. In this case the thermal boundary state is simply

$$|B_n\rangle = P_n\ e^{2\pi i\lambda J_1}|N\rangle. \tag{17.4}$$

Here

$$|N\rangle = 2^{-1/4}\sum_{j,m}|j;m,-m\rangle\rangle \tag{17.5}$$

is the standard $SU(2)$ Neumann boundary state and $|j;m,-m\rangle\rangle$ is the Ishibashi state associated with the SU(2) primary field $|j;m,-m\rangle$. The SU(2) rotation J_1 acts only on right-movers, and P_n is the projection operator onto the allowed sublattice defined by (17.3). For $n = 1$, P_1 is the identity. In the non-compact case, $n \to \infty$ and P_∞ projects onto $p_L = p_R$.

Let us now consider the part of the boundary state which involves no oscillators. There are four such terms for every j, namely $|j;\pm j,\pm j\rangle$. Now, since

$$\langle j;j,j|P_n = \langle j;j,j|P_\infty, \qquad \langle j;-j,-j|P_n = \langle j;-j,-j|P_\infty \tag{17.6}$$

for any n, the $p_L = p_R$ components of the state are the same as in [120]. For real λ they may be written

$$\big[1 + 2\sum_{j\neq 0}(-\sin(\pi\lambda))^{2j}\cos(2j\phi(0))\big]|0\rangle = \frac{\cos^2(\pi\lambda)}{1+\sin^2(\pi\lambda)+2\sin(\pi\lambda)\cos\phi(0)}|0\rangle. \tag{17.7}$$

For finite n, there are also terms with $p_L = -p_R = 2nj \neq 0$. These are related to the $p_L = p_R$ terms by the rotation $e^{i\pi J_1}$, which corresponds to a shift of λ by $\frac{1}{2}$. Hence in addition to (17.7), $|B_n\rangle$ has a winding-sector component

$$2\sum_{j\neq 0}(\cos\pi\lambda)^{2nj}\cos(2nj\tilde\phi(0))|0\rangle = \frac{2\cos^n(\pi\lambda)\cos(n\tilde\phi(0)) - 2\cos^{2n}(\pi\lambda)}{1+\cos^{2n}(\pi\lambda)-2\cos^n(\pi\lambda)\cos(n\tilde\phi(0))}|0\rangle. \tag{17.8}$$

In this expression $\tilde\phi(z,\bar z) = \frac{1}{2}(\phi(z)-\phi(\bar z))$ is the T-dual of ϕ.

The continuation $\phi \to -iX^0$ of these expressions to the timelike theory

$$S = -\frac{1}{2\pi}\int_\Sigma \partial X^0\bar\partial X^0 + \lambda\int_{\partial\Sigma}\cosh X^0 \tag{17.9}$$

is straightforward. The theory (17.9) contains the currents[42]

$$j_\pm(z) = e^{\pm X^0(z)}, \qquad j_3(z) = \frac{1}{2}\partial X^0(z), \tag{17.10}$$

which generate the usual level one SU(2) current algebra. Note however that with the standard norm $X^{0\dagger} = X^0$, j_3 is anti-hermitian while $j^\pm$ are both hermitian. Nevertheless the charges

$$J_\pm = \oint\frac{dz}{2\pi i}j_\pm(z), \qquad J_3 = \oint\frac{dz}{2\pi i}j_3(z), \tag{17.11}$$

[42] In our conventions $X(z,\bar z) = \frac{1}{2}(X(z)+X(\bar z))$, $X(z)X(w)\sim 2\ln(z-w)$ and $\alpha' = 1$.

obey the usual commutation relations

$$[J_-, J_+] = -2J_3, \qquad [J_3, J_\pm] = \pm J_\pm. \tag{17.12}$$

States can therefore be characterized by their SU(2) representations. Under $\phi \to -iX$, $J_k \to J_k$ and hence $|j; m, m'\rangle\rangle \to |j; m, m'\rangle\rangle$. Therefore the Sine Gordon boundary state written in the form (17.4) can also be viewed as a boundary state for the timelike theory (17.9). Expressions (17.7) and (17.8) become

$$\begin{aligned}\big[1 + 2\sum_{j\neq 0}(-\sin(\pi\lambda))^{2j}\cosh(2jX^0(0))\big]|0\rangle \\ = \frac{\cos^2(\pi\lambda)}{1+\sin^2(\pi\lambda)+2\sin(\pi\lambda)\cosh X^0(0)}|0\rangle\end{aligned} \tag{17.13}$$

and

$$\begin{aligned}\sum_{j\neq 0}(\cos\pi\lambda)^{2nj}\cosh(2nj\tilde{X}^0(0))|0\rangle \\ = \frac{2\cos^n(\pi\lambda)\cosh(n\tilde{X}^0(0)) - 2\cos^{2n}(\pi\lambda)}{1+\cos^{2n}(\pi\lambda)-2\cos^n(\pi\lambda)\cosh(n\tilde{X}^0(0))}|0\rangle.\end{aligned} \tag{17.14}$$

Here $\tilde{X}^0(z,\bar{z}) = \frac{1}{2}(X^0(z) - X^0(\bar{z}))$.

17.2. The superstring

In this subsection we sketch the finite-temperature generalization for the superstring of the zero-temperature boundary state of [121]. For the superstring, instead of the boundary interaction (14.1), one has

$$\lambda \int d\tau \psi^0 \sinh\frac{X^0}{\sqrt{2}} \otimes \sigma_1. \tag{17.15}$$

We follow the notation of [119,121,131] in which σ_1 acts on Chan-Paton factors, and (17.15) arises from a tachyon field proportional to $\cosh\frac{X^0}{\sqrt{2}}$. After integrating out ψ^0 one obtains a boundary interaction of the form (14.4). This interaction is invariant under

$$X^0 \to X^0 + 2\sqrt{2}\pi i. \tag{17.16}$$

We can therefore consider thermal boundary states at temperatures

$$T = \frac{1}{2\sqrt{2}\pi n}. \tag{17.17}$$

This corresponds to the superstring Hagedorn temperature $T_H = \frac{1}{2\sqrt{2}\pi}$ for the minimal value $n = 1$, rather than the $n = 2$ we encountered in the bosonic string. The bosonic zero mode part of the boundary state with no winding is then

$$\frac{1 - \sin^4(\pi\lambda)}{1 + \sin^4(\pi\lambda) + 2\sin^2(\pi\lambda)\cosh(\sqrt{2}X^0(0))}|0\rangle. \tag{17.18}$$

The winding component is

$$\frac{2\cos^{2n}(\pi\lambda)\cosh(\sqrt{2}n\tilde{X}^0(0)) - 2\cos^{4n}(\pi\lambda)}{1 + \cos^{4n}(\pi\lambda) - 2\cos^{2n}(\pi\lambda)\cosh(\sqrt{2}n\tilde{X}^0(0))}|0\rangle. \tag{17.19}$$

These components are similar to those of the bosonic string, with the replacement $\sin\pi\lambda \to \sin^2\pi\lambda$ and the factors of $\sqrt{2}$. In computing the fermionic components, twisted boundary conditions around the thermal circle must be taken into account.

18. The $\lambda = \pm\frac{1}{2}$ sD-brane limit

In this section we will consider the very interesting limits $\lambda \to \pm\frac{1}{2}$. In [131] it was shown that in a certain $\lambda \to -\frac{1}{2}$ limit, the general bosonic s-brane boundary state (17.4) (at zero temperature) reduces to the boundary state of [118] which imposes a Dirichlet boundary condition $X^0 = 0$ in the time direction. In other words $\lambda = -\frac{1}{2}$ is an sD-brane. The relation to sD-branes follows immediately from the fact that the $\lambda = \pm\frac{1}{2}$ boundary interaction is an $SU(2)$ rotation by π which transforms a Neumann boundary state into a Dirichlet state.

On the other hand, in [120] it was shown that in a certain $\lambda \to \frac{1}{2}$ limit, the general s-brane boundary state in some sense reduces to nothing – i.e. in this limit there is no brane present at all.[43] In fact, we will see that the limiting closed string

[43] As can be seen from (17.18), the superstring case for both $\lambda \to \frac{1}{2}$ and $\lambda \to -\frac{1}{2}$ is qualitatively similar to the $\lambda \to \frac{1}{2}$ bosonic case.

configuration is not unambiguously determined from the boundary state for any value of λ. Additional boundary conditions on the fields are needed. In general the limit is not the trivial one described in [120], but rather is a very special type of s-brane configuration described by spacelike Dirichlet branes located on the imaginary time axis.

In the next subsection, we will describe this ambiguity in the limit $\lambda \to \frac{1}{2}$. In section 6.2 we will derive the linearized RR-field sourced by an sD-brane and see that it carries a non-trivial s-charge for all λ. In 6.3 the long range graviton and dilaton fields of an s-brane are computed. In 6.4 we determine the force between an ordinary D-brane and a $\lambda = \frac{1}{2}$ sD-brane from a computation of the annulus diagram. in 6.5 the calculation is generalized to finite temperature. Finally, in section 6.6 we discuss the relation between s-branes and D-instantons.

18.1. The classical closed string field

Consider the state

$$|C\rangle = \frac{1}{L_0 + \bar{L}_0}|B\rangle. \tag{18.1}$$

This can be viewed as a quantum state of a single closed string. Alternately, since the states in the Fock basis of the single closed string are identified as spacetime components of the classical string field, $|C\rangle$ can be viewed as a classical string field configuration. By construction it obeys

$$(L_0 + \bar{L}_0)|C\rangle = |B\rangle. \tag{18.2}$$

These are the linearized spacetime wave equations with sources for the components of the classical string field. The source is the boundary state $|B\rangle$ whose support is confined to the brane. Hence we conclude that $|C\rangle$ is the linearized classical closed string field sourced by the brane.

For ordinary static supersymmetric D-branes, it has been explicitly verified that $|C\rangle$ as defined in (18.1) reproduces the linearized dilaton, metric and RR fields

sourced by the brane [151]. When the brane is static, the Fock component states in $|B\rangle$ carry no p^0, and all of its components are off-shell. A unique static $|C\rangle$ may then be determined from (18.1). Time-dependent boundary states differ crucially in this regard. They have components with non-vanishing p^0 which correspond to on-shell closed string states and hence are annihilated by $L_0 + \bar{L}_0$. It follows that $L_0 + \bar{L}_0$ is not invertible and $|C\rangle$ is not unambiguously determined from $|B\rangle$. This is just the usual problem of specifying the homogenous part of the solution emanating from a time-dependent source. Some additional boundary conditions must be specified.[44]

For general λ, the Fock components of the string field wave equation (18.2) are of the form

$$\begin{aligned} \eta^{ab}\partial_a\partial_b\phi(\vec{x},t) &= \delta^{25-p}(\vec{x})\frac{\cos^2(\pi\lambda)}{1+\sin^2(\pi\lambda)+2\sin(\pi\lambda)\cosh t} \\ &= \delta^{25-p}(\vec{x})\left(\frac{1}{1+e^t\sin\pi\lambda}+\frac{1}{1+e^{-t}\sin\pi\lambda}-1\right). \end{aligned} \tag{18.3}$$

This follows from (17.13) after replacing the operator X^0 by its eigenvalue t. Here $\vec{x}$ are the transverse spatial dimensions, and longitudinal spatial dimensions are suppressed. For notational simplicity we henceforth specialize to $p = 22$, so that only four spacetime dimensions are relevant. For $\lambda = \frac{1}{2}$ the wave equation (18.3) reduces to

$$\eta^{ab}\partial_a\partial_b\phi(\vec{x},t) = 2\pi i\delta^3(\vec{x})\sum_{m=-\infty}^{\infty}\delta(t+\pi i+2m\pi i). \tag{18.4}$$

Since the source on the right hand side vanishes for real t, an obvious solution of (18.4) for real t is simply

$$\phi(\vec{x},t) = 0. \tag{18.5}$$

This is the solution implicit in [120]. However, there is another solution which "knows" about the sources at imaginary t. Recall that the wave equation with a

[44] We note that this closed string ambiguity remains even after we have fixed the quantum state of the open strings on the brane.

delta function source

$$\eta^{ab}\partial_a\partial_b\phi(\vec{x},t) = \delta^3(\vec{x})\delta(t-t_0) \tag{18.6}$$

is solved by Feynman propagator

$$\phi(\vec{x},t) = -\Delta_F(\vec{x},t;\vec{0},t_0) = \frac{i}{4\pi^2}\lim_{\epsilon\to 0}\frac{1}{(t-t_0)^2 - r^2 + i\epsilon}, \tag{18.7}$$

where $r^2 = \vec{x}^2$. Continuing this to imaginary t_0 we find that (18.3) is solved by

$$\begin{aligned}\phi(\vec{x},t) &= -2\pi i\sum_{m=-\infty}^{\infty}\Delta_F(\vec{x},t;\vec{0},\pi i + 2\pi m i) \\ &= \frac{1}{2\pi}\sum_{m=-\infty}^{\infty}\frac{1}{r^2 - (t-\pi i - 2\pi m i)^2}.\end{aligned} \tag{18.8}$$

Since the denominator is non-vanishing for real (r,t), we have set ϵ to zero here. Performing the sum over m yields

$$\phi(\vec{x},t) = -\frac{1}{4\pi r}\big(\tanh\frac{r+t}{2} + \tanh\frac{r-t}{2}\big). \tag{18.9}$$

Note that at large t and fixed r this vanishes exponentially. On the other hand, at fixed time t this has the $\frac{1}{r}$ falloff at large r characteristic of a static source, yet it is nonsingular for all real r,t. With 25-p transverse dimensions we would find a characteristic $\frac{1}{r^{23-p}}$ falloff. Solutions of this general form were discussed in [118].

In section 6.3 we will compute the annulus diagram connecting an sD-brane and an ordinary D-brane using a straightforward adaptation of the standard string theory prescription [152], which involves a Euclidean continuation of the worldsheet field X^0. Since this calculation gives a definite answer, it must contain an implicit prescription for inverting $L_0+\bar{L}_0$. We shall find that at large separation the graviton falls off like $\frac{1}{r^{23-p}}$. This indicates that non-trivial solutions of the form (18.9) rather than the trivial solution (18.5) are implicit in this formulation of worldsheet string theory.

We note that at $\lambda = \frac{1}{2}$, the branes have no support at real t, and therefore there can be no on-shell open strings propagating at real time. Hence the problem [129] of a Hagedorn-like divergence in open string pair production disappears.

18.2. RR field strength and s-charge

In this subsection we will use (18.1) to determine the RR field sourced by an sD-brane in superstring theory. We will find that it carries one unit of "s-charge" defined below as an integral of the RR field strength over a complete spacelike surface.

In the presence of an s-brane described by the boundary deformation (17.15), the source for RR fields is proportional to [153]

$$\sin(\pi\lambda)\left[\frac{e^{X^0/\sqrt{2}}}{1+\sin^2(\pi\lambda)e^{\sqrt{2}X^0}}-\frac{e^{-X^0/\sqrt{2}}}{1+\sin^2(\pi\lambda)e^{-\sqrt{2}X^0}}\right] \tag{18.10}$$

up to an overall normalization, which can be determined as follows. If we analytically continue

$$\lambda\to -i\lambda,\quad X^0\to X^0+\pi i/\sqrt{2}, \tag{18.11}$$

the boundary interaction (17.15) becomes $\lambda\psi^0\cosh X^0/\sqrt{2}$, which describes the tachyon rolling over the barrier. The corresponding s-brane should carry ± 1 unit of RR charge, with the sign depending on the sign of λ. The integral of the source is now $\sqrt{2}\pi\,\mathrm{sign}(\lambda)$, which determines the normalization factor to be $(\sqrt{2}\pi)^{-1}$ times the unit RR charge.

Let us now return to the case (17.15). After Euclidean continuation $X^0\to i\phi$, the RR source can be written as

$$\frac{1}{\sqrt{2}\pi}\sin(\pi\lambda)\left[\sum_{n=0}^{\infty}(-1)^n\sin^{2n}(\pi\lambda)e^{i(2n+1)\phi/\sqrt{2}}-\sum_{n=0}^{\infty}(-1)^n\sin^{2n}(\pi\lambda)e^{-i(2n+1)\phi/\sqrt{2}}\right]. \tag{18.12}$$

When $\lambda=1/2$, this is the source corresponding to an array of branes and antibranes located along the Euclidean time axis

$$-i\sqrt{2}\sum_{n=-\infty}^{\infty}(-1)^n\delta(\sqrt{2}\phi+\pi+2n\pi) \tag{18.13}$$

The wave equation is then

$$\partial^a \partial_a C_{9-p,\cdots,9} = \sqrt{2} \sum_{n=-\infty}^{\infty} (-1)^n \delta(\sqrt{2}X^0 + i\pi + 2\pi n i)\delta(\vec{r}_\perp). \tag{18.14}$$

For simplicity, we will consider the case of an s5-brane in type IIB theory, so that there are 4 transverse directions. As in the previous section, we can solve the wave equation in Euclidean space and analytically continue back to find

$$\begin{aligned} C_{4\cdots 9} &= \frac{i}{2\pi^2} \sum_{n=-\infty}^{\infty} \frac{(-1)^n}{(\sqrt{2}t + \pi i + 2\pi n i)^2 - 2r^2} \\ &= \frac{1}{8\sqrt{2}\pi^2 r} \left[\frac{1}{\cosh \frac{r-t}{\sqrt{2}}} - \frac{1}{\cosh \frac{r+t}{\sqrt{2}}} \right]. \end{aligned} \tag{18.15}$$

The RR potential for sp-branes, $p \neq 5$, in type IIB theory can be obtained from the above by, say, taking derivatives in r.

The s-brane with $\lambda = 1/2$ has no RR source located at real time, so the RR flux through any transverse spacelike 3-surface is conserved. The conserved charge is

$$Q_s = \int_{\Sigma_3} *dC. \tag{18.16}$$

If we take Σ_3 to be the plane located at $X^0 = t$ and extending in $X^{1,2,3}$ directions, then

$$(dC)_{04\cdots 9} = \frac{\partial}{\partial_t} C_{4\cdots 9} = \frac{1}{16\pi^2 r} \left[\frac{\sinh \frac{r-t}{\sqrt{2}}}{\cosh^2 \frac{r-t}{\sqrt{2}}} + \frac{\sinh \frac{r+t}{\sqrt{2}}}{\cosh^2 \frac{r+t}{\sqrt{2}}} \right] \tag{18.17}$$

yields

$$Q_s = \int_0^\infty dr 4\pi r^2 (dC)_{04\cdots 9} = \frac{1}{2}\ . \tag{18.18}$$

We conclude that the $\lambda = \frac{1}{2}$ closed string configuration carries half a unit of spacelike Ramond-Ramond charge.

18.3. Long-range graviton/dilaton fields

In this subsection we compute the long-distance Coulomb fields for the graviton and dilaton sourced by the sp-brane. We will restrict to the bosonic case, although the generalization to the superstring is straightforward.

The spatial components of the boundary state of an sp-brane are

$$|B\rangle_{\vec{X}} = \frac{T_{p+1}}{2}\delta^{24-p}(\vec{x}_\perp)\exp\left(-\sum_{n=1}^{\infty} S_{ij}a^i_{-n}\tilde{a}^i_{-n}\right)|0\rangle \tag{18.19}$$

where T_{p+1} is the tension of the D$(p+1)$-brane and S_{ij} $(1 \le i,j \le 25)$ is given by

$$S_{ij} = (\delta_{\alpha\beta}, -\delta_{ab}) \tag{18.20}$$

where α,β $(a,b$ $)$ label the directions with Neumann (Dirichlet) boundary conditions.

The relevant parts of the time component of the boundary state are [120]

$$|B\rangle_{X^0} = f(X^0)|0\rangle + a^0_{-1}\tilde{a}^0_{-1}g(X^0)|0\rangle + \cdots \tag{18.21}$$

where

$$\begin{aligned} f(X^0) &= \frac{1}{1+e^{X^0}\sin\pi\lambda} + \frac{1}{1+e^{-X^0}\sin\pi\lambda} - 1, \\ g(X^0) &= 1+\cos(2\pi\lambda) - f(X^0), \end{aligned} \tag{18.22}$$

and a^0_{-1} is an oscillator in the expansion of X^0. Combining (18.19) and (18.21), we get the total source for graviton and dilaton

$$|B\rangle = \frac{T_{p+1}}{2}\delta^{24-p}(\vec{x}_\perp)\left[-S_{ij}a^i_{-1}\tilde{a}^j_{-1}f(X^0) + a^0_{-1}\tilde{a}^0_{-1}g(X^0)\right]|0\rangle + \cdots \tag{18.23}$$

The massless part of the closed string field is then

$$|C\rangle = \frac{T_{p+1}}{2}V_{p+1}\int dt'\,\Delta(\vec{X},X^0;0,t')\left[-S_{ij}a^i_{-1}\tilde{a}^j_{-1}f(t') + a^0_{-1}\tilde{a}^0_{-1}g(t')\right]|0\rangle + \cdots \tag{18.24}$$

where V_{p+1} is the spatial volume of the s-brane. Our prescription for the t' integral employs the Euclidean imaginary time axis. Defining

$$J^{\mu\nu}(k) = \langle 0;k|a^\mu_1\tilde{a}^\nu_1|C\rangle \tag{18.25}$$

one finds

$$\begin{aligned} J_{ij}(x) &= -\frac{T_{p+1}}{2}V_{p+1}S_{ij}\int dt'\,\Delta(\vec{x},t;0,t')f(t'), \\ J_{00}(x) &= \frac{T_{p+1}}{2}V_{p+1}\int dt'\,\Delta(\vec{x},t;0,t')g(t'). \end{aligned} \tag{18.26}$$

For simplicity let us first consider the case $p = 21$, where there are 4 transverse directions to the sp-brane. For $r = |\vec{x}| > |t|$,[45]

$$J_{ij}(\vec{x},t) = -\frac{T_{p+1}V_{p+1}}{2}\frac{S_{ij}}{4\pi r}\left[\frac{1}{1+e^{t-r}\sin\pi\lambda}+\frac{1}{1+e^{-t-r}\sin\pi\lambda}-1\right],$$
$$J_{00}(\vec{x},t) = -\frac{T_{p+1}V_{p+1}}{2}\frac{1}{4\pi r}\left[\frac{1}{1+e^{t-r}\sin\pi\lambda}+\frac{1}{1+e^{-t-r}\sin\pi\lambda}-2-\cos(2\pi\lambda)\right]. \tag{18.27}$$

In the limit of large r, we have

$$J_{ij} \to -\frac{T_{p+1}V_{p+1}}{2}\frac{S_{ij}}{4\pi r}, \qquad J_{00} \to \frac{T_{p+1}V_{p+1}}{2}\frac{\cos(2\pi\lambda)}{4\pi r} \tag{18.28}$$

For general sp-branes

$$J_{ij} \to -N_p\frac{S_{ij}}{r^{22-p}}, \qquad J_{00} \to N_p\frac{\cos(2\pi\lambda)}{r^{22-p}},$$
$$N_p = \frac{T_{p+1}V_{p+1}}{4}\pi^{\frac{p-24}{2}}\Gamma\left(\frac{24-p}{2}\right). \tag{18.29}$$

We see that in the string frame the graviton and dilaton fields fall off like $\frac{1}{r^{22-p}}$. This is consistent with the results of the next subsection in which the force between an s-brane and a D-brane is computed.

18.4. The annulus diagram

In this subsection we compute the bosonic annulus diagram in the presence of an ordinary D(p+1)-brane and sp-brane with general λ. $\lambda = 0$ corresponds to two D(p+1)-branes while $\lambda = \frac{1}{2}$ is an sDp-brane and a D(p+1)-brane. We will deduce the long range force from this computation and find that it is in agreement with the results of the previous section.

Let us denote the boundary state associated to the D(p+1)-brane by $|D_{p+1}\rangle$ and the boundary state associated to the sp-brane with coupling λ by $|s_p,\lambda\rangle$. They

[45] The full solution is discontinuous (but obeys the wave equation) on the light cone for $\lambda < \frac{1}{2}$. The $\lambda = 0$ case corresponds to a D-brane with some radiation inside the light cone.

are factorized as the product of time components and spatial components as

$$\begin{aligned} |D_{p+1}\rangle &= |N\rangle^0 \otimes |N\rangle^{1,\cdots,p+1} \otimes |D\rangle^{p+2,\cdots,25} \otimes |\text{ghost}\rangle, \\ |s_p\rangle &= |B,\lambda\rangle \otimes |N\rangle^{1,\cdots,p+1} \otimes |D\rangle^{p+2,\cdots,25} \otimes |\text{ghost}\rangle. \end{aligned} \tag{18.30}$$

Here $|B,\lambda\rangle$ is the zero-temperature boundary state (as in [142], [120] and equation (17.4))

$$\begin{aligned} |B,\lambda\rangle &= P_\infty e^{2\pi i \lambda J_1} |N\rangle, \\ &= 2^{-1/4} \sum_{j,m} D^j_{m,-m}(2\pi\lambda) |j,m,m\rangle\rangle. \end{aligned} \tag{18.31}$$

Here $J_1 = \cosh X^0$, P_∞ projects onto $p_L = p_R$ and $D^j_{m,m'}$ is the $SU(2)$ representation matrix element

$$D^j_{m,m'}(2\pi\lambda) = \langle j,m|e^{i2\pi\lambda J_1}|j,m'\rangle. \tag{18.32}$$

For the state $|j,m,m'\rangle\rangle$ the left and right momenta are related by $p_L = 2m', p_R = 2m$.

The annulus diagram connecting $|D_{p+1}\rangle$ and $|s_p,\lambda\rangle$ is given by[46]

$$Z_A = \int_0^\infty dt\ I_\lambda(t), \tag{18.33}$$

with

$$I_\lambda(t) \equiv \langle s_p|e^{-t(L_0+\widetilde{L}_0)}|D_{p+1}\rangle. \tag{18.34}$$

The integrand of Z_A is a product $I_\lambda(t) = I^0_\lambda(t) I^S(t)$ of contributions from time components and spatial plus ghost components. The contribution from these latter

[46] To compute the force between the D-brane and the s-branes we must multiply this expression by a factor of 2, since the string can stretch in either orientation.

components is the same as in the free theory, namely[47]

$$\begin{aligned} I^S(t) &= \frac{1}{2t} V_{p+1} \int \frac{d^{p+1}\vec{p}}{(2\pi)^{p+1}} e^{-\frac{2\pi\vec{p}^2}{t} - \frac{y^2}{2\pi t}} \sum e^{-2\pi(h_i-1)/t} \\ &= \frac{V_{p+1}}{2t} \left(\frac{8\pi^2}{t}\right)^{-(p+1)/2} e^{-\frac{y^2}{2\pi t}} \eta(i/t)^{-23} \\ &= \frac{V_{p+1}}{2} (8\pi^2)^{-(p+1)/2} t^{(p-24)/2} e^{-\frac{y^2}{2\pi t}} \eta(it)^{-23}. \end{aligned} \tag{18.35}$$

The timelike components were computed in [142] (up to the factor of i from analytic continuation of the volume) as

$$I^0_\lambda(t) = \langle B| e^{-\pi t(L_0 + \widetilde{L}_0)} |N\rangle = \frac{iV_0}{\sqrt{2}} \sum_{j=0,1,\cdots} D^j_{00}(2\pi\lambda)\ \chi^{Vir}_j(e^{-2\pi t}), \tag{18.36}$$

where

$$D^j_{00}(2\pi\lambda) = \frac{1}{j!} \frac{d^j}{d\xi^j} \left[\xi^j (1-\xi)^j\right], \quad \xi = \sin^2(\pi\lambda), \tag{18.37}$$

and V_0 is the real volume in the X^0 direction and

$$\chi^{Vir}_j(q) = q^{-1/24}(q^{j^2} - q^{(j+1)^2}) \prod_{n=1}^{\infty} \frac{1}{1-q^n} \tag{18.38}$$

is the Virasoro character. The total integrand from large t goes as

$$I_\lambda(t) = i\frac{V_0 V_{p+1}}{2} (8\pi^2)^{-(p+1)/2} \int dt\ t^{(p-24)/2} e^{-y^2/2\pi\alpha' t} (e^{2\pi t} + 23 + \cos(2\pi\lambda) + \cdots). \tag{18.39}$$

When $\lambda = 0$ we have two D(p+1)-branes and (18.39)reduces to the usual expression. As usual the force between the D-brane and s-brane is obtained by differentiating with respect to y. As λ ranges from 0 to $\frac{1}{2}$ and the D-brane goes to an s-brane and then an sD-brane, the force decreases by a factor of $\frac{11}{12}$.

[47] In general when there is on-shell closed strings exchange one must include an ordering and $i\epsilon$ prescription for the t and $\vec{p}$ integrations. However when one of the boundary states is a D-brane, local energy conservation prohibits emission/absorption of an on-shell closed string.

18.5. The finite-temperature annulus

In this subsection we compute the bosonic annulus diagram at general λ and temperature $T = \frac{1}{2\pi n}$. We will find that the $T \to 0$ limit reproduces the results of the previous section.

At finite temperature $T = \frac{1}{2\pi n}$ one naturally computes the Euclidean thermal partition function. This is obtained by Wick rotation $X^0 \to i\phi$ with the Euclidean time ϕ compactified on a circle of radius n[154,152]. We consider a D(p+1)-brane located at $X^m = 0$, $m = p+2, \cdots, 25$, with world-volume extending in the $X^1, \cdots, X^{p+1}$ directions and wrapped around the ϕ circle. There is also an sp-branes located at $X^m = y^m$ and parallel to the D-brane in the spatial directions. When λ vanishes, we simply have the Euclidean annulus connecting two finite temperature D(p+1)-branes. The open string 1-loop calculation gives (before integrating over t)

$$\begin{aligned} \mathrm{Tr}\, e^{-2\pi L_0/t} &= \frac{1}{\eta(i/t)} \sum_m e^{-\frac{2\pi}{t}\frac{m^2}{n^2}} \\ &= \frac{1}{\eta(i/t)} \vartheta(0, \frac{2i}{n^2 t}) \\ &= \frac{n}{\sqrt{2}\eta(it)} \vartheta(0, in^2 t/2). \end{aligned} \tag{18.40}$$

We will recover this result below in the special case $\lambda = 0$.

We will now turn to the Euclidean s-brane boundary state. At the self-dual temperature ($n = 1$), the time component of the boundary state describing an s-brane is[142]

$$|B\rangle_{SU(2)} = e^{i2\pi\lambda J_1} |N\rangle_{SU(2)}. \tag{18.41}$$

For other values of n the boundary state describing an array of n s-branes is, up to a normalization factor, simply the projection of $|B\rangle_{SU(2)}$ onto allowed momentum and winding modes. For $\lambda = \pm 1/2$, this boundary state describes n Dirichlet branes

on a circle. The boundary state $|B\rangle$ at temperature $T = 1/2\pi n$ is

$$\begin{aligned} |B\rangle_{R=2\pi n} &= 2^{-1/4} \sum_{j=0,1/2,\cdots} P_n e^{i\theta^a J^a} |j, m, -m\rangle\rangle \\ &= 2^{-1/4} \sum_j \sum_{m,w} D^j_{m-wn,-m}(2\pi\lambda) |j, m, m - wn\rangle\rangle. \end{aligned} \tag{18.42}$$

At $\lambda = \pm 1/2$ equation (18.42) simplifies to

$$2^{-1/4} \sum_{j=0,1/2,\cdots} e^{\pm i\pi j} |j, m, m\rangle\rangle. \tag{18.43}$$

The Neumann boundary state at $T = 1/2\pi n$ is

$$|N\rangle_{R=2\pi n} = 2^{-1/4} \sum_{j=0,1/2,\cdots} \sum_w |j, wn/2, -wn/2\rangle\rangle. \tag{18.44}$$

Here the second sum is over allowed values of w, i.e. wn is restricted to be even (odd) when j is integer (half integer). The time component of the annulus amplitude is

$$\langle B| e^{-\pi t(L_0 + \widetilde{L_0})} |N\rangle_{R=2\pi n} = \frac{n}{\sqrt{2}} \sum_{j=0,1/2,1,\cdots} \sum_w D^j_{\frac{wn}{2},\frac{wn}{2}}(2\pi\lambda)\ \chi_j^{Vir}(e^{-2\pi t}). \tag{18.45}$$

The prefactor n comes from the volume of the ϕ zero mode.

The trivial case $\lambda = 0$ corresponds to a Neumann boundary condition. We should be able to recover from (18.45) the answer for ordinary D-branes (18.40). We can write (18.45) as

$$\langle N| e^{-\pi t(L_0 + \widetilde{L_0})} |N\rangle_{R=2\pi n} = \frac{n}{\sqrt{2}} \sum_{j=0,1/2,1,\cdots} C_{n,j}\ \chi_j^{Vir}(e^{-2\pi t}), \tag{18.46}$$

where

$$C_{n,j} = \sum_{wn/2 \in \{-j, -j+1, \cdots, j\}} 1. \tag{18.47}$$

Suppose n is even. Then the $wn/2$ are integers, so the contribution to (18.47) comes from integer values of j. Equation (18.46) can then be rewritten as

$$\frac{n}{\sqrt{2}\eta(it)} \sum_{j=0}^{\infty} (C_{n,j} - C_{n,j-1}) e^{-2\pi j^2 t}. \tag{18.48}$$

For n even,

$$C_{n,j} - C_{n,j-1} = \begin{cases} 2, & j = kn/2, k(\text{A.1})1; \\ 1, & j = 0; \\ 0, & \text{otherwise} \end{cases} \tag{18.49}$$

so we can evaluate the sum (18.46)

$$\frac{n}{\sqrt{2}\eta(it)} \sum_{k=-\infty}^{\infty} e^{-\pi n^2 k^2 t/2} = \frac{n}{\sqrt{2}\eta(it)} \vartheta(0, in^2 t/2), \tag{18.50}$$

which agrees with (18.40). A similar analysis yields the same expression for odd n.

At the special values $\lambda = \pm 1/2$ only the $w = 0$ sector will contribute to the amplitude (18.45), so j is therefore restricted to be an integer. The amplitude (18.45) then reduces to

$$\frac{n}{\sqrt{2}} \eta(it)^{-1} \sum_{j=-\infty}^{\infty} e^{-2\pi t j^2 + \pi i j} = \frac{n}{\sqrt{2}\eta(it)} \vartheta(1/2, 2it). \tag{18.51}$$

Combining this with (18.35), we find that the annulus partition function at generic λ and n is

$$\begin{aligned} &\int_0^\infty dt \ \langle s_p | e^{-\pi t (L_0 + \widetilde{L}_0)} | D_{p+1} \rangle \\ &\qquad = \int_0^\infty dt \frac{n V_{p+1}}{2\sqrt{2}} (8\pi^2)^{-\frac{p+1}{2}} t^{\frac{p-24}{2}} e^{-\frac{y^2}{2\pi t}} \eta(it)^{-24} \\ &\qquad\qquad \sum_{j=0,1/2,1,\cdots} \sum_{w} D^j_{\frac{wn}{2}, \frac{wn}{2}} (2\pi\lambda) \ (e^{-2\pi t j^2} - e^{-2\pi t (j+1)^2}). \end{aligned} \tag{18.52}$$

For $\lambda = \pm 1/2$ and all n, the contribution from large t goes like

$$n V_{p+1} \int dt \ t^{(p-24)/2} e^{-y^2/2\pi\alpha' t} (e^{2\pi t} + 22 + \cdots). \tag{18.53}$$

As usual, the first term in the sum corresponds to the amplitude of tachyon exchange. The graviton exchange amplitude, given by the second term in the sum, falls off like $|y|^{p-22} = |y|^{2-(25-(p+1))}$, as in the zero-temperature case. This agrees with (18.39) up to the factor of i, which is due to the fact that (18.53) comes from the Euclidean rather than Lorentzian one loop diagram.

18.6. S-branes and D-instantons

In this subsection we discuss the relation between s-branes and D-instantons.

Instantons fall into two general categories: those with and those without a time reversal symmetry. An example of the latter is the Yang-Mills instanton. It describes tunneling between topologically distinct vacua. Any attempt to continue it to real time yields an imaginary solution. There is a topological Lorentzian configuration – the creation and decay of a sphaleron – which interpolates between the distinct vacua, but it is not obtained by analytic continuation of the Euclidean instanton solution.

The situation is different when there is a time reversal symmetry, as in the Euclidean bubble describing the decay of the false vacuum. The analytic continuation to real time yields a real solution describing a contracting/expanding bubble of the true vacuum inside the false vacuum. Indeed, the semi-classical decay process is quantum tunneling followed by the real time expanding bubble solution. In this case both the Euclidean and Lorentzian solutions are real and meaningful.

The sD-branes (and most of the s-branes) discussed herein are of this latter character. They are processes in which the tachyon rolls up one side of the barrier and back down the same side, and so are time symmetric. While we have been focusing on the Lorentzian solutions, there are also Euclidean solutions which represent tunneling through the tachyon barrier at $\mathcal{T} = 0$. For example, we could consider a semi-classical process in which the tachyon is incident on the barrier from $\mathcal{T} = -\infty$, tunnels through it, and then proceeds to $\mathcal{T} = +\infty$. The tunneling phase of this evolution would be described by the Euclidean continuation of the s-brane. It connects two time-symmetric solutions in which $\mathcal{T}$ bounces off the barrier. Alternately the periodically identified instanton can be interpreted as a finite-temperature tunneling in which the energy comes from the thermal bath. Such tunneling processes could become important near the Hagedorn transition.

There are also of course non-time symmetric solutions with large enough energy to classically pass over the barrier. These solutions, largely the focus of [118], will result in a change in the RR s-charge Q_s evaluated at $t = \pm\infty$. They are analogs of baryon-number-violating sphaleron creation/decay in the standard model. They do not have a real continuation to Euclidean space (at least by the usual method). In the superstring, one has a cosh rather than a sinh in (17.15), while in the bosonic string one has a sinh rather than a cosh in (14.4).

19. Timelike Holography

An interesting potential application of s-branes is to the problem of finding a string theory configuration with a timelike holographic dual. We close this paper with some speculation on this topic.

The sD-brane boundary state for the superstring at temperature $T = \frac{1}{2\sqrt{2}\pi n}$ describes $2n$ Euclidean D-branes spaced along a circle at intervals $\sqrt{2}\pi$. According to (18.14), these have alternating RR charge, and hence are really n D-branes and n anti-D-branes. One may also consider beginning with a boundary interaction on N coincident Lorentzian D(p+1)-branes, in which case the individual Euclidean (anti) Dp-branes become replaced by a collection of N coincident (anti) Dp-branes.

According to the discussion of Section 4, this finite temperature configuration determines an effective long-distance Euclidean field theory. This field theory evidently contains $2n$ supersymmetric $U(N)$ gauge theories. Additionally, the $\sqrt{2}\pi$ spacing is precisely such that the would-be tachyonic open string connecting a D-brane and an anti-D-brane is massless. (A similar massless mode appears in the bosonic sD-brane.) This couples the $U(N)$ theories with bifundamentals in a manner that breaks supersymmetry.

Assuming they do exist, what could the dual supergravity solutions be? In part these should be determined by the symmetries. A number of potentially dual

solutions have appeared in the literature. Many of them have an R-symmetry corresponding to Lorentz transformations transverse to the brane. This symmetry is clearly spontaneously broken in all the s-branes discussed herein, and hence should not appear in the supergravity solution. Some solutions that do have the appropriate symmetries have appeared in [136,132,135]. Particularly intriguing in this connection is a class of solutions [135] that exhibit thermal particle production and are periodic in Euclidean time.

Acknowledgements

We are grateful to M. Fabinger, S. Gubser, M. Gutperle, J. Karczmarek, M. Kruczenski, F. Leblond, J. Maldacena, S. Minwalla, L. Motl, R. Myers, A. Sen, T. Takayanagi and J. Wacker for useful conversations. This work was supported in part by DOE grant DE-FG02-91ER40654.

References

[1] R. Bousso, A. Maloney and A. Strominger, "Conformal vacua and entropy in de Sitter space," Phys. Rev. D **65**, 104039 (2002) [arXiv:hep-th/0112218].

[2] A. Maloney, E. Silverstein and A. Strominger, "De Sitter space in noncritical string theory," arXiv:hep-th/0205316.

[3] A. Maloney, A. Strominger and X. Yin, "S-brane thermodynamics," arXiv:hep-th/0302146.

[4] I. Antoniadis, P. O. Mazur and E. Mottola "Comment on *Nongaussian isocirvature perturbations from inflation*", astro-ph/9705200.

[5] C. M. Hull, "Timelike T-duality, de Sitter space, large N gauge theories and topological field theory," JHEP **9807**, 021 (1998) [hep-th/9806146].

[6] J. M. Maldacena and A. Strominger, "Statistical entropy of de Sitter space," JHEP **9802**, 014 (1998) [arXiv:gr-qc/9801096].

[7] F. Lin and Y. Wu, "Near-horizon Virasoro symmetry and the entropy of de Sitter space in any dimension," Phys. Lett. B **453**, 222 (1999) [hep-th/9901147].

[8] W. T. Kim, "Entropy of 2+1 dimensional de Sitter space in terms of brick wall method," Phys. Rev. D **59**, 047503 (1999) [hep-th/9810169].

[9] R. Bousso, "Bekenstein bounds in de Sitter and flat space," JHEP **0104**, 035 (2001) [hep-th/0012052].

[10] V. Balasubramanian, P. Horava and D. Minic, "Deconstructing de Sitter," JHEP **0105**, 043 (2001) [hep-th/0103171].

[11] M. Banados, T. Brotz and M. E. Ortiz, "Quantum three-dimensional de Sitter space," Phys. Rev. D **59**, 046002 (1999) [hep-th/9807216].

[12] R. Bousso, "Holography in general space-times," JHEP **9906**, 028 (1999) [hep-th/9906022].

[13] T. Banks, "Cosmological breaking of supersymmetry or little Lambda goes back to the future. II," hep-th/0007146.

[14] R. Bousso, "Positive vacuum energy and the N-bound," JHEP **0011**, 038 (2000) [hep-th/0010252].

[15] E. Witten, "Quantum gravity in de Sitter space" Strings 2001 online proceedings http://theory.theory.tifr.res.in/strings/Proceedings

[16] A. Strominger, "The dS/CFT Correspondence," hep-th/0106113.

[17] J. Maldacena, "The large N limit of superconformal field theories and supergravity," Adv. Theor. Math. Phys. **2**, 231 (1998) [hep-th/9711200].

[18] S. S. Gubser, I. R. Klebanov and A. M. Polyakov, "Gauge theory correlators from non-critical string theory," Phys. Lett. B **428**, 105 (1998) [arXiv:hep-th/9802109].

[19] E. Witten, "Anti-de Sitter space and holography," Adv. Theor. Math. Phys. **2**, 253 (1998) [hep-th/9802150].
[20] E. Witten, "Quantum gravity in de Sitter space," arXiv:hep-th/0106109.
[21] E. Silverstein, "(A)dS backgrounds from asymmetric orientifolds," hep-th/0106209.
[22] S. Nojiri and S. D. Odintsov, "Conformal anomaly from dS/CFT correspondence," Phys. Lett. B **519**, 145 (2001) [arXiv:hep-th/0106191].
[23] M. Li, "Matrix model for de Sitter," arXiv:hep-th/0106184.
[24] A. Chamblin and N. D. Lambert, "de Sitter space from M-theory," Phys. Lett. B **508**, 369 (2001) [arXiv:hep-th/0102159].
[25] Y. Gao, "Symmetries, matrices, and de Sitter gravity," hep-th/0107067.
[26] J. Bros, H. Epstein and U. Moschella, "The asymptotic symmetry of de Sitter spacetime," hep-th/0107091.
[27] S. Nojiri and S. D. Odintsov, "Quantum cosmology, inflationary brane-world creation and dS/CFT correspondence," hep-th/0107134.
[28] A. J. Tolley and N. Turok, "Quantization of the massless minimally coupled scalar field and the dS/CFT correspondence," hep-th/0108119.
[29] A. Volovich, "Discreteness in deSitter space and quantization of Kahler manifolds," hep-th/0101176.
[30] T. Shiromizu, D. Ida and T. Torii, "Gravitational energy, dS/CFT correspondence and cosmic no-hair," hep-th/0109057.
[31] R. Kallosh, "N = 2 supersymmetry and de Sitter space," arXiv:hep-th/0109168.
[32] N. C. Tsamis and R. P. Woodard, "The quantum gravitational back-reaction on inflation," Annals Phys. **253**, 1 (1997) [hep-ph/9602316].
[33] A. C. Petkou and G. Siopsis, "dS/CFT correspondence on a brane," arXiv:hep-th/0111085.
[34] P. O. Mazur and E. Mottola, "Weyl cohomology and the effective action for conformal anomalies," Phys. Rev. D **64**, 104022 (2001) [arXiv:hep-th/0106151].
[35] S. Nojiri, S. D. Odintsov and S. Ogushi, "Cosmological and black hole brane world universes in higher derivative gravity," arXiv:hep-th/0108172.
[36] S. Cacciatori and D. Klemm, "The asymptotic dynamics of de Sitter gravity in three dimensions," arXiv:hep-th/0110031.
[37] Y. S. Myung, "Entropy of the three dimensional Schwarzschild-de Sitter black hole," arXiv:hep-th/0110123.
[38] B. G. Carneiro da Cunha, "Three-dimensional de Sitter gravity and the correspondence," arXiv:hep-th/0110169.
[39] R. G. Cai, Y. S. Myung and Y. Z. Zhang, "Check of the mass bound conjecture in de Sitter space," arXiv:hep-th/0110234.
[40] S. Ogushi, "Holographic entropy on the brane in de Sitter Schwarzschild space," arXiv:hep-th/0111008.

[41] A. Strominger, "Inflation and the dS/CFT correspondence," arXiv:hep-th/0110087.
[42] C. M. Hull, "De Sitter Space in Supergravity and M Theory," hep-th/0109213.
[43] E. Mottola, "Particle Creation In De Sitter Space," Phys. Rev. D **31**, 754 (1985)
[44] B. Allen, "Vacuum States In De Sitter Space," Phys. Rev. D **32**, 3136 (1985)
[45] D. Klemm, "Some aspects of the de Sitter/CFT correspondence," [hep-th/0106247].
[46] G. W. Gibbons and S. W. Hawking, "Cosmological Event Horizons, Thermodynamics, And Particle Creation," Phys. Rev. D **15**, 2738 (1977).
[47] A. Strominger, "Black hole entropy from near-horizon microstates," JHEP **9802**, 009 (1998) [hep-th/9712251].
[48] M. I. Park, "Statistical entropy of three-dimensional Kerr-de Sitter space," Phys. Lett. B **440**, 275 (1998) [hep-th/9806119].
[49] V. Balasubramanian, J. de Boer and D. Minic, "Mass, entropy and holography in asymptotically de Sitter spaces," arXiv:hep-th/0110108.
[50] U. H. Danielsson, "A black hole hologram in de Sitter space," arXiv:hep-th/0110265.
[51] R. G. Cai, "Cardy-Verlinde Formula and Asymptotically de Sitter Spaces," arXiv:hep-th/0111093.
[52] E. Halyo, "De Sitter entropy and strings," hep-th/0107169.
[53] S. Hawking, J. Maldacena and A. Strominger, "DeSitter entropy, quantum entanglement and AdS/CFT," JHEP **0105**, 001 (2001) [hep-th/0002145].
[54] N. A. Chernikov and E. A. Tagirov, "Quantum Theory Of Scalar Fields In De Sitter Space-Time," Annales Poincare Phys. Theor. A **9** (1968) 109.
[55] E. A. Tagirov, "Consequences Of Field Quantization In De Sitter Type Cosmological Models," Annals Phys. **76**, 561 (1973).
[56] R. Figari, R. Hoegh-Krohn and C. R. Nappi, "Interacting Relativistic Boson Fields In The De Sitter Universe With Two Space-Time Dimensions," Commun. Math. Phys. **44**, 265 (1975).
[57] H. Rumpf and H. K. Urbantke, "Covariant 'In-Out' Formalism For Creation By External Fields," Annals Phys. **114**, 332 (1978).
[58] L. F. Abbott and S. Deser, "Stability Of Gravity With A Cosmological Constant," Nucl. Phys. B **195**, 76 (1982).
[59] A. H. Najmi and A. C. Ottewill, "Quantum States And The Hadamard Form. I. Energy Minimization For Scalar Fields," Phys. Rev. D **30**, 1733 (1984).
[60] L. H. Ford, "Quantum Instability Of De Sitter Space-Time," Phys. Rev. D **31**, 710 (1985).
[61] B. Allen and A. Folacci, "The Massless Minimally Coupled Scalar Field In De Sitter Space," Phys. Rev. D **35**, 3771 (1987).
[62] C. J. Burges, "The De Sitter Vacuum," Nucl. Phys. B **247**, 533 (1984).

[63] N. D. Birrell and P. C. W. Davies, *Quantum Fields in Curved Space,* Cambridge University Press, Cambridge (1982).

[64] B. McInnes, "Exploring the similarities of the dS/CFT and AdS/CFT correspondences," arXiv:hep-th/0110062.

[65] M. Spradlin, A. Strominger and A. Volovich, "Les Houches lectures on de Sitter space,"hep-th/0110007.

[66] I. S. Gradshteyn and I. M. Ryzhik, *Table of Integrals, Series and Products*, Academic Press (1994).

[67] I. Sachs and S. N. Solodukhin, "Horizon holography," arXiv:hep-th/0107173.

[68] M. Spradlin and A. Volovich, to appear.

[69] M. Abramowitz and I. Stegun, *Handbook of Mathematical Functions*, Dover (1972).

[70] W. G. Unruh, "Notes On Black Hole Evaporation," Phys. Rev. D **14**, 870 (1976).

[71] T. M. Fiola, J. Preskill, A. Strominger and S. P. Trivedi, "Black Hole Thermodynamics and Information Loss in Two Dimensions," Phys. Rev. D **50**, 3987 (1994) [hep-th/9403137].

[72] J. D. Bekenstein, "Black Holes And Entropy," Phys. Rev. D **7**, 2333 (1973).

[73] S. W. Hawking, "Particle Creation By Black Holes," Commun. Math. Phys. **43**, 199 (1975).

[74] S. Deser and R. Jackiw, "Three-Dimensional Cosmological Gravity: Dynamics Of Constant Curvature," Annals Phys. **153**, 405 (1984).

[75] R. Bousso and S. W. Hawking, "Pair Creation of Black Holes During Inflation," Phys. Rev. D **54**, 6312 (1996) [gr-qc/9606052].

[76] J. D. Brown and J. W. York, "Quasilocal energy and conserved charges derived from the gravitational action," Phys. Rev. D **47**, 1407 (1993).

[77] V. Balasubramanian and P. Kraus, "A stress tensor for anti-de Sitter gravity," Commun. Math. Phys. **208**, 413 (1999) [hep-th/9902121].

[78] L. F. Abbott and S. Deser, "Stability Of Gravity With A Cosmological Constant," Nucl. Phys. B **195**, 76 (1982).

[79] J. L. Cardy, "Operator Content Of Two-Dimensional Conformally Invariant Theories," Nucl. Phys. B **270**, 186 (1986).

[80] S. J. Gates and B. Zwiebach, "Gauged N=4 Supergravity Theory With A New Scalar Potential," Phys. Lett. B **123**, 200 (1983).

[81] G. W. Gibbons and C. M. Hull, "de Sitter space from warped supergravity solutions," arXiv:hep-th/0111072.

[82] C. M. Hull, "de Sitter space in supergravity and M theory," JHEP **0111**, 012 (2001) [arXiv:hep-th/0109213].

[83] P. Berglund, T. Hubsch and D. Minic, "de Sitter spacetimes from warped compactifications of IIB string theory," arXiv:hep-th/0112079.

[84] P. Fre, M. Trigiante and A. Van Proeyen, "Stable de Sitter Vacua from N=2 Supergravity," arXiv:hep-th/0205119.

[85] K. Pilch, P. van Nieuwenhuizen and M. F. Sohnius, "De Sitter Superalgebras And Supergravity," Commun. Math. Phys. **98**, 105 (1985).

[86] E. Silverstein,"(A)dS backgrounds from asymmetric orientifolds,"arXiv:hep-th/0106209.

[87] S. P. de Alwis, J. Polchinski and R. Schimmrigk, "Heterotic Strings With Tree Level Cosmological Constant," Phys. Lett. B **218**, 449 (1989).

[88] A. M. Polyakov, "The wall of the cave," Int. J. Mod. Phys. A **14**, 645 (1999) [arXiv:hep-th/9809057].

[89] B. Craps, D. Kutasov and G. Rajesh, "String Propagation in the Presence of Cosmological Singularities," arXiv:hep-th/0205101.

[90] R. Bousso and J. Polchinski,"Quantization of four-form fluxes and dynamical neutralization of the cosmological constant,"JHEP **0006**, 006 (2000)[arXiv:hep-th/0004134].

[91] L. Dyson, J. Lindesay and L. Susskind, "Is there really a de Sitter/CFT duality,"arXiv:hep-th/0202163.

[92] P. Ginsparg and M. J. Perry, "Semiclassical Perdurance Of De Sitter Space," Nucl. Phys. B **222**, 245 (1983).

[93] J. L. Feng, J. March-Russell, S. Sethi and F. Wilczek, "Saltatory relaxation of the cosmological constant," Nucl. Phys. B **602**, 307 (2001) [arXiv:hep-th/0005276].

[94] J. Preskill, P. Schwarz, A. D. Shapere, S. Trivedi and F. Wilczek, "Limitations on the statistical description of black holes," Mod. Phys. Lett. A **6**, 2353 (1991).

[95] R. Bousso, "Adventures in de Sitter space", hep-th/0205177.

[96] R. Bousso, O. DeWolfe and R. C. Myers, "Unbounded entropy in spacetimes with positive cosmological constant," arXiv:hep-th/0205080. .

[97] J. D. Brown and C. Teitelboim,"Neutralization Of The Cosmological Constant By Membrane Creation,"Nucl. Phys. B **297**, 787 (1988).

[98] L. F. Abbott,"A Mechanism For Reducing The Value Of The Cosmological Constant,"Phys. Lett. B **150**, 427 (1985).

[99] A. H. Chamseddine, "A Study of noncritical strings in arbitrary dimensions," Nucl. Phys. B **368**, 98 (1992).

[100] K. Dasgupta, G. Rajesh and S. Sethi, "M theory, orientifolds and G-flux," JHEP **9908**, 023 (1999) [arXiv:hep-th/9908088].

[101] S. Kachru, M. Schulz and S. Trivedi, "Moduli stabilization from fluxes in a simple IIB orientifold," arXiv:hep-th/0201028.

[102] A. R. Frey and J. Polchinski, "N = 3 warped compactifications," arXiv:hep-th/0201029.

[103] S. Gukov, C. Vafa and E. Witten, "CFT's from Calabi-Yau four-folds," Nucl. Phys. B **584**, 69 (2000) [Erratum-ibid. B **608**, 477 (2001)] [arXiv:hep-th/9906070].

[104] S. B. Giddings, S. Kachru and J. Polchinski, "Hierarchies from fluxes in string compactifications," arXiv:hep-th/0105097.

[105] K. Becker and M. Becker, "M-Theory on Eight-Manifolds," Nucl. Phys. B **477**, 155 (1996) [arXiv:hep-th/9605053].

[106] J. Polchinski and A. Strominger, "New Vacua for Type II String Theory," Phys. Lett. B **388**, 736 (1996) [arXiv:hep-th/9510227].

[107] A. Strominger, "The Inverse Dimensional Expansion In Quantum Gravity," Phys. Rev. D **24**, 3082 (1981).

[108] R. Rohm, "Spontaneous Supersymmetry Breaking In Supersymmetric String Theories," Nucl. Phys. B **237**, 553 (1984).

[109] S. R. Coleman and F. De Luccia,"Gravitational Effects On And Of Vacuum Decay,"Phys. Rev. D **21**, 3305 (1980).

[110] L. Susskind, "Twenty years of debate with Stephen," arXiv:hep-th/0204027.

[111] A. D. Linde, "Hard art of the universe creation (stochastic approach to tunneling and baby universe formation)," Nucl. Phys. B **372**, 421 (1992) [arXiv:hep-th/9110037].

[112] J. Garriga and A. Vilenkin, "Recycling universe," Phys. Rev. D **57**, 2230 (1998) [arXiv:astro-ph/9707292].

[113] T. Banks, "Cosmological Breaking Of Supersymmetry?," Int. J. Mod. Phys. A **16**, 910 (2001).

[114] R. Bousso, "Positive vacuum energy and the N-bound," JHEP **0011**, 038 (2000) [arXiv:hep-th/0010252].

[115] W. Fischler, unpublished.

[116] J. M. Maldacena and L. Susskind, "D-branes and Fat Black Holes," Nucl. Phys. B **475**, 679 (1996) [arXiv:hep-th/9604042].

[117] S. Kachru, J. Pearson and H. Verlinde, "Brane/flux annihilation and the string dual of a non-supersymmetric field theory," arXiv:hep-th/0112197.

[118] M. Gutperle and A. Strominger, "Spacelike branes," JHEP **0204**, 018 (2002) [arXiv:hep-th/0202210].

[119] A. Sen, "Non-BPS states and branes in string theory," arXiv:hep-th/9904207.

[120] A. Sen, "Rolling tachyon," JHEP **0204**, 048 (2002) [arXiv:hep-th/0203211].

[121] A. Sen, "Tachyon matter," arXiv:hep-th/0203265.

[122] C. M. Chen, D. V. Gal'tsov and M. Gutperle, "S-brane solutions in supergravity theories," Phys. Rev. D **66**, 024043 (2002) [arXiv:hep-th/0204071].

[123] S. Mukohyama, "Brane cosmology driven by the rolling tachyon," Phys. Rev. D **66**, 024009 (2002) [arXiv:hep-th/0204084].

[124] M. Kruczenski, R. C. Myers and A. W. Peet, "Supergravity S-branes," JHEP **0205**, 039 (2002) [arXiv:hep-th/0204144].

[125] B. McInnes, "dS/CFT, censorship, instability of hyperbolic horizons, and spacelike branes," arXiv:hep-th/0205103.

[126] S. Roy, "On supergravity solutions of space-like Dp-branes," JHEP **0208**, 025 (2002) [arXiv:hep-th/0205198].

[127] N. S. Deger and A. Kaya, "Intersecting S-brane solutions of D = 11 supergravity," JHEP **0207**, 038 (2002) [arXiv:hep-th/0206057].

[128] J. E. Wang, "Spacelike and time dependent branes from DBI," JHEP **0210**, 037 (2002) [arXiv:hep-th/0207089].

[129] A. Strominger, "Open string creation by s-branes," arXiv:hep-th/0209090.

[130] V. D. Ivashchuk, "Composite S-brane solutions related to Toda-type systems," Class. Quant. Grav. **20**, 261 (2003) [arXiv:hep-th/0208101].

[131] T. Okuda and S. Sugimoto, "Coupling of rolling tachyon to closed strings," Nucl. Phys. B **647**, 101 (2002) [arXiv:hep-th/0208196].

[132] F. Quevedo, G. Tasinato and I. Zavala, "S-branes, negative tension branes and cosmology," arXiv:hep-th/0211031.

[133] N. Ohta, "Intersection rules for S-branes," arXiv:hep-th/0301095.

[134] M. Gutperle and A. Strominger, "Timelike boundary Liouville theory," arXiv:hep-th/0301038.

[135] C. P. Burgess, P. Martineau, F. Quevedo, G. Tasinato and I. Zavala C., "Instabilities and particle production in S-brane geometries," arXiv:hep-th/0301122.

[136] H. Lu, S. Mukherji and C. N. Pope, "From p-branes to cosmology," Int. J. Mod. Phys. A **14**, 4121 (1999) [arXiv:hep-th/9612224].

[137] C. M. Hull, "Timelike T-duality, de Sitter space, large N gauge theories and topological field theory," JHEP **9807**, 021 (1998) [arXiv:hep-th/9806146].

[138] N. Lambert, H. Liu and J. Maldacena to appear.

[139] S. Minwalla and K. Pappododimas, unpublished.

[140] A. Sen, unpublished.

[141] P. Mukhopadhyay and A. Sen, "Decay of unstable D-branes with electric field," JHEP **0211**, 047 (2002) [arXiv:hep-th/0208142].

[142] C. G. Callan, I. R. Klebanov, A. W. Ludwig and J. M. Maldacena, "Exact solution of a boundary conformal field theory," Nucl. Phys. B **422**, 417 (1994) [arXiv:hep-th/9402113].

[143] F. Larsen, A. Naqvi and S. Terashima, "Rolling tachyons and decaying branes," arXiv:hep-th/0212248.

[144] N. W. McLachlan, *Theory and Application of Mathieu Functions*, Clarendon Press, Oxford, UK (1947).

[145] S. S. Gubser and A. Hashimoto, "Exact absorption probabilities for the D3-brane," Commun. Math. Phys. **203**, 325 (1999) [arXiv:hep-th/9805140].

[146] I. R. Klebanov, "World-volume approach to absorption by non-dilatonic branes," Nucl. Phys. B **496**, 231 (1997) [arXiv:hep-th/9702076].

[147] M. Spradlin, A. Strominger and A. Volovich, "Les Houches lectures on de Sitter space," arXiv:hep-th/0110007.

[148] J. Polchinski and L. Thorlacius, "Free Fermion Representation Of A Boundary Conformal Field Theory," Phys. Rev. D **50**, 622 (1994) [arXiv:hep-th/9404008].

[149] M. B. Green and M. Gutperle, "Symmetry Breaking at enhanced Symmetry Points," Nucl. Phys. B **460**, 77 (1996) [arXiv:hep-th/9509171].

[150] M. R. Gaberdiel and A. Recknagel, "Conformal boundary states for free bosons and fermions," JHEP **0111**, 016 (2001) [arXiv:hep-th/0108238].

[151] P. Di Vecchia, M. Frau, I. Pesando, S. Sciuto, A. Lerda and R. Russo, "Classical p-branes from boundary state," Nucl. Phys. B **507**, 259 (1997) [arXiv:hep-th/9707068].

[152] J. Polchinski, "String Theory. Vol. 1: An Introduction To The Bosonic String."

[153] A. Sen, "Field Theory of Tachyon matter," arXiv:hep-th/0204143.

[154] J. Polchinski, "Evaluation Of The One Loop String Path Integral," Commun. Math. Phys. **104**, 37 (1986).